DOCTOR OF PHILOSOPHY

Travelling Wave Analysis of a Nonlinear Diffusion Equation

Alzubadi, Hanadi

Award date:
2019

Awarding institution:
University of Dundee

Travelling Wave Analysis of a Nonlinear Diffusion Equation

By

Hanadi Alzubadi

A Thesis submitted for the degree of Doctor of Philosophy

Division of Mathematics

University of Dundee

Dundee

2019

Contents

List of Figures

List of Tables

Acknowledgements

Praise be to (ALLAH) that gave me strength and power to succeed in this thesis. Then foremost, I would like to thank my supervisor Dr. Philip Murray for his guidance, patience and motivation. His guidance helps me to make this thesis possible. He has always been available to advise me. I also thank all members of the staff of the Department of mathematics, especially Prof. Fordyce Davidson for his advice. I am very blessed to have been given the opportunity to work on a very interesting topic in cell population dynamics.

My sincere thanks to my wonderful husband, Abdulmuoeen, for his understanding and love during the past a few years to make my studying successful which is very difficult as we have two kids (Wissam and Leen). I am much indebted to my father, Mother, brother (Abdulaziz), sisters for encouragements, prayers and support during my studies. My great pleasure and appreciation go to my friend, Haneen Hamam, for supporting me since I arrived to Dundee. As well, my friend Tahani Binaoun for lending a hand in the last stage of submitting the thesis.

Finally, I would like to thank (Umm Al-Qura University), and the embassy of Saudi Arabia for giving me this opportunity to study PhD in Dundee University.

Declaration

I declare that the following thesis is my own composition and that it has not been submitted before in application for a higher degree.

Hanadi Alzuabdi

Certification

This is to certify that Hanadi Alzubadi has complied with all the requirements for the submission of this Doctor of Philosophy thesis to the University of Dundee.

Philip Murray

Abstract

Cell monolayers are a widely used tool in tumour and tissue repair studies. In many cell lines, cell proliferation is contact-inhibited such that the cell population reaches confluence at long times. Given suitable initial conditions, moving fronts of proliferation and migration can be observed prior to confluence, with two key measurable quantities being the width and propagation speed of the proliferating region. In this thesis we consider the continuum limit of a model of an off-lattice, cell-based simulation of a contact-inhibited cell monolayer. Numerical solutions of the continuum model, which can be formulated as a nonlinear diffusion free boundary (nonlinear Stefan) problem, indicate a travelling wave behaviour that is subsequently investigated using a travelling wave analysis. Considering first a simplified linear problem, we perform a travelling wave analysis that identifies a small parameter, the natural logarithm of the compression ratio of cells at which contact inhibition stops proliferation, from which asymptotic expressions for the wave speed and proliferating rim width are derived. Subsequently, we use perturbation theory to derive approximations for the wave speed and proliferating rim width in the case of nonlinear diffusion coefficients that represents the continuum limit of a discrete model in which cells interact via a nonlinear force law. The related results depend on which force law in which diffusion coefficient type is considered. We investigate the solution of nonlinear diffusion models for a number of different inter- cellular force laws (e.g. Hertz, linear, cubic) where the power of the force law has a profound effect on the qualitative behaviour.

Chapter 1

Introduction

Cell monolayer cultures are a fundamental tool that allow phenomena such as collective migration, wound healing and cell proliferation to be studied in a controlled environment. In cell monolayer cultures that exhibit contact inhibition of proliferation, (i.e. cells divide only if there is sufficient space to do so), the cell population typically reaches confluence at long times. On intermediate time scales, moving cell fronts of proliferation and migration can arise given suitable initial conditions. Analysis of front dynamics can be used to infer proliferation and migration rates for tumours and wound healing (tissue repair) studies.

Mathematical models in cell populations are an essential tool in the study of collective or emergent behaviours. For instance, in a situation where an experimentalist can measure individual cell behaviours and tissue scale phenomena, such as the speed of a propagating front, modelling can play a crucial role in identifying how micro-scale interactions give rise to tissue scale phenomena.

There are two types of mathematical modelling of cell populations: discrete (individual

or agent) based models, which treat each biological cell or part therefore as an individual entity; Continuum models, which describe the macro-scale behaviour of a cell population. Both approaches address the model-building problem in different ways and have advantages and disadvantages.

By treating each cell as an individual, discrete models capture measurable biological behaviour at the single cell scale and effects such as cell heterogeneity and stochasticity. However, they are typically computationally intensive and can require a prohibitive amount of simulation time in order to qualitatively describe model behaviour.

Continuum models describe locally averaged quantities. There are a whole host of techniques from the applied mathematics literature (e.g. perturbation theory and bifurcation theory) that can be used to study model behaviour. However, models often rely on constitutive assumptions that can be difficult to explicitly relate to cell biology.

In some cases it is possible to derive a corresponding continuum model from a discrete counterpart. This approach has the advantage that the underlying assumptions are made at the discrete cellular scale where they can in principle be validated by the experimental biologist. The derived continuum form allows qualitative insight to be gained into the behaviour of simulations.

In this thesis we consider a continuum model of a proliferating cell monolayer in one spatial dimension that has previously been derived from a discrete cell-based model. Using a combination of numerical and analytic tools we demonstrate travelling wave behaviour and compute asymptotic expressions for emergent tissue scale quantities. We attempt to identify which details of the discrete cell-based model are important in cell population dynamic.

1.1 The model

Consider a population of cells in one spatial dimension. Letting $x_i(t)$ represent the position of the i^{th} cell at time t, we assume over-damped motion of the form

$$\begin{aligned} \eta \dot{x}_1 &= 0, \\ \eta \dot{x}_i &= \sum_j F(|x_i - x_j|); \qquad i = 2, \ldots n-1, \\ \eta \dot{x}_n &= F(|x_n - x_{n-1}|), \end{aligned} \tag{1.1}$$

where η is the cell damping constant, F is the force exerted on the i^{th} cell by its nearest neighbours and n is the total number of cells. We assume that cells divide with a period of T_C hours but only if there is sufficient space to do so, i.e. if the average distance between a cell and its two neighbours is greater than a threshold, d_c.

It has previously been shown that the aforementioned discrete cell based model can be described by the reaction diffusion equation

$$\frac{\partial q}{\partial t} = \frac{\partial}{\partial x}(D(q)\frac{\partial q}{\partial x}) + rqH(q_c - q), \tag{1.2}$$

where $q(x,t)$ is the cell density, x is the position variable, t is time, $D(q)$ is a nonlinear diffusion coefficient, r is a proliferation rate, q_c is a cell density above which cell proliferation is contact inhibited and the Heaviside function, $H(q_c - q)$, is given by

$$H(x) = \begin{cases} 1, & x > 0, \\ 0, & x \leq 0. \end{cases}$$

Equation (1.2) is solved on the domain $[0, s(t)]$, where $s(t)$ represents the position of a

moving boundary. The boundary conditions are given by

$$\left.\frac{\partial q}{\partial x}\right|_{x=0} = 0, \tag{1.3}$$

and

$$\left.\frac{\partial q}{\partial x}\right|_{x=s(t)} = -\frac{q(x,t)}{D(q)}\frac{ds}{dt}. \tag{1.4}$$

The moving boundary satisfies the ordinary differential equation:

$$\frac{ds}{dt} = F(q(s(t),t)), \tag{1.5}$$

and the initial condition

$$q(x,0) = f(x). \tag{1.6}$$

In this thesis we will consider the behaviour of equations (1.2)-(1.6) for different forms of the force law, F. For each case, we will analyse the system numerically by directly solving the diffusion model. We will then using a shooting method to compute the wave speed. Finally, we will derive asymptotic expressions for the travelling wave.

The results highlight the emergence of two tissue-scale, experimentally measurable quantities: the speed of propagation of the edge of the tissue, c, and the proliferating rim width, ρ. The analysis identifies a small parameter, the natural logarithm of the compression ratio of cells at which contact inhibition stops proliferation, from which asymptotic expressions for the wave speed and proliferating rim width are obtained. Moreover, the analysis yields a relationship between the proliferating rim width and wave front speed that was documented in previous discrete cell-based model simulations. The approach allows us to understand how the choice for the force law, F, affects tissue scale observables c and ρ.

1.2 Thesis overview

The layout of this thesis is as follows. In Chapter 2, we summarise our current biological knowledge by reviewing some pre-existing work related to our study. We discuss some essential biological knowledge of diffusion models, and introduce several previous results. We also discuss some techniques to solve our problem that are particalarly relevant.

In Chapter 3 we consider a simplified case in which the diffusion coefficient is assumed to be a constant. We then discuss two different classes of boundary condition on the moving front and calculate asymptotic expressions for the wave speed and proliferating rim width. The analysis identifies a small parameter, the natural logarithm of the compression ratio of cells, at which contact inhibition stops proliferation.

In Chapter 4 we consider the case of a non-linear diffusion coefficient that represents cells interacting via a linear force law [53]. Using the methodology outlined in Chapter 3, we show that the effect of nonlinear diffusion does not appear at leading order of the asymptotic solutions. These results suggest that in many cases a simple reaction diffusion model with Dirichlet boundary conditions and a constant diffusion coefficient is adequately able to quantitatively explain behaviour in the discrete simulations. We then show that the above conclusions are valid for a generalised force law.

Case number	diffusion $D(q)$	Boundary at $z=0$	Section
(1)	constant	$\frac{1}{q}$	3.1
(2)	a^2k constant	$\frac{1}{a\left(1-\frac{c}{ak}\right)}$	3.2
(3)	$\frac{k}{q^2}$	$\frac{1}{a}$	4.1.1
(4)	$\frac{k}{q^2}$	$\frac{1}{a\left(1-\frac{c}{ak}\right)}$	4.1.2
(5)	$\frac{a^2k}{(aq)^n}$	$\frac{1}{a}$	4.2.1
(6)	$\frac{a^2k}{(aq)^n}$	$\frac{1}{a\left(1-\frac{c}{ak}\right)}$	4.2.2
(7)	$\frac{a^2k}{(aq)^n}$	$\frac{1}{a(1-\frac{c(n-1)}{ak})^{1/(n-1)}}$	4.2.3
(8)	$\frac{nk}{q^2}\left(1-\frac{1}{aq}\right)^{n-1}$	$\frac{1}{a\left(1-\left(\frac{c}{ak}\right)^{\frac{1}{n}}\right)}$	5.1

Table 1.1: A table illustrating the different cases considered in this thesis.

Murray et al. [53] derived nonlinear diffusion models for a number of different intercellular force laws used in the literature (e.g. Hertz, linear, cubic). In Chapter 5 we extend our analysis to consider these cases. This case is qualitatively different to what was previously considered. Hence we adjust the approach taken in the previous chapter and show that the power of the force law has a profound effect on the qualitative behaviour of the model.

Chapter 6, meanwhile, concludes our thesis with the primary results, and describes avenues for future work investigation.

Chapter 2

Literature Review

Introduction

This review subdivided into three main topics: (i) biological background; (ii) mathematical modelling background; and (iii) algorithm implementation.

2.1 Biological background

In this section we provide an introduction to relevant features of biological cells and their surroundings. In Section 2.1.1 we will provide a brief description of fundamental properties of cells. In Section 2.1.2 we consider aspects of cell monolayers growth.

2.1.1 Introductory biology

A cell is a complex system that is the structural unit of any living organism. Cells contain organic molecules that all living things are composed of. A cell can perform

a range of functions, e.g. metabolise its nutrients, synthesise molecules, provide its energy and replicate itself [34].

Deoxyribonucleic acid (DNA) refers to the hereditary material of living organisms [31]. Most DNA is located on chromosomes in the nucleus of a cell. Information is stored in the form of four essential bases: adenine (A), guanine (G), thymine (T) and cytosine (C). It is the ordering of these bases that primarily determines the information that will build and maintain an organism (Crick and Watson [16]).

A parent cell can divide into two or more daughter cells in a process known as cell division. Cell division introduced in two types: vegetative and reproductive. In the former, a daughter cell is genetically identical to its parent. It ensures maintenance of the original cell's genome. In contrast, during reproductive cell division, also known as meiosis [35], DNA is inherited by a daughter cell. Cell division is essential as it is used in sexual reproduction to bring about new organisms.

The cell cytoskeleton is a network of filaments and tubules that ran through a cell and the cytoplasm. The cytoskeleton is composed of components such as actin, microtubules and intermediate filaments [9]. The cytoskeleton provides a range of cellular function, e.g it provides support to the cell, gives it shape, helps in molecular transport, helps in cell division and, finally, it aids in cell signalling. Although a cytoskeleton is found in all cells, the proteins that form it may vary from one organism to the other [71].

Elasticity is the ability of a body or substance to return to its original size and shape after being deformed if the forces causing the deformation are removed. Cell elasticity mainly originates in the cytoskeleton which can exert forces on the cellular environment. This process is essential in the regulation of elasticity where the forces are generating the tension in the actin network [60].

Intercell adhesion occurs when cells interact with neighbouring cells with the help of

specific molecules, cell adhesion molecules (CAMs) [29]. This may occur through direct contact between cell surfaces or indirectly where cells attach to the extracellular matrix (ECM). The functional units of cell adhesion are usually multiprotein complexes made up of three general classes of proteins: cell adhesion molecules, adhesion receptor and the extracellular matrix (ECM) [29]. The primary role played by cell adhesion is regulation of fundamental cellular processes such as cell survival and proliferation.

Cells in higher organisms can interact with one another to form tissues and organs. This requires intercellular communication which is usually mediated via signalling molecules. Cell-cell interactions can lead to tissue level phenomena such as homeostasis.

2.1.2 Monolayer growth

Cell monolayers are a primary in *vitro* tool that can be used to study aspects of tissue behaviour. For many cell lines cultured in *vitro*, cells seeded at low population densities proliferate and migrate until confluence is attained (i.e. some upper limit on cell density where proliferation is arrested [42]).

Monolayer growth is highly relevant to the study of wound healing. For example, in a scratch assay a wound is created in a cell by scratching a section of cells and observing the recovery of the 'wound'. The assay is simple, cheap and conditions are easily regulated. Typically, via a combination of proliferation and migration the scratch is filled in. Wound healing assays typically exhibit travelling wave type solutions whereby cells migrate in response to the wound [44, 15, 8, 58].
Cell monolayers are also a fundamental tool used to characterise properties of cancer cell lines such as migration and proliferative capacity. When many cancer cell lines are

cultured as a monolayer the population is found to grow to confluence. Notably, behaviour in a monolayer is typically much simpler than a tumour spheroid as diffusion limited growth does not occur [66, 55, 59, 18].

2.2 Mathematical models of cell proliferation and migration

The mathematical modelling of cell population dynamics is a rich and active area of research. It is useful to classify models into one of two categories: discrete and continuum. In discrete models a cell, or part thereof, is modelled as a discrete entity. In continuum models, the individual cell description is lost and one describes the evolution of macroscopic quantities such as cell density.

2.2.1 Discrete models

Discrete models can be separated into on-lattice and off-lattice.

2.2.1.1 Lattice-based models

Lattice-based models can be subdivided into cellular automata and cellular Potts models.

Cellular automata

A cellular automaton is an on-lattice, discrete dynamical system. A biological cell, typically represented by a state vector, can occupy discrete positions on a fixed lattice. Prescribed rules are used to update the state vector at each time step of a simulation. Rules are chosen to compute individual-level interactions between cells.

In lattice-gas cellular automata, cells are defined to have positions on a fixed lattice and velocities. Collision rules can be chosen to model biological interaction [30]. Cellular automata have been study to model tissue maintenance of biological observation [54, 17, 30, 45].

Cellular Potts model

The cellular Potts model (CPM) is an on-lattice model that was originally used to study problems in statistical physics [28, 46, 56]. In a CPM a cell is represented by a number of lattice points. Biological features are described using a Hamiltonian which is minimised using a Metropolis algorithm. Typically, the Hamiltonian is defined to constrain features such as cell volume, cell perimeter or chemotactic movement. The model of CPM was introduced by Glazier and Graner [27].

2.2.1.2 Off-lattice models

In off lattice models, cell coordinates are continuous functions of space and time.

2.2.1.3 Vertex models

Vertex models represent biological cells by describing the motion of boundary vertices. They are particularly well suited to describing cell mechanics in tight epithelial tissues [38], where cells can be accurately represented as polygons. Typically each vertex satisfies an equation of motion of the form

$$\gamma \frac{dx_i}{dt} = -\nabla_i U \quad i = 1, ..., n, \tag{2.1}$$

where U is a function of vertex position, x_i is the spatial position of vertex i, ∇_i is the nabla differential operation and $\frac{dx_i}{dt}$ is the vertex velocity. Honda et al. [33] used 3D cell model to treats the interfaces between neighbouring cells and volumes of polyhedral cells. Vertex dynamics models investigated by Fletcher et al. [23]

2.2.1.4 Cell centre models

Cell centre models represent the position of a cell as a single point. Cellular biophysics is represented by a force that describes repulsive and attractive forces that cells exert upon one another [61].

Letting x_i represent the location of cell i, Newton's Second Law yields

$$\Sigma_j F_{ij} - \mu \frac{dx_i}{dt} = m_i \frac{d^2 x_i}{dt^2}, \tag{2.2}$$

where m_i is the mass, F_{ij} is force on cell i due to cell j, μ is a drag coefficient and the sum is taken over nearest neighbours. Typically over-damped motion is assumed,

hence inertial terms are neglected and

$$\frac{dx_i}{dt} = \frac{1}{\mu_i}\Sigma_j F_{ij}. \tag{2.3}$$

Cell centre models have been used to study tissue homoeostasis, epithelial layer and tumour growth [e.g. 20, 25, 19]. Examples of cell centre models found in [68, 48, 3, 64, 47].

2.2.2 Continuum models

Continuum models of cell population dynamics describe smoothly varying properties, such as cell density or pressure fields. Amongst their advantages are that there is a vast number of numerical and analytical techniques available to analyse the models. Moreover, continuum models readily deal with the large number of cells often found in biological systems.

Continuum models have been used to successfully study many aspects of cell population dynamics [e.g. 26, 70, 36]. As in this thesis we will ultimately consider reaction diffusion models of cell population dynamics, here we focus the literature review on reaction diffusion models of one variable.

2.2.2.1 Derivation of reaction-diffusion equations

In a continuum setting, conservation of cell number can be described by the conservation equation

$$\frac{\partial q}{\partial t} + \nabla.\mathbf{J} = 0,$$

where q is a cell number density and J a cell flux. Fick's law assumes that the flux is proportional to the local gradient, i.e.

$$\mathbf{J} = -D\nabla q \tag{2.4}$$

where D is a diffusion coefficient. Substituting for $\mathbf{J}$ in the conservation equation yields

$$\frac{\partial q}{\partial t} = \nabla.\left(D(\nabla q)\right).$$

Given reactions, represented by $f(q)$, we obtain the reaction diffusion equation

$$\frac{\partial q}{\partial t} = \nabla.(D\nabla q) + f(q). \tag{2.5}$$

Model (2.5) is known as a reaction-diffusion system (Murray [51] and Britton [12]). Other examples of reaction diffusion models found in Britton et al. [13]; Kuttler [41]; Volpert and Petrovskii [69]. Spatial studies investigated with Turing [67] in chemical basis of morphogenesis; Gatenby and Gawlinski [26] in cancer invasion.

2.2.2.2 Fisher's equation

One of the early important examples of a reaction diffusion equation was described by Fisher [22, 40]. The model is given by

$$\frac{\partial q}{\partial t} = D\frac{\partial^2 q}{\partial^2 x} + rq(1 - \frac{q}{k}), \tag{2.6}$$

where q is the density, D is the diffusion coefficient and the positive constant r represents the growth rate. This equation has many solutions depending on the boundary condition. Fisher defined travelling wave solutions and studied their existence, stability and speed of propagation.

Development of the Fisher and Kolmogorov model with a nonlinear diffusion coefficient

Shakeel [63] extended the analysis of Fisher by introducing a nonlinear diffusion coefficient. Hence they obtained the non-linear diffusion of the Fisher and Kolmogorov model

$$\frac{\partial q}{\partial t} = \frac{\partial}{\partial x}\left(D(q)\frac{\partial q}{\partial x}\right) + \chi q(1-q), \tag{2.7}$$

where q is the density, x is the position, χ is the ratio of cell growth rate to speed of growth front and the diffusion coefficient given by

$$D(q) = \exp(\gamma(q-1)), \tag{2.8}$$

where γ controls how fast cells are spreading in the domain.

King and McCabe [39] study a modification of the Fisher-KPP equation with fast nonlinear diffusion that is given by

$$\frac{\partial q}{\partial t} = \nabla.\left(q^{-n}\nabla q\right) + q(1-q). \tag{2.9}$$

They explore travelling wave behaviours and estimate the wave speed and position of wavefront for small value n. Notably the boundary conditions differ from those considered in this thesis.

2.2.2.3 Aggregation reaction-diffusion model

In ecological modelling the aggregation behaviour of individuals in a population occurs to avoid predators or for reproduction [17, 2]. The reaction aggregation diffusion model involves the density depending on nonlinear diffusion, D, which has a sign that changes as a function of the density. A negative value describes aggregation and the positive value describes dispersion:

$$\frac{\partial q}{\partial t} = \frac{\partial}{\partial x}[D(q)\frac{\partial q}{\partial x}] + g(q), \tag{2.10}$$

where $q(x,t)$ is the population density, D illustrates the reaction aggregation at ($D < 0$) and diffusion at ($D > 0$), and g is the nonlinear growth rate.

2.2.3 From discrete to continuum models

Coarse graining of discrete models can in some cases yield continuum models. Such approaches have been developed for many classes of discrete models: crowding effects have been be accounted for lattice-based simulations [e.g. 65, 21, 5]; Deutsch and Dormann [17] studied the continuum limit of LGCA; Alber et al. [1] and Lushnikov et al. [43] demonstrated that nonlinear diffusion equations can describe continuum properties of cellular Potts simulations; Fozard et al. [24] studied the continuum limit of vertex models; Murray et al. [49, 53, 52] showed that nonlinear diffusion coefficients can be used to represent continuum behaviour in a class of off-lattice cell-based models; Bodnar and Velazquez [11] considered the continuum limit of a general class of off-lattice models; and Anderson et al. [4] investigated the successful application of their hybrid discrete-continuum method to tumour growth and invasion.

2.2.3.1 Continuum limit of a Cellular Potts model

Lushnikov et al. [43] derived continuous macroscopic limits of CPMs in 1D and 2D. The continuum model equations describe the dynamic of a cell density moving chemotactically in a chemical gradient. In one spatial dimension, the macroscopic nonlinear diffusion equation of cellular density, $q(r,t)$, is given by

$$\partial_t q = D_2 \nabla . \left(\frac{1 + \left(\frac{q}{q_0}\right)^2}{(1 - \left(\frac{q}{q_0}\right))^2} \nabla_r q \right), \tag{2.11}$$

where $q(x,t)$ evolution of cellular density, D_2 is the diffusion coefficient and q_0 is the maximum cell density.

2.2.3.2 Continuum limit of lattice

Deutsch and Dormann [17] showed that a LGCA can be described in the continuum limit by

$$\frac{\partial q(x,t)}{\partial t} = D \frac{\partial^2 q(x,t)}{\partial x^2}, \tag{2.12}$$

where

$$D := \frac{m_\sigma}{2} \lim_{\varepsilon \to 0} \frac{\varepsilon^2}{\delta} = \frac{1}{2} a m_\sigma^2, \tag{2.13}$$

where ε is a space interval, δ is a time interval and m_σ is speed of each cell σ,

2.2.3.3 Continuum limit of individual cell-based models

Bodnar and Velazquez [11] considered an interaction potential of the form

$$c_N(x) = N^{\beta} V_1(N^{\beta} X),$$

where V is a potential. Equation of motion given by

$$\frac{d}{dt} X_k^N(t) = -\frac{1}{N} \Sigma_{i=1}^N \nabla V_N(X_k^N(t) - X_i(t)) + \sigma \xi_k(t), \quad k = 1, ..., N, \tag{2.14}$$

where $X_k(t)$ is the position of the centre of cells at time t and N is the number of cells that interact with potential c. $\xi_k(t)$ represent uncorrelated random noise.
Bodnar and Velazquez [11] derived the continuum limit approximation

$$\frac{\partial q}{\partial t} = \frac{\partial}{\partial x} \left(D(q) \frac{\partial q}{\partial x} \right). \tag{2.15}$$

The precise form of $D(q)$ depended on features of the interaction potential with one particular form, similar to the CPM diffusion coefficient, given by

$$D(q) = \frac{\sigma^2 q_x}{(1 - cq)^2}, \tag{2.16}$$

where c is the speed of each cell and q is the density. In the case where d the average distance between cells equal to R the range of interactions of the potential and $\sigma \neq 0$.

2.2.3.4 Continuum limit of a vertex model

Fozard et al. [24], considering a one-dimensional vertex model of epithelial monolayers, derived corresponding continuum models in the slow-growth-rate and long-time

limits. The authors showed that in the continuum limit

$$\frac{\partial q}{\partial t} + \frac{\partial}{\partial x}(qu) = 0, \tag{2.17}$$

where q is cell density and u is the local cell velocity. u was shown to satisfy

$$\begin{aligned} \mu u - V\frac{\partial}{\partial x}(\delta l \frac{\partial u}{\partial x}) &= -\frac{\partial p}{\partial x}, \\ p &= \lambda(a-l) \\ \frac{Da}{Dt} &= \alpha\Gamma(a,l,p,\gamma), \end{aligned} \tag{2.18}$$

where l is cell length, a is mean target length, μ is the cell-substrate damping constant, λ is the cell elastic constant, p is cell pressure, Γ is cell growth rate, V is the viscosity coefficient of the cells and α is the rate of cell elongation.
We observe that in the case $\delta = 0$ the model reduces to a form similar to that considered in this thesis.

2.2.3.5 Continuum limit of a lattice-based model

Simpson et al. [65] considered a lattice-based model of cell proliferation and migration and showed that it could be represented in the continuum limit by the nonlinear diffusion equation

$$\frac{\partial q}{\partial t} = D_0 \nabla.[D(q)\nabla q], \tag{2.19}$$

where q is the continuum density and the diffusion coefficient is

$$D_0 = \frac{P}{2d}\lim_{\Delta,\tau\to 0}(\frac{\Delta^2}{\tau}),$$

and P is the probability that any agent is motile in the time interval of duration τ and d is the dimension of the problem.

The nonlinear diffusivity function is given by

$$D(q) = 1 - 2q(1-q)\frac{f'(q)}{f(q)}.$$

where $f(c) = e^{Ak}$ is a function describing lattice occupancy. The study shows that discrete and continuum are in good agreement except when f, f' are sufficiently large.

2.2.3.6 Continuum limit of a one-dimensional cell centre model

Murray et al. [53] showed that the discrete equation of motion (equations (2.3)) transforms into continuum nonlinear diffusion equations. In this section, we highlight the derivation of the diffusion coefficient, which enables us to derive the main PDE model, which we will introduce in detail.

Let us consider a population of similar cells in one spatial dimension, where the interaction between the cells is a function of the distance between their centres. The equations of motion are

$$\mu\frac{dx_i}{dt} = F(x_i - x_{i-1}) - F(x_{i+1} - x_i), \quad i = 1,2,...N.$$

The continuum description of cell dynamic by introducing Δi.

$$\hat{\mu}\frac{dx_i}{dt} = \hat{F}(x_i - x_{i-\Delta i}) - \hat{F}(x_{i+\Delta i} - x_i), \quad i = 1,2,...N, \tag{2.20}$$

where x_i is the position of the i^{ith} cell, F is the intercellular force and $\hat{\mu}$ is the cell damping constant. Murray et al. [53] assumed that the spatial coordinates of the cell

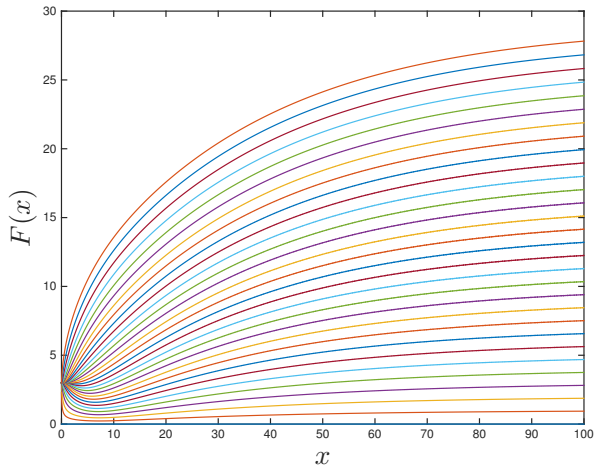

Figure 2.1: The force law, $F(x) = k((x_{i-1} - x_i) + a)$, is plotted against spatial position, x, at different time t. $k = 10$, $a = 1$ and $N = 30$.

positions along the axis are a continuous function of i, hence

$$x_i = x(i,t).$$

Using Taylor expansions

$$\begin{aligned} x_{i+\Delta i} &= x_i + \frac{\partial x}{\partial i}\Delta i + \frac{1}{2}\frac{\partial^2 x}{\partial i^2}\Delta i^2 + O(\Delta i^3), \\ x_{i-\Delta i} &= x_i - \frac{\partial x}{\partial i}\Delta i + \frac{1}{2}\frac{\partial^2 x}{\partial i^2}\Delta i^2 + O(\Delta i^3). \end{aligned} \tag{2.21}$$

Substituting equation (2.21) in to (2.20) and using a Taylor expansion again for $\hat{F}$ yields

$$\begin{aligned} \hat{\mu}\frac{\partial x}{\partial t} = \hat{F}(\frac{\partial x}{\partial i}\Delta i) + \hat{F}'\left(\frac{\partial x}{\partial i}\Delta i\right)\left(-\frac{1}{2}\frac{\partial^2 x}{\partial i^2}\Delta i^2 + O(\Delta i^3)\right) + O(\Delta i^4) \\ - \hat{F}(\frac{\partial x}{\partial i}\Delta i) - \hat{F}'\left(\frac{\partial x}{\partial i}\Delta i\right)\left(\frac{1}{2}\frac{\partial^2 x}{\partial i^2}\Delta i^2 + O(\Delta i^3)\right) + O(\Delta i^4). \end{aligned}$$

It is assumed that the damping coefficient scales like

$$\hat{\mu} = \mu \Delta i,$$

and that the force between two volume element scales inversely with Δi , hence

$$\hat{F}(x\Delta i) = \frac{F(x)}{\Delta i}.$$

After cancelation, substitution yields

$$\mu \frac{\partial x}{\partial t} = -\frac{\partial^2 x}{\partial i^2} F'\left(\frac{\partial x}{\partial i}\right) + O(\Delta i^2). \tag{2.22}$$

Using a coordinate transformation from the old independent i and t to new variables x and τ, the Jacobian matrix is

$$\begin{pmatrix} \frac{\partial x}{\partial i}|_t & \frac{\partial x}{\partial t}|_i \\ \frac{\partial \tau}{\partial i}|_t & \frac{\partial \tau}{\partial t}|_i \end{pmatrix} = \begin{pmatrix} \frac{\partial i}{\partial x}|_\tau & \frac{\partial i}{\partial \tau}|_x \\ \frac{\partial t}{\partial x}|_\tau & \frac{\partial t}{\partial \tau}|_x \end{pmatrix}^{-1}$$

$$= \frac{1}{\frac{\partial i}{\partial r}|_\tau \frac{\partial t}{\partial \tau}|_x - \frac{\partial i}{\partial \tau}|_x \frac{\partial t}{\partial x}|_\tau} \begin{pmatrix} \frac{\partial t}{\partial \tau}|_x & -\frac{\partial i}{\partial \tau}|_x, \\ -\frac{\partial t}{\partial x}|_\tau & \frac{\partial i}{\partial x}|_\tau \end{pmatrix}.$$

Letting $t = \tau$

$$dx = \frac{\partial x}{\partial i} di + \frac{\partial x}{\partial t} dt,$$

$$d\tau = \frac{\partial \tau}{\partial x} di + \frac{\partial \tau}{\partial t} dt,$$

$$\begin{pmatrix} dx \\ d\tau \end{pmatrix} = \begin{pmatrix} \frac{\partial x}{\partial \tau} & \frac{\partial x}{\partial t} \\ \frac{\partial \tau}{\partial x} & \frac{\partial x}{\partial t} \end{pmatrix} \begin{pmatrix} di \\ dt \end{pmatrix},$$

$$\left.\frac{\partial x}{\partial i}\right|_t = \frac{1}{(\frac{\partial i}{\partial x})|_\tau}, \tag{2.23}$$

$$\left.\frac{\partial x}{\partial t}\right|_i = -\frac{(\frac{\partial i}{\partial \tau})|_x}{(\frac{\partial i}{\partial x})|_\tau}. \tag{2.24}$$

Substituting equations (2.24) and (2.23) into equation (2.22) we obtain

$$\frac{\partial i}{\partial \tau} = \frac{-F'\left(\frac{1}{\frac{\partial i}{\partial x}}\right)}{\mu\left(\frac{\partial i}{\partial x}\right)^2}\frac{\partial^2 i}{\partial x^2}. \tag{2.25}$$

Defining

$$q(x,\tau) = \frac{\partial i(x,\tau)}{\partial x}, \tag{2.26}$$

differentiating both sides of equation (2.25) with respect to r, using the chain rule and cancelling terms yields

$$\frac{\partial q}{\partial \tau} = \frac{\partial}{\partial x}\left(\frac{-F'\left(\frac{1}{q}\right)}{\mu q^2}\frac{\partial q}{\partial x}\right). \tag{2.27}$$

This results describe the collective motion of cells in the one-dimensional chain via a nonlinear diffusion equation.

Murray et al. [49] shows how the continuum limit of equations (2.3) with a reaction term can be approximated by

$$\frac{\partial q}{\partial t} = \frac{\partial}{\partial x}\left(D(q)\frac{\partial q}{\partial x}\right) + rqH(q_c - q), \tag{2.28}$$

where $D(q)$ is a non-linear diffusion coefficient given by

$$D(q) = -\frac{F'(x=\frac{1}{q})}{\eta q^2}, \tag{2.29}$$

and $q(x,t)$ is the cell number density, x is the position, t is time.

2.2.4 Mathematical modelling of monolayer growth

In this section we focus specifically on a key mathematical model of monolayer growth.

In a study of a cell monolayer that exhibited contact inhibition of cell proliferation, Byrne and Drasdo [14] compared simulations of a discrete cell-based model, using a JKR(Johnson, Kendall and Roberts) force law, with a continuum model.
In the simulations, Byrne and Drasdo found that the proliferating monolayers exhibited travelling wave-like behaviour, in which cell density at the centre of the tissue was the contact inhibition density. Besides, they found there was a proliferating outer rim of cells that propagated at speed, c, and had constant width, ρ. Intriguingly, they found that the speed was inversely proportional to the proliferating rim width, i.e.

$$c \propto \frac{1}{\rho},$$

and that the wave speed in the asymptotic linear growth regime satisfies

$$c \propto \sqrt{r},$$

where r is the cell proliferation rate. We observe that, in this previous work, the ratio of the contact inhibition density to the equilibrium cell density was approximately $5/4$. Further, the mechanical time-scale was much faster than the proliferation time-scale

[25].

2.3 Review of relevant techniques

Here we describe a number of techniques that are used throughout this thesis.

2.3.1 Travelling wave analysis

Let $q(x,t)$ represent cell density, x represent spatial position and t represent time. Making the change of variables

$$z = x - ct, \tag{2.30}$$

a solution, q, is a travelling wave if it is time- independent in the travelling wave frame, i.e

$$q = q(z).$$

2.3.1.1 Travelling wave solution of Fisher equation

Consider the Fisher equation

$$\frac{\partial q}{\partial t} = D\frac{\partial^2 q}{\partial^2 x} + rq(1-q), \tag{2.31}$$

with boundary conditions

$$q(-\infty,t) = 1 \quad \text{and} \quad q(\infty,t) = 0. \tag{2.32}$$

Assume that $z = x - ct$, equation (2.31) transforms to the second order ODE

$$D\frac{d^2q}{dz^2} + c\frac{dq}{dz} + rq(1-q) = 0. \tag{2.33}$$

Rewriting as system of first order ODEs

$$\begin{aligned} \frac{du}{dz} &= v, \\ D\frac{dv}{dz} &= -cv - u(1-u). \end{aligned} \tag{2.34}$$

A steady state is observed at $(0,0)$ and $(1,0)$. By imposing that steady state at the origin is not a spiral (which is biologically not realistic as the density would be negative) . We obtain the condition

$$c > 2\sqrt{rD}. \tag{2.35}$$

2.3.2 Perturbation method

Perturbation theory is a technique used to develop approximate solutions to equations [32, 37, 57]. In this section we introduce the important notation and definitions used in an asymptotic expression using a simple example. We generally work with a few initial series terms and use the O notation to describes neglected terms in the series, i.e.

$$\sin(x) = w(x) + O(x^5) \quad \textbf{as} \quad x \to 0, \quad w(x) = x - \frac{x^3}{6}. \tag{2.36}$$

2.3.3 Method of lines

In this thesis the model given by equations ((1.2)-(1.6)) is solved using a Method of Lines. The Method of Lines is a technique in numerical methods that solve partial differential equations (PDEs) in which all but one dimension is discretised [62, 57]. To deal with the moving boundary condition, we transform to a Lagrangian form.

Letting

$$v = -\frac{D(q)}{q}\frac{\partial q}{\partial x},$$

then

$$\frac{\partial v}{\partial x} = -\frac{D(q)}{q}\frac{\partial^2 q}{\partial x^2} - (\frac{qD'(q) - D(q)}{q^2})(\frac{\partial q}{\partial x})^2.$$

Hence the material derivative is

$$\frac{Dq}{Dt} = -q\frac{\partial v}{\partial x} + rqH(q_c - q_0), \tag{2.37}$$

with

$$\frac{dx}{dt} = v.$$

Discretising the spatial domain by letting

$$x = \frac{i}{N}S_0, \quad i = 0...N,$$

equation (1.2) are discretised as follows

$$\frac{dq_1}{dt} = D(q_1)\left(\frac{q_2 - q_1}{(x_2 - x_1)^2}\right) + rq_1S(q_c - q_1), \tag{2.38}$$

$$\frac{dq_n}{dt} = D(q_i)\left(\left(\frac{-\frac{ds}{dt}\frac{q_i}{D(q_n)} - \frac{q_i - q_{i-1}}{x_i - x_{i-1}}}{x_i - x_{i-1}}\right) - \left(D(q_i)' - (D(q_i)/q_i)\right)\left(\frac{q_i - q_{i-1}}{x_i - x_{i-1}}\right)^2\right)$$
$$+ rq_n S(q_c - q_i), \tag{2.39}$$

$$\frac{dq_i}{dt} = D(q_i)\left(\frac{\frac{q_{i+1}-q_i}{x_{i+1}-x_i} - \frac{q_i - q_{i-1}}{x_i - x_{i-1}}}{\frac{x_{i+1}-x_i}{2}}\right)$$
$$-\left(D(q_i)' - (D(q_i)/q_i)\right)\left(\frac{q_{i+1} - q_{i-1}}{x_{i+1} - x_{i-1}}\right)^2 + rq_i S(q_c - q_i) \quad 1 < i < n. \tag{2.40}$$

Similarly

$$\begin{aligned}
\frac{dx_i}{dt} &= -\frac{D(q_i)}{q_i}\left(\frac{q_{i+1} - q_{i-1}}{x_{i+1} - x_{i-1}}\right) \quad 1 < i < n, \\
\frac{dx_i}{dt} &= -\frac{D(q_i)}{q_i}\left(\frac{q_i - q_{i-1}}{x_i - x_{i-1}}\right) \quad , i = n. \\
\frac{dx_i}{dt} &= 0, \quad i = 1.
\end{aligned} \tag{2.41}$$

The Heaviside function is approximated numerically by the function

$$S(x) = \frac{1}{2}(\tanh(\gamma x) + 1), \tag{2.42}$$

where γ is a parameter chosen to be large such that equation (2.42) is an approximation to the Heaviside function.

Throughout Chapter 3, 4 and 5, we apply the Method of Lines using this method and we will examine the numerical solution.

2.3.4 Shooting method

When the solution of an ordinary differential equation has to satisfy boundary conditions at more than one value of the independent variable, the main problem is known as a two-point boundary value problem. Typically, such problems require one to satisfy one of the boundary conditions and run some form of optimisation algorithm to identify a solution that satisfies both boundary conditions simultaneously. Such a process is known as a shooting method [57, 10].

Chapter 3

The model of constant diffusion

In this chapter we consider the continuum model given by equations (1.2)-(1.6), in the case where D is a constant.Consider the model given by

$$\frac{\partial q}{\partial t} = D\frac{\partial^2 q}{\partial x^2} + rqH(q_c - q), \tag{3.1}$$

with the boundary conditions given by

$$\left.\frac{\partial q}{\partial x}\right|_{x=0} = 0, \quad \left.\frac{\partial q}{\partial x}\right|_{x=s(t)} = -\frac{q(s(t),t)\frac{ds}{dt}}{D}, \tag{3.2}$$

where

$$\frac{ds}{dt} = k(a - \frac{1}{q}), \tag{3.3}$$

and the initial conditions satisfy

$$q(x,0) = f(x), \quad s(0) = s_0. \tag{3.4}$$

parameter	value	description	Unit	source
D	10	diffusion constant	$c.d^2.h^{-1}$	estimate
q_c	1.4	proliferation density threshold	$\frac{1}{c.d}$	Byrne and Drasdo [14]
k	100	spring constant	h^{-1}	estimate
r	$\log(2)/14$	growth rate	h^{-1}	Byrne and Drasdo [14]
a	1	resting spring length	$c.d.$	estimate
s_0	50	initial domain length	$c.d$	estimate
γ	1000	scaling of $H(q-q_c)$	$c.d$	estimate

Table 3.1: A table with model parameters. Unit length is taken to be one cell diameter $(c.d.) \sim 10\mu m$, unit of single mass $(c.m)$.

The layout of this chapter is as follows: in Section 3.1 we consider a simplified case in which the Robin boundary condition is replaced with a Dirichlet boundary condition; in Section 3.2 we consider the case with the Robin boundary condition; and in Section 3.3 we discuss the results.

3.1 A constant diffusion coefficient and Dirichlet boundary condition

In this section we replace the Robin boundary condition in equation (3.3) with the Dirichlet boundary condition

$$q(s(t),t) = \frac{1}{a}.$$

Hence, equations (3.1) transform to

$$\frac{\partial q}{\partial t} = D\frac{\partial^2 q}{\partial x^2} + rqH(q_c - q), \tag{3.5}$$

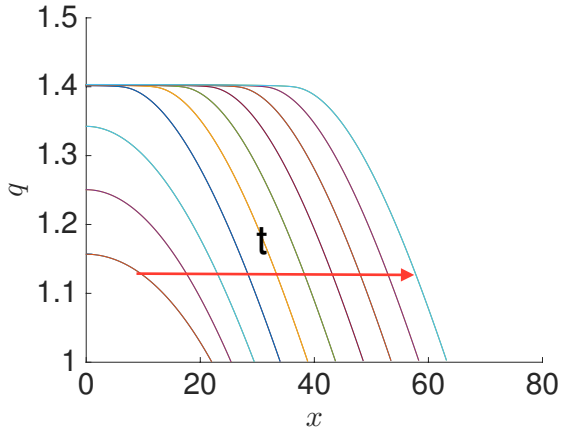

Figure 3.1: Numerical solution of equations (3.5)- (3.7). The cell density, q, is plotted against spatial position, x, at different times, t. See Table 3 for parameters values.

the boundary conditions are

$$\left.\frac{\partial q}{\partial x}\right|_{x=0} = 0, \quad q(s(t),t) = \frac{1}{a}, \quad \frac{ds}{dt} = -aD\left.\frac{\partial q}{\partial x}\right|_{x=s(t)}, \tag{3.6}$$

and the initial conditions are

$$q(x,0) = f(x), \quad s(0) = s_0. \tag{3.7}$$

3.1.1 Numerical solution

The numerical solutions of equations (3.5)- (3.7) was computed using the Method of Lines (see Section 2.3.3). Representative results are plotted in Figure 3.1. The numerical analysis is suggestive of a travelling wave solution with a constant front speed. Behind the wave front, there is a non-proliferating core of cells at density, q_c. At the front there is a proliferating rim of fixed width.

3.1.2 Phase plane solution

Upon introducing the travelling wave coordinate

$$z = x - ct,$$

where c is a constant wave speed, equations (3.5)-(3.7) transform to

$$-c\frac{dq}{dz} = D\frac{d^2q}{dz^2} + rqH(q_c - q), \tag{3.8}$$

and

$$\left.\frac{dq}{dz}\right|_{z\to-\infty} = 0, \quad q(0) = \frac{1}{a} \quad \text{and} \quad \left.\frac{dq}{dz}\right|_{z=0} = -\frac{c}{aD}. \tag{3.9}$$

Translating the travelling reference frame so that initial conditions are defined at the origin, I define

$$\bar{z} = z - \rho.$$

Letting

$$u = q, \quad v = \frac{dq}{d\bar{z}}, \tag{3.10}$$

equations (3.8)–(3.9) transform to the first order ODE system

$$\begin{aligned} \frac{du}{d\bar{z}} &= v, \\ \frac{dv}{d\bar{z}} &= \frac{1}{D}\left(-cv - ru\right), \end{aligned} \tag{3.11}$$

and the initial conditions are

$$u(0) = \frac{1}{a} \quad \text{and} \quad v(0) = 0. \tag{3.12}$$

Defining ρ such that

$$u(\rho) = q_c, \tag{3.13}$$

for a given initial guess for c we seek a solution that satisfies

$$v(\rho) = -\frac{c}{aD}, \tag{3.14}$$

by minimising the function

$$E(c) = \left(v(\rho) + \frac{c}{aD} \right)^2. \tag{3.15}$$

Using a shooting method, a value of c is identified that minimises equation (3.15). In Figure 3.2 we plot representative results. In Figure 3.2 (a) we plot the error defined in equation (3.15) against a range of values for the unknown wave speed, c. Note that there is a unique minimum. In Figure 3.2 (b) we plot the solution of equations (3.11) in the phase plane. Note that solution trajectories originate at the point $(q_c, 0)$ and end at the boundary condition $(\frac{1}{a}, \frac{-cq_0}{D})$. In Figure 3.2 (c) we plot the computed wave speed as a function of the model parameter q_c. Note that the wave speed increases with density threshold q_c. In Figure 3.2 (d) we plot the computed wave speed as a function of the model parameter r. Note that wave speed increases with proliferation rate.

The goal of the rest of this section is to derive approximate expressions for the wave speed and proliferating rim width.

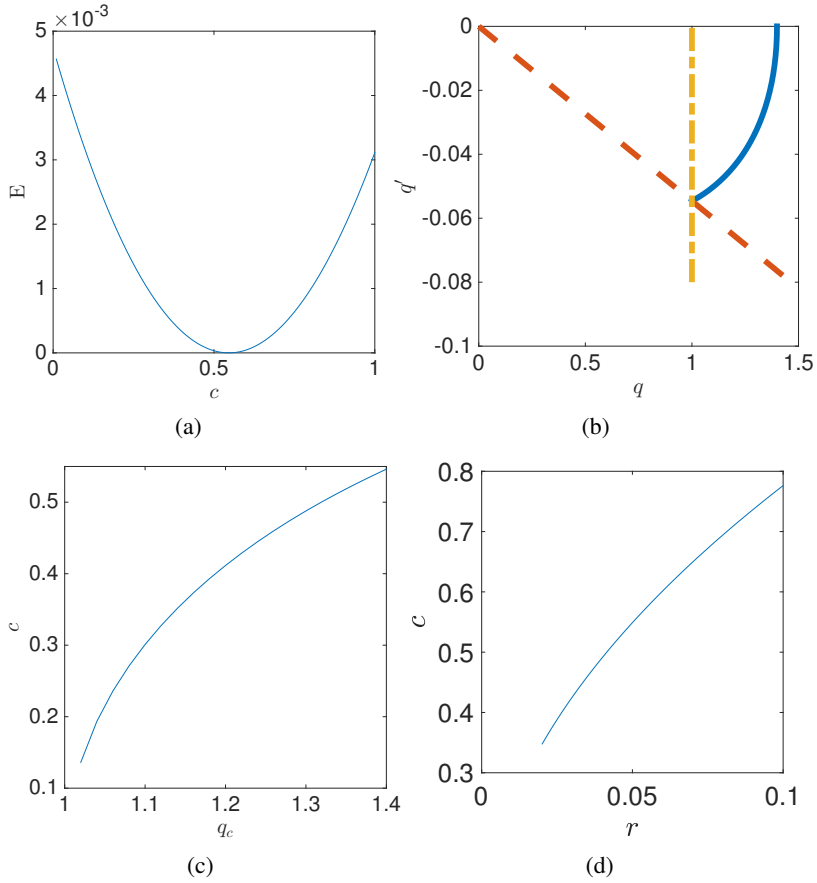

Figure 3.2: Using a shooting method to compute wave speed, c. (a) A unique wave speed, c^*, is identified. Error, $E(c)$, is plotted against wave speed, c (see equation (3.15)). (b) A representative phase plane trajectory is presented for wave speed $c = c^*$. q' is plotted against q. Equations (3.8) were solved numerically (blue line). Dashed and dot-dashed lines represent boundary conditions (3.13) and (3.14), respectively. (c) The wave speed, c, is plotted against the proliferation threshold density, q_c. (d) The wave speed, c, is plotted against proliferation rate, r. Parameter values as in Table 3.

3.1.3 Exact solution

As a consequence of the simplifying assumptions of a Dirichlet boundary condition and a constant diffusion coefficient, equations (3.8)-(3.9) are linear and an exact solution can be constructed.

Defining ρ to be the value of the travelling wave coordinate upon which

$$q(-\rho) = q_c, \tag{3.16}$$

we construct solutions in the domains $z \in [-\infty, -\rho]$ (Region I) and $z \in [-\rho, 0]$ (Region 2 see Figure 3.3).

In Region I, where $z < -\rho$,

$$-c\frac{dq_l}{dz} = D\frac{d^2q_l}{dz^2}, \tag{3.17}$$

the solution is

$$q_l(z) = A_1 \exp\left(-\frac{c}{D}z\right) + A_2, \tag{3.18}$$

where A_1 and A_2 are integration constants.

Applying boundary conditions (3.6) yields

$$A_1 = 0 \qquad \text{and} \quad A_2 = q_c. \tag{3.19}$$

Hence the solution for Region I is

$$q_1(z) = q_c. \tag{3.20}$$

In Region II, where $z > -\rho$, equations (3.8) are given by

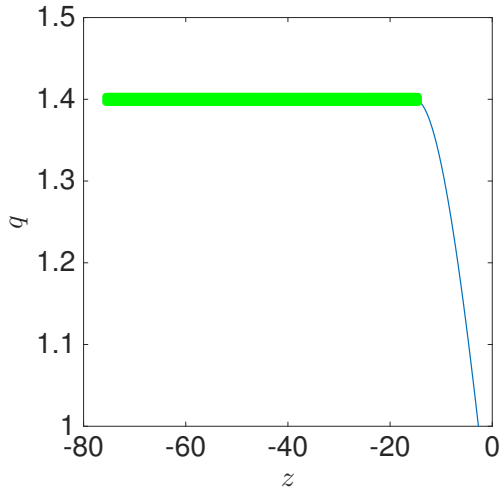

Figure 3.3: A schematic diagram of the model solution. The green line denotes Region 1 ($z < -\rho$) and the blue line denotes Region 2 ($z > -\rho$).

$$-c\frac{dq_r}{dz} = D\frac{d^2q_r}{dz^2} + rq_r. \tag{3.21}$$

Assuming that the solution and its derivative are continuous on the boundary $z = -\rho$, the boundary conditions are

$$q_r(-\rho) = q_c, \tag{3.22}$$

$$q_r^{'}(-\rho) = 0, \tag{3.23}$$

$$q_r(0) = \frac{1}{a}, \tag{3.24}$$

$$q_r^{'}(0) = -\frac{c}{aD}. \tag{3.25}$$

Letting

$$q_r(z) = \exp(\gamma z),$$

the characteristic polynomial equation for equation (3.21) is

$$D\gamma^2 + c\gamma + r = 0. \tag{3.26}$$

Hence,

$$\gamma = \frac{-c \pm \sqrt{c^2 - 4Dr}}{2D}. \tag{3.27}$$

The general solution to equations (3.21) - (3.25) is

$$q_r(z) = e^{\delta z}(A_3 \cos(\beta z) + A_4 \sin(\beta z)), \tag{3.28}$$

where A_3 and A_4 are integration constants and

$$\delta = -\frac{c}{2D} \quad \text{and} \quad \beta = \frac{\sqrt{4rD - c^2}}{2D}. \tag{3.29}$$

Applying boundary condition (3.24) yields

$$A_3 = \frac{1}{a}. \tag{3.30}$$

Applying boundary condition (3.25) yields

$$q'(0) = A_4\beta + \delta A_3 = -\frac{c}{aD}. \tag{3.31}$$

Substituting for A_3 from equation (3.30) into equation (3.31) yields

$$A_4 = -\frac{1}{a\beta}\left(\frac{c}{D} + \delta\right). \tag{3.32}$$

Noting from equation (3.29) that

$$\frac{c}{D} = -2\delta, \tag{3.33}$$

$$A_4 = \frac{\delta}{a\beta}. \tag{3.34}$$

Applying boundary condition (3.23) yields

$$0 = \delta A_3 \cos(\beta\rho) - \delta A_4 \sin(\beta\rho) + \beta A_3 \sin(\beta\rho) + \beta A_4 \cos(\beta\rho). \tag{3.35}$$

Now we need to find the value for $\sin(\beta\rho)$ and $\cos(\beta\rho)$. Recall that the tangent function can be defined as

$$\tan(\beta\rho) = \frac{\sin(\beta\rho}{\cos(\beta\rho)}.$$

hence we rearranging equation (3.35)

$$\tan(\beta\rho) = \frac{(\beta A_4 + \delta A_3)}{\beta A_3 - \delta A_4}. \tag{3.36}$$

Substituting for A_3 and A_4 from equations (3.30) and (3.32), respectively, into equation (3.36) yields

$$\tan(\beta\rho) = \frac{2\delta\beta}{\beta^2 - \delta^2}. \tag{3.37}$$

Applying Pythagoras theorem, the value of hypotenuse is

$$h = \sqrt{(\beta^2 - \delta^2)^2 + 4\delta^2\beta^2} = \delta^2 + \beta^2,$$

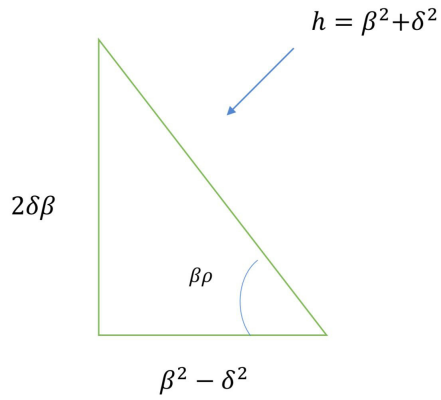

Figure 3.4: A graphical representation the values of triangle side using Pythagoras theorem equation (see equation (3.37)).

and

$$\cos(\beta\delta) = \frac{\beta^2 - \delta^2}{\delta^2 + \beta^2} \quad \text{and} \quad \sin(\beta\delta) = \frac{2\delta\beta}{\delta^2 + \beta^2}. \tag{3.38}$$

Applying boundary condition (3.22) yields

$$q(-\rho) = e^{-\delta\rho}\left(A_3\cos(\beta\rho) + A_4\sin(\beta\rho)\right) = q_c. \tag{3.39}$$

Substituting for A_3, A_4, $\cos(\beta\rho)$ and $\sin(\beta\rho)$ from equations (3.30), (3.32) and (3.38), respectively, yields

$$e^{-\delta\rho}\left(\left(\frac{1}{a}\right)\left(\frac{\beta^2 - \delta^2}{\delta^2 + \beta^2}\right) + \left(\frac{\delta}{a\beta}\right)\left(\frac{2\delta\beta}{\delta^2 + \beta^2}\right)\right) = q_c. \tag{3.40}$$

Upon cancellation

$$e^{-\delta\rho} = aq_c. \tag{3.41}$$

Hence

$$\rho = -\frac{1}{\delta}\ln(q_c a). \tag{3.42}$$

Substituting for δ from equation (3.29) yields

$$\rho = \frac{2D}{c}\ln(q_c a). \tag{3.43}$$

Returning to equation (3.37), note that

$$\beta\rho = \frac{\sqrt{4rD-c^2}}{2D}\frac{2D}{c}\ln(q_c a) = \hat{x}\ln(q_c a).$$

Hence the left-hand side of equation (3.37) can be written

$$\tan(\hat{x}\ln(q_c a)), \tag{3.44}$$

where

$$\hat{x} = \frac{\sqrt{4rD-c^2}}{c}. \tag{3.45}$$

Substituting for δ and β, the right-hand side of equation (3.37) can be written as

$$\frac{2\left((-\frac{c}{2D})(\frac{\sqrt{4rD-c^2}}{2D})\right)}{(\frac{4rD-c^2}{4D^2})-(\frac{c^2}{4D^2})}.$$

Simplifying yields

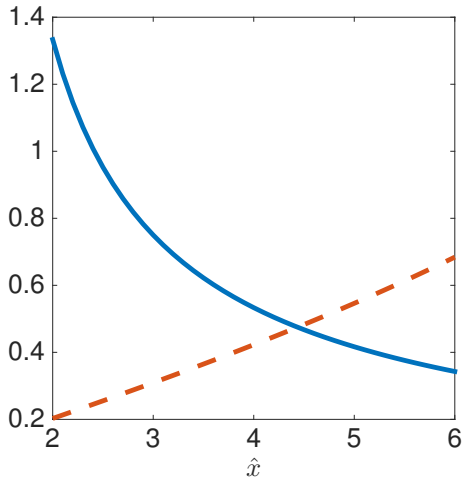

Figure 3.5: A graphical representation of the transcendental equation (3.47). The left- (dashed lines) and right- (solid lines) hand sides of equation (3.47) are plotted against $\hat{x}$. Here $\varepsilon = 0.1$.

$$\frac{\hat{x}}{\frac{1}{2}(\hat{x}^2 - 1)}. \tag{3.46}$$

Equating equations (3.44) and (3.46) yields the transcendental equation

$$\tan(\hat{x}\varepsilon) = \frac{\hat{x}}{\frac{1}{2}(\hat{x}^2 - 1)}, \tag{3.47}$$

where

$$\varepsilon = \ln(q_c a), \tag{3.48}$$

Rearranging equation (3.45) yields

$$c = \frac{2rD}{\sqrt{\hat{x}^2 + 1}}. \tag{3.49}$$

Note that the parameter ε represents the log of ratio of the density at which prolifera-

tion stops to the equilibrium density. As previous models of contact inhibition of cell proliferation have assumed $\varepsilon = 0.3$ [14], we seek a power series solution of equation (3.49). Using a Taylor series

$$\tan(\hat{x}\varepsilon) = \varepsilon\hat{x} + \frac{1}{3}\varepsilon^3\hat{x}^3 + O(\varepsilon^5),$$

hence equation (3.47) can be approximated as

$$\varepsilon\hat{x} + \frac{1}{3}\varepsilon^3\hat{x}^3 + o(\varepsilon\hat{x})^5 = \frac{\hat{x}}{\frac{1}{2}(\hat{x}^2 - 1)}.$$

Upon rearrangement

$$\frac{1}{2}(\hat{x}^2 - 1)\varepsilon\hat{x} + \frac{1}{6}\hat{x}^3\varepsilon^3(\hat{x}^2 - 1) = \hat{x} + O(\varepsilon^5),$$

and we obtain, at leading order, the quadratic equation

$$\hat{x}^2\varepsilon - \varepsilon + \frac{1}{3}\hat{x}^4\varepsilon^3 - \frac{1}{3}\hat{x}^2\varepsilon^3 = 2.$$

Defining

$$z = \hat{x}^2,$$

we obtain

$$z^2\varepsilon^2 + z(3 - \varepsilon^2) - \left(3 + \frac{6}{\varepsilon}\right) = 0. \tag{3.50}$$

The positive root of the quadratic equation (3.50) is

$$z = \frac{-(3 - \varepsilon^2) + 3\sqrt{1 + \frac{8\varepsilon}{3}\left(1 + \frac{1}{4}\varepsilon + \frac{3}{72}\varepsilon^3\right)}}{2\varepsilon^2}. \tag{3.51}$$

Applying the binomial expansion

$$(1+x)^n = 1+nx+\frac{n(n-1)}{2}x^2+\frac{n(n-1)(n-2)}{6}x^3+O(x^4),$$

the term inside the square root of equation (3.51) is approximated as

$$\sqrt{1+\frac{8\varepsilon}{3}\left(1+\frac{1}{4}\varepsilon+\frac{3}{72}\varepsilon^3\right)} = 1+\frac{4}{3}\varepsilon-\frac{5}{9}\varepsilon^2+O(\varepsilon^3). \tag{3.52}$$

Substituting in equation (3.51) gives

$$z = \frac{2}{\varepsilon}-\frac{1}{3} = \frac{2}{\varepsilon}(1-\frac{\varepsilon}{6}+o(\varepsilon^2)).$$

Hence

$$\hat{x} = \sqrt{\frac{2}{\varepsilon}}\left(1-\frac{\varepsilon}{6}+o(\varepsilon^2)\right)^{1/2}. \tag{3.53}$$

Now we derive an interesting formula for wave speed, c. Upon substitution for $\hat{x}$ from equation (3.53), we obtain

$$\begin{aligned} c &= 2\sqrt{rD}\left(\sqrt{\frac{\varepsilon}{2}}(1+\frac{1}{12}\varepsilon)-(\sqrt{\frac{2}{\varepsilon}})^{3/2}(1+\frac{\varepsilon}{4})+O(\varepsilon^2)\right), \\ &= 2\sqrt{rD}\sqrt{\frac{\varepsilon}{2}}\left(1+\frac{1}{12}\varepsilon-\frac{\varepsilon}{4}+O(\varepsilon^2)\right). \end{aligned} \tag{3.54}$$

Upon rearrangement, we obtain

$$c = \sqrt{2rD\varepsilon}\left(1-\frac{1}{6}\varepsilon+O(\varepsilon^2)\right). \tag{3.55}$$

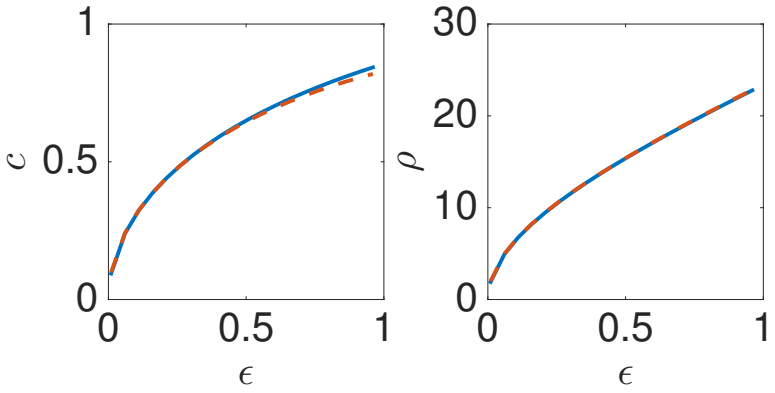

(a) (b)

Figure 3.6: Comparing numerical and asymptotic approximations to the wave speed and proliferating rim width. The wave speed, c, is plotted against ε (equation (3.55)). The proliferation width, ρ, is plotted against ε (equation (3.56)). Dashed lines - shooting method, solid lines - asymptotic solution. See Table 3 for parameter values.

Substituting for c in equation (3.43) yields

$$\rho = \sqrt{\frac{2\varepsilon D}{r}}\left(1+\frac{1}{6}\varepsilon+O(\varepsilon^2)\right). \tag{3.56}$$

In Figure 3.6 numerical solution of equations (3.6) are compared with the asymptotic formulae given by equations (3.55) and (3.56). Note the excellent agreement for biologically relevant values of the parameter ε. These results show that in the case of a constant diffusion coefficient with a Dirichlet boundary condition, asymptotic expressions for the wave speed, c, and the proliferating rim width, ρ, can be obtained for biologically relevant parameters values.

Note that the wave speed is less than that obtained in a classical analysis of the Fisher equation [22]. This is possible because in this case the domain on which the travelling wave front is defined is semi-infinite. In fact, it can be shown that the origin is a stable spiral but this does not lead to minimum wave speed because the boundary condition is not enforced at $q = 0$.

Note also that the relationship found between c and ρ is precisely that observed in simulating by Byrne and Drasdo [14]. However, whilst Byrne and Drasdo simulate force of a discrete model to empirically infer their result, here we derive a solution.
This results its new in our knowledge there is no research study has been done finding the approximate solution for wave speed and proliferation width ρ.

3.1.4 Perturbation solution

Perturbation methods, such as those introduced in (section 2.3.2), are particularly useful in cases where exact solutions cannot be defined. As later in this thesis we will consider problems that do not have an exact solution, in this section we use perturbation theory to construct approximate solutions.
Making the change of independent variable

$$y = \frac{z}{\rho}, \tag{3.57}$$

equation (3.5) transforms to

$$-c\rho q' = Dq'' + r\rho^2 q, \tag{3.58}$$

and the boundary conditions are given by

$$q(-1) = q_c, \quad q'(-1) = 0, \quad q(0) = \frac{1}{a} \quad \text{and} \qquad q'(0) = -\frac{c\rho}{aD}. \tag{3.59}$$

Following the analysis in Section 3.1.3, we define

$$q_c = \frac{1}{a}e^{\varepsilon}, \tag{3.60}$$

and seek asymptotic solutions of equations (3.58)-(3.59) of the form

$$\begin{aligned} c &= c_0\varepsilon^{1/2} + c_1\varepsilon^{3/2} + O(\varepsilon^2), \\ \rho &= \rho_0\varepsilon^{1/2} + \rho_1\varepsilon^{3/2} + O(\varepsilon^2), \\ q &= q_0(y) + q_1(y)\varepsilon + q_2(y)\varepsilon^2 + O(\varepsilon^2). \end{aligned} \tag{3.61}$$

Substituting in equation (3.58), we obtain

$$\begin{aligned} -(c_0\varepsilon^{1/2} + c_1\varepsilon^{3/2})(\rho_0\varepsilon^{1/2} + \rho_1\varepsilon^{3/2})(q_0'(y) + q_1'(y)\varepsilon + q_2'(y)\varepsilon^2) = D(q_0''(y) \\ + q_1''(y)\varepsilon + q_2''(y)\varepsilon^2) + r(\rho_0\varepsilon^{1/2} + \rho_1\varepsilon^{3/2})^2(q_0 + \varepsilon q_1 + \varepsilon^2 q_2)). \end{aligned} \tag{3.62}$$

Substituting for q in boundary condition (3.60) yields

$$q_0(-1) + \varepsilon q_1(-1) + O(\varepsilon^2) = \frac{1}{a}e^{\varepsilon},$$

which, after applying the Taylor expansion on the right-hand side, yields

$$q_0(-1) + \varepsilon q_1(-1) + \varepsilon^2 q_2(-1) + O(\varepsilon^3) = \frac{1}{a}\left(1 + \varepsilon + \frac{\varepsilon^2}{2}\right) + O(\varepsilon^3). \tag{3.63}$$

Noting that

$$q'(y) = q_0'(y) + \varepsilon q_1'(y) + O(\varepsilon^2),$$

the other boundary condition transform to

$$\begin{aligned} q_0'(-1) + \varepsilon q_1'(-1) + \varepsilon^2 q_2'(-1) &= 0, \\ q_0(0) + \varepsilon q_1(0) + \varepsilon^2 q_2(0) &= \frac{1}{a}, \\ q_0'(0) + \varepsilon q_1'(0) + \varepsilon^2 q_2'(0) &= -\frac{1}{aD}(c_0\rho_0\varepsilon + (c_1\rho_0 + c_0\rho_1)\varepsilon^2). \end{aligned} \tag{3.64}$$

At $O(1)$

$$q_0'' = 0, \tag{3.65}$$

with the boundary conditions given by

$$q_0(-1) = \frac{1}{a}, \quad q_0(0) = \frac{1}{a} \quad q_0'(-1) = 0 \quad \text{and} \quad q_0'(0) = 0. \tag{3.66}$$

The general solution to equation (3.65) is

$$q_0(y) = A_0 y + B_0, \tag{3.67}$$

where A_0 and B_0 are integration constants.

Application of boundary conditions (3.66) yields

$$A_0 = 0 \quad \text{and} \quad B_0 = \frac{1}{a}. \tag{3.68}$$

Hence

$$q_0(y) = \frac{1}{a}.$$

At $O(\varepsilon)$

$$Dq_1'' + \frac{r\rho_0^2}{a} = 0, \tag{3.69}$$

and the boundary conditions are

$$q_1(-1) = \frac{1}{a}, \tag{3.70}$$

$$q_1'(-1) = 0, \tag{3.71}$$

$$q_1(0) = 0, \tag{3.72}$$

$$q_1'(0) = -\frac{c_0\rho_0}{aD}. \tag{3.73}$$

Integrating equation (3.69) yields

$$q_1'(y) = -\frac{r\rho_0^2}{aD}y + A_1, \tag{3.74}$$

and a further integration yields

$$q_1(y) = -\frac{r\rho_0^2}{2aD}y^2 + A_1 y + B_1, \tag{3.75}$$

where A_1 and B_1 are integration constants.

Application of boundary condition (3.72) yields

$$B_1 = 0. \tag{3.76}$$

Application of boundary condition (3.73) yields

$$A_1 = -\frac{c_0\rho_0^2}{aD}, \tag{3.77}$$

and application of boundary condition (3.71) yields

$$A_1 = -\frac{r\rho_0^2}{aD}. \tag{3.78}$$

Equating equations (3.77) and (3.78) yields

$$c_0 = r\rho_0. \tag{3.79}$$

Application of boundary condition (3.70) yields

$$-\frac{r\rho_0^2}{2Da} - A_1 = \frac{1}{a}. \tag{3.80}$$

Substituting for A_1 from equation (3.78) yields

$$-\frac{r\rho_0^2}{2Da} + \frac{r\rho_0^2}{aD} = \frac{1}{a},$$

Hence, taking the positive root,

$$\rho_0 = \sqrt{\frac{2D}{r}}. \tag{3.81}$$

Substituting equation (3.81) into equation (3.79) yields

$$c_0 = \sqrt{2Dr}. \tag{3.82}$$

Upon simplification we find

$$A_1 = -\frac{c_0\rho_0}{aD} = -\frac{2}{a}. \tag{3.83}$$

Hence the solution to equations (3.69)-(3.73) is

$$c_0 = \sqrt{2Dr}, \quad \rho_0 = \sqrt{\frac{2D}{r}} \quad \text{and} \quad q_1(y) = -\frac{y(y+2)}{a}. \tag{3.84}$$

Note that at leading order in the case of constant diffusion coefficient and a Dirichlet

boundary condition, the wavefront can be approximated as being a quadratic function.

At $O(\varepsilon^2)$

$$-c_0\rho_0 q_1' = Dq_2'' + 2\rho_0\rho_1\left(\frac{1}{a}\right)r + q_1\rho_0^2 r, \tag{3.85}$$

and the boundary conditions are

$$q_2(-1) = \frac{1}{2a}, \tag{3.86}$$

$$q_2'(-1) = 0, \tag{3.87}$$

$$q_2(0) = 0, \tag{3.88}$$

$$q_2'(0) = -\left(\frac{\rho_1 c_0 + \rho_0 c_1}{aD}\right). \tag{3.89}$$

Substituting for c_0 and ρ_0 from equation (3.84) into equation (3.85) yields

$$q_2''(y) = \frac{1}{a}\left(y^2 + 8y + \left(4 - 2\sqrt{\frac{2r}{D}}\rho_1\right)\right). \tag{3.90}$$

Integration of equation (3.90) yields

$$q_2'(y) = \frac{1}{a}\left(\frac{2}{3}y^3 + 4y^2 + \left(4 - 2\sqrt{\frac{2r}{D}}\rho_1\right)y\right) + A_2, \tag{3.91}$$

and a further integration yields

$$q_2(y) = \frac{1}{a}\left(\frac{1}{6}y^4 + \frac{4}{3}y^3 + \left(4 - 2\sqrt{\frac{2r}{D}}\rho_1\right)\frac{y^2}{2}\right) + A_2 y + B_2, \tag{3.92}$$

where A_2 and B_2 are integration constants.

Application of boundary condition (3.86) yields, after rearrangement,

$$A_2 = \frac{1}{a}\left(\frac{1}{3} - \sqrt{\frac{2r}{D}}\rho_1\right). \tag{3.93}$$

Application of boundary condition (3.88) yields

$$B_2 = 0, \tag{3.94}$$

application of boundary condition (3.87) yields, after rearrangement,

$$A_2 = \frac{1}{a}\left(\frac{2}{3} - 2\sqrt{\frac{2r}{D}}\rho_1\right). \tag{3.95}$$

Equating equations (3.93) and (3.95) yields

$$\frac{1}{3} - \sqrt{\frac{2r}{D}}\rho_1 = \frac{2}{3} - 2\sqrt{\frac{2r}{D}}\rho_1,$$

hence

$$\rho_1 = \frac{1}{6}\sqrt{\frac{D}{r}}. \tag{3.96}$$

Application of boundary condition (3.89) yields

$$A_2 = -\left(\frac{\rho_1 c_0 + \rho_0 c_1}{aD}\right). \tag{3.97}$$

Substituting for c_0 and ρ_0 from equations (3.84) into equation (3.97) yields

$$A_2 = -\left(\frac{\rho_1\sqrt{2rD} + c_1\sqrt{\frac{2D}{r}}}{aD}\right). \tag{3.98}$$

Rearranging and substituting for ρ_1 from equation (3.96) yields

$$c_1 = -\frac{1}{6}\sqrt{2rD}. \tag{3.99}$$

Substituting for ρ_1 from equation (3.96) into equation (3.93) yields

$$A_2 = 0. \tag{3.100}$$

Hence the solution to equation (3.85)-(3.89) is

$$\rho_1 = \frac{1}{6}\sqrt{\frac{D}{r}}, \quad c_1 = -\frac{1}{6}\sqrt{2rD} \quad \text{and} \quad q_2(y) \quad = \frac{1}{a}\left(\frac{1}{6}y^2 + \frac{4}{3}y + \frac{5}{3}\right)y^2. \tag{3.101}$$

Hence, the asymptotic solution takes the form

$$\begin{aligned} q(y) &= \frac{1}{a}\left(1 - y(y+2)\varepsilon + y^2\left(\frac{1}{6}y^2 + \frac{4}{3}y + \frac{5}{3}\right)\varepsilon^2 + O(\varepsilon^3)\right), \\ c &= \sqrt{2rD\varepsilon}\left(1 - \frac{1}{6}\varepsilon + O(\varepsilon^2)\right), \\ \rho &= \sqrt{\frac{2D\varepsilon}{r}}\left(1 + \frac{1}{6}\varepsilon + O(\varepsilon^2)\right). \end{aligned} \tag{3.102}$$

Note that the wave speed and proliferation rim width expansions takes the same form as equations (3.55) and (3.56), respectively. The form for the cell density, q, is an expansion of the trigonometric form for q given by equation (3.102). In this section we have shown that Perturbation Theory can be applied in order to derive accurate

approximation to the propagation speed and proliferating rim width of a proliferating monolayer in the case of a constant diffusion coefficient and a Dirichlet boundary condition.

3.2 A constant diffusion coefficient and a Robin boundary condition

In this section we reintroduce boundary condition (3.6) but still retain the simplifying assumption that D is constant. Without loss of generality we let D take the form

$$D = ka^2,$$

in equations (1.2)-(1.6) and obtain

$$\frac{\partial q}{\partial t} = ka^2 \frac{\partial^2 q}{\partial x^2} + rqH(q_c - q), \tag{3.103}$$

with boundary conditions

$$\left.\frac{\partial q}{\partial x}\right|_{x=0} = 0, \quad \text{and} \quad \left.\frac{\partial q}{\partial x}\right|_{x=s(t)} = -\frac{ds}{dt}\frac{q(s(t),t)}{ka^2}. \tag{3.104}$$

The moving boundary, $s(t)$, satisfies

$$\frac{ds}{dt} = k\left(a - \frac{1}{q(s(t),t)}\right), \tag{3.105}$$

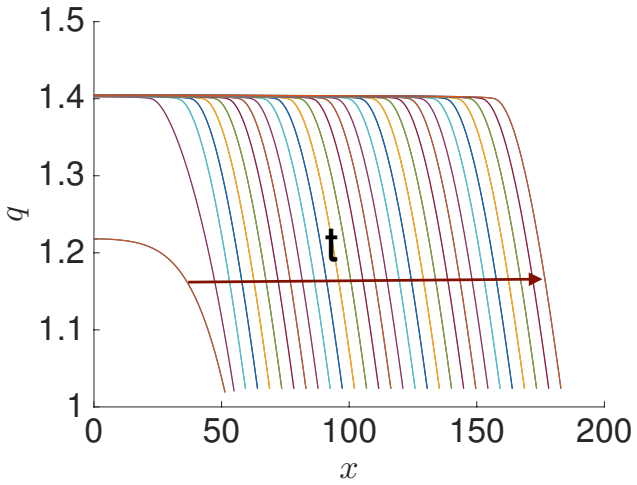

Figure 3.7: Numerical solution of equations (3.103)- (3.106). The cell density, q, is plotted against spatial position, x, at different times, t. See Table 3 for parameters values.

and the initial conditions satisfy

$$q(x,0) = f(x), \quad s(0) = s_0. \tag{3.106}$$

3.2.1 Numerical solution

The numerical solutions of equations (3.103)- (3.106) was computed using the Method of Lines (see Section 2.3.3). The results are showed in Figure 3.7. The numerical analysis is suggestive of a travelling wave solution with a constant front speed. We can clearly see that behind the wave front there is a non-proliferating core of cells at density, q_c. At the front there is a proliferating rim of fixed width that propagates with a constant wave speed. Note that unlike in Figure 3.7, the cell density, q, does not take the value $\frac{1}{a}$ on the boundary $y = 0$.

3.2.2 Phase plane solution

Following Section 3.1.2, we introduce the travelling wave coordinate

$$z = x - ct, \tag{3.107}$$

equation (3.103) transforms to

$$-cq' = ka^2 q'' + rq, \tag{3.108}$$

and boundary conditions (3.104) transform to

$$\begin{aligned} &q(-1) = q_c, \quad q'(-1) = 0, \\ &q(0) = \frac{1}{a\left(1 - \frac{c}{ak}\right)} \qquad \text{and} \quad q'(0) = -\frac{c}{ka^3}\left(\frac{1}{1 - \frac{c}{ak}}\right). \end{aligned} \tag{3.109}$$

To define initial conditions at the origin of the travelling wave coordinate, I define

$$\bar{z} = z - \rho.$$

Letting

$$u = q, \quad v = \frac{dq}{d\bar{z}}, \tag{3.110}$$

equations (3.108)-(3.109) transform to the ODE system

$$\begin{aligned} \frac{du}{d\bar{z}} &= v, \\ \frac{dv}{d\bar{z}} &= \frac{1}{a^2 k}\left(-cv - ru\right), \end{aligned} \tag{3.111}$$

and the initial conditions are

$$u(0) = q_c \qquad \text{and} \qquad v(0) = 0. \tag{3.112}$$

For a given initial guess for c, we numerically identify ρ such that

$$u(\rho) = \frac{1}{a\left(1 - \frac{c}{ak}\right)}. \tag{3.113}$$

We then seek a solution that satisfies

$$v(\rho) = -\frac{c}{ka^3}\left(\frac{1}{1 - \frac{c}{ak}}\right), \tag{3.114}$$

by minimising the function

$$E(c) = \left(v(\rho) + \frac{c}{ka^3}\left(\frac{1}{1 - \frac{c}{ak}}\right)\right)^2. \tag{3.115}$$

Using a shooting method a value of c is identified that minimises equation (3.115). In Figure 3.8 we plot representative results. In Figure 3.8 (a) we plot the error defined in equation (3.115) against a range of values for the unknown wave speed c. Note that there is a unique minimum. In Figure 3.8 (b) solution of equations (3.111) in the phase plane. Note that solution trajectories originate at point $(q_c, 0)$. In Figure 3.8 (c) we plot the computed wave speed as a function of the model parameters q_c. Note that wave speed increases with density threshold, q_c. In Figure 3.8 (d) we plot the computed

wave speed as a function of the model parameter r. Note that the wave speed increases with proliferation rate.

3.2.3 Perturbation solution

In this section we seek asymptotic solutions to equations (3.103)-(3.104). Making a change of independent variable

$$y = \frac{z}{\rho}, \tag{3.116}$$

equation (3.103) transforms to

$$-cq' = ka^2 q'' + r\rho^2 q, \tag{3.117}$$

and the boundary conditions (3.104) are given by

$$q(-1) = q_c, \tag{3.118}$$

$$q'(-1) = 0, \tag{3.119}$$

$$q(0) = \frac{1}{a\left(1 - \frac{c}{ak}\right)}, \tag{3.120}$$

$$q'(0) = -\frac{c\rho}{a^3 k}\left(\frac{1}{1 - \frac{c}{ak}}\right). \tag{3.121}$$

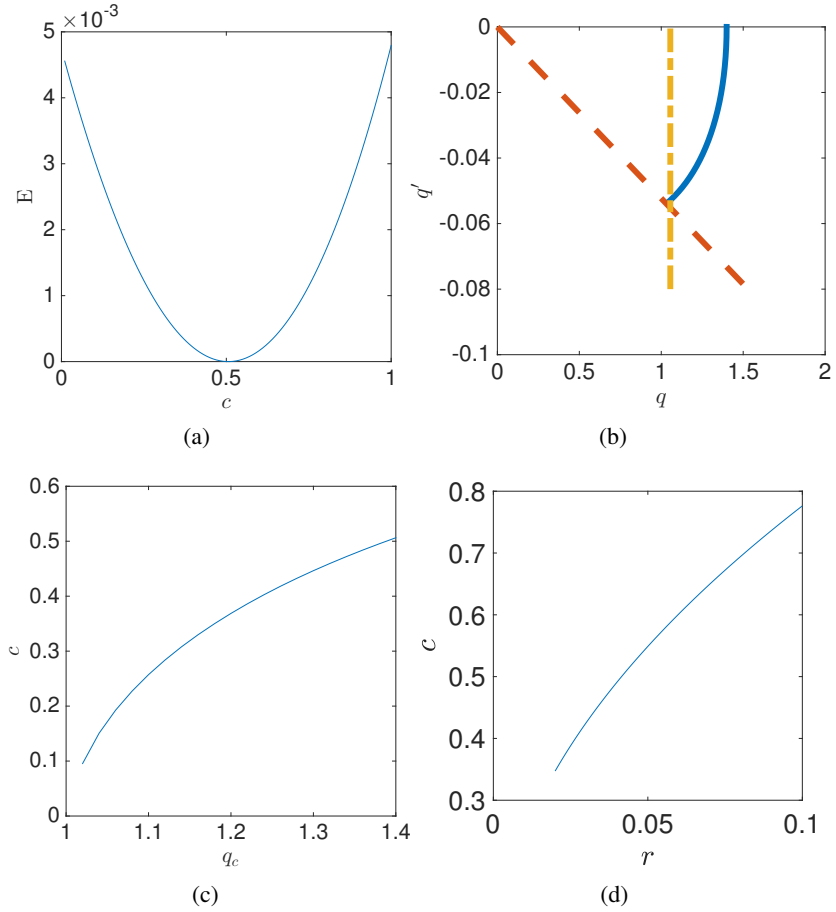

Figure 3.8: Using a shooting method to compute wave speed, c. (a) A unique wave speed, c^*, is identified using a shooting method. Error, $E(c)$, is plotted against wave speed, c (equation (3.115)). (b) A representative phase plane trajectory is presented for wave speed $c = c^*$. q' is plotted against q. Equations (3.111) were solved numerically (blue lines). Red and yellow lines represent boundary conditions (3.113) and (3.114), respectively. (c) The wave speed, c, is plotted against the proliferation threshold density, q_c. (d) The wave speed, c, is plotted against proliferation rate, r. Other parameter values as in Table 3.

Motivated by the exact solution derived in section 3.1.3, I define ε to be a small parameter

$$\varepsilon = \log(aq_c).$$

Hence

$$q_c = \frac{1}{a}e^{\varepsilon}. \tag{3.122}$$

Expanding boundary condition (3.118) yields

$$q(-1) = \frac{1}{a}e^{\varepsilon} = \frac{1}{a}\left(1+\varepsilon+\frac{1}{2}\varepsilon^2+O(\varepsilon^3)\right). \tag{3.123}$$

Hence we propose that q is an expansion in integer powers of ε, i.e

$$q = q_0 + \varepsilon q_1 + \varepsilon^2 q_2 + O(\varepsilon^3).$$

Substituting the proposed expansion for q in boundary condition (3.120) and rearranging, we obtain that c must also be an expansion in powers of ε, i.e.

$$c = c_0\varepsilon + \varepsilon^2 c_1 + O(\varepsilon^3).$$

Substituting the proposed expansions for c and q in boundary condition (3.121) and rearranging, we find that ρ must be an expansion of the form

$$\rho = \rho_0 + \varepsilon\rho_1 + O(\varepsilon^3).$$

Hence we seek asymptotic solutions of the form

$$\begin{aligned} c &= c_0\varepsilon + c_1\varepsilon^2 + O(\varepsilon^3), \\ \rho &= \rho_0 + \rho_1\varepsilon + O(\varepsilon^2), \\ q &= q_0(y) + q_1(y)\varepsilon + q_2(y)\varepsilon^2 + O(\varepsilon^3). \end{aligned} \tag{3.124}$$

Substitution of equations (3.124) into equation (3.117) yields

$$\begin{aligned} -(c_0\varepsilon + c_1\varepsilon^2)(\rho_0 + \rho_1\varepsilon)(q_0'(y) + q_1'(y)\varepsilon + q_2'(y)\varepsilon^2) = ka^2(q_0''(y) \\ +q_1''(y)\varepsilon + q_2''(y)\varepsilon^2) + r(\rho_0 + \rho_1\varepsilon)^2(q_0(y) + \varepsilon q_1(y) + q_2(y)\varepsilon^2). \end{aligned} \tag{3.125}$$

Following a dominant balance argument Bender and Orszag [7], at leading order we obtain

$$k\varepsilon q_1'' \sim r\rho_0, \tag{3.126}$$

which, assuming q_1'' is order one, yields the scaling relationship

$$\frac{r}{k} \propto \varepsilon.$$

Finally, assuming that the proliferation timescale ($\frac{1}{r}$, typically tens of hours) is much longer than the diffusion timescale, we assume that

$$\frac{r}{k} = \alpha^2\varepsilon, \tag{3.127}$$

where $\alpha \ll 1$. It is small because it comes from biological/physical considerations: the time scale of inter-cell forces is much shorter than that of proliferation. This a commonly made assumption in continuum models of tissue growth and can be observed in

discrete models of tissues.

Hence

$$r = \frac{\alpha^2 \varepsilon k}{2}.$$

and

$$\alpha = \sqrt{\frac{2r}{k\varepsilon}}. \tag{3.128}$$

Hence equation (3.125) transforms to

$$\begin{aligned} -(c_0\varepsilon + c_1\varepsilon^2)(\rho_0 + \rho_1\varepsilon)(q_0'(y) + q_1'(y)\varepsilon + q_2'(y)\varepsilon^2) = \\ ka^2(q_0''(y) + q_1''(y)\varepsilon + q_2''(y)\varepsilon^2) + \frac{\alpha^2\varepsilon k}{2}(\rho_0 + \rho_1\varepsilon)^2(q_0(y) + \varepsilon q_1(y) + q_2(y)\varepsilon^2). \end{aligned} \tag{3.129}$$

Substituting equation (3.124) into boundary conditions (3.118)-(3.119), and expanding the right-hand sides yields

$$\begin{aligned} q_0(-1) + \varepsilon q_1(-1) + \varepsilon^2 q_2(-1) &= \frac{1}{a}\left(1 + \varepsilon + \frac{1}{2}\varepsilon^2\right) + O(\varepsilon^3), \\ q_0'(-1) + \varepsilon q_1'(-1) + \varepsilon^2 q_2'(-1) &= 0. \end{aligned} \tag{3.130}$$

Noting that

$$\begin{aligned} \frac{1}{a(1-\frac{c}{ak})} &= \frac{1}{a}\left(\frac{1}{1-\frac{1}{ak}\left(c_0\varepsilon + c_1\varepsilon^2\right)}\right) \\ &= \frac{1}{a}\left(1 + \frac{1}{ka}\left(c_0\varepsilon + c_1\varepsilon^2\right) + \frac{1}{a^2k^2}\left(c_0^2\varepsilon^2\right)\right) \\ &= \frac{1}{a}\left(1 + \frac{c_0}{ak}\varepsilon + \left(\frac{c_1}{ak} + \frac{c_0^2}{a^2k^2}\right)\varepsilon^2\right), \end{aligned} \tag{3.131}$$

and

$$-\frac{c\rho}{a^3k}\left(\frac{1}{1-\frac{c}{ak}}\right) = -\frac{1}{a^3k}\left(\varepsilon c_0\rho_0+\varepsilon^2(c_1\rho_0+c_0\rho_1)\right)\left(1+\frac{c_0}{ak}\varepsilon+(\frac{c_0}{ak}+\frac{c_0^2}{a^2k^2})\varepsilon^2\right)$$
$$= -\frac{1}{a^3k}\left(c_0\rho_0\varepsilon+\left(c_1\rho_0+c_0\rho_1+\frac{c_0^2\rho_0}{ak}\right)\varepsilon^2\right), \tag{3.132}$$

the boundary conditions (3.120)-(3.121) are given by

$$q_0(0)+\varepsilon q_1(0)+\varepsilon^2 q_2(0) = \frac{1}{a}\left(1+\frac{c_0}{ak}\varepsilon+\left(\frac{c_1}{ak}+\frac{c_0^2}{a^2k^2}\right)\varepsilon^2\right),$$
$$q_0'(0)+\varepsilon q_1'(0)+\varepsilon^2 q_2'(0) = -\frac{1}{a^3k}\left(c_0\rho_0\varepsilon+\left(c_1\rho_0+\rho_1c_0+\frac{c_0^2\rho_0}{ak}\right)\varepsilon^2\right). \tag{3.133}$$

At $O(1)$

$$q_0'' = 0, \tag{3.134}$$

and the boundary conditions are

$$q_0(-1)=\frac{1}{a}, \quad q_0(0)=\frac{1}{a}, \quad q_0'(-1)=0 \quad \text{and} \quad q_0'(0)=0. \tag{3.135}$$

The general solution to equation (3.134) is

$$q_0 = A_0y+B_0, \tag{3.136}$$

where A_0 and B_0 are integration constants.

Application of boundary conditions (3.135) yields

$$A_0=0 \quad \text{and} \quad B_0=\frac{1}{a}. \tag{3.137}$$

Hence the solution is

$$q_0(y) = \frac{1}{a}. \tag{3.138}$$

At $O(\varepsilon)$

$$0 = ka^2 q_1'' + \frac{k\alpha^2}{2}\rho_0^2 q_0,$$

which, upon rearrangement and substitution for q_0, yields

$$q_1'' = -\frac{\alpha^2\rho_0^2}{2a^3}. \tag{3.139}$$

The boundary conditions are

$$q_1(0) = \frac{c_0}{a^2 k}, \tag{3.140}$$

$$q_1(-1) = \frac{1}{a}, \tag{3.141}$$

$$q_1'(-1) = 0, \tag{3.142}$$

$$q_1'(0) = -\frac{c_0\rho_0}{ka^3}. \tag{3.143}$$

Integrating equation (3.139) yields

$$q_1'(y) = -\frac{\alpha^2\rho_0^2}{2a^3}y + A_1. \tag{3.144}$$

The general solution to equation (3.139) is

$$q_1(y) = -\frac{\alpha^2\rho_0^2}{4a^3}y^2 + A_1 y + B_1, \tag{3.145}$$

where A_1 and B_1 are integration constants.

Application of boundary conditions (3.140) yields

$$B_1 = \frac{c_0}{a^2 k}. \tag{3.146}$$

Application of boundary conditions (3.141) yields

$$-\frac{\alpha^2\rho_0^2}{4a^3} - A_1 + B_1 = \frac{1}{a}.$$

Substituting for B_1 and rearranging yields

$$A_1 = -\frac{\alpha^2\rho_0^2}{4a^3} + \frac{c_0}{ka^2} - \frac{1}{a}. \tag{3.147}$$

Application of boundary conditions (3.142) yields

$$\frac{\alpha^2\rho_0^2}{2a^3} + A_1 = 0,$$

hence

$$A_1 = -\frac{\alpha^2\rho_0^2}{2a^3}. \tag{3.148}$$

Application of boundary conditions (3.143) yields

$$A_1 = -\frac{c_0\rho_0}{ka^3}. \tag{3.149}$$

Equating equations (3.148) and (3.149) and rearranging yields

$$c_0 = \frac{\alpha^2 \rho_0 k}{2}. \tag{3.150}$$

Substituting equation (3.148) and (3.150) into (3.147) yields

$$\frac{\alpha^2 \rho_0^2}{4a^3} + \frac{\alpha^2 \rho_0}{2a^2} - \frac{1}{a} = 0. \tag{3.151}$$

Rearranging we obtain the quadratic equation

$$\rho_0^2 + 2a\rho_0 - \frac{4a^2}{\alpha^2} = 0. \tag{3.152}$$

Taking the positive root, the solution for ρ_0 is

$$\rho_0 = -a + \frac{2a}{\alpha}\left(1 + \frac{\alpha^2}{4}\right)^{\frac{1}{2}}. \tag{3.153}$$

Application of binomial expansion wherte $\alpha \ll 1$ yields

$$\rho_0 = -a + \frac{2a}{\alpha}(1 + \frac{1}{8}\alpha^2 + O(\alpha^3)). \tag{3.154}$$

Hence ρ_0 can be written as

$$\rho_0 = \frac{2a}{\alpha}(1 - \frac{\alpha}{2} + O(\alpha^2)). \tag{3.155}$$

Substituting for ρ_0 from equation (3.155) into equation (3.150) yields

$$c_0 = k\alpha a(1 - \frac{\alpha}{2} + O(\alpha^2)). \tag{3.156}$$

Hence the solution for equations (3.139)-(3.143) at $O(\varepsilon)$ take the form

$$\begin{aligned}
\rho_0 &= \frac{2a}{\alpha}\left(1-\frac{\alpha}{2}+O(\alpha^2)\right),\\
c_0 &= k\alpha a\left(1-\frac{\alpha}{2}+O(\alpha^2)\right),\\
q_1(y) &= \frac{1}{a}\left(-(1-\alpha+O(\alpha^2)y\,(y+2)+\alpha\left(1-\frac{\alpha}{2}+O(\alpha^2)\right)\right).
\end{aligned} \tag{3.157}$$

At $O(\varepsilon^2)$

$$-\frac{c_0\rho_0 q_1'}{ka^2} = q_2'' + \frac{\alpha^2}{2a^2}\left(q_1\rho_0^2 + 2\rho_0\rho_1 q_0\right), \tag{3.158}$$

and the boundary conditions are

$$\begin{aligned}
q_2(-1) = \frac{1}{2a}, \quad q_2'(-1) = 0, \quad q_2(0) = \frac{c_1}{a^2k} + \frac{c_0^2}{a^3k^2}\\
\text{and} \quad q_2'(0) = -\frac{1}{ka^3}\left(c_0\rho_1 + c_1\rho_0 + \frac{c_0^2\rho_0}{ak}\right).
\end{aligned} \tag{3.159}$$

We seek asymptotic solution of equations (3.158)-(3.159) by writing the series of α (Note here that $\alpha \ll 1$).

$$\begin{aligned}
q_2 &= q_{21} + \alpha q_{22} + O(\alpha^2),\\
c_1 &= c_{01}\alpha + c_{11}\alpha^2 + O(\alpha^3),\\
\rho_1 &= \frac{1}{\alpha}\rho_{01} + \rho_{11} + O(\alpha).
\end{aligned} \tag{3.160}$$

After substitution for c_0 and ρ_0 from equations (3.156) and (3.157), respectively, and

expressing as a series in α yields

$$q_{21}'' + \alpha q_{22}'' = \frac{1}{a}(\left(2y^2+8y+4\right) + \alpha\left(-4y^2-16y-10-\frac{2}{a}(\frac{1}{\alpha}\rho_{01}+\rho_{11})\right) + \alpha^2\left(\frac{5}{2}y^2+15y+13+\frac{1}{a}(\frac{1}{\alpha}\rho_{01}+\rho_{11})\right) + O(\alpha^3)). \tag{3.161}$$

Hence

$$q_{21}'' + \alpha q_{22}'' = \frac{1}{a}\left(2y^2+8y+4-\frac{2}{a}\rho_{01}\right) + \frac{\alpha}{a}\left(-4y^2-16y-10+\frac{\rho_{01}}{a}-\frac{2}{a}\rho_{11}\right). \tag{3.162}$$

The boundary condition are given by

$$\begin{aligned} q_{21}(-1) + q_{22}(-1)\alpha &= \frac{1}{2a}, \\ q_{21}(0) + q_{22}(0)\alpha &= \frac{c_{01}}{ka^2}\alpha, \\ q_{21}'(-1) + q_{22}'(-1)\alpha &= 0, \\ q_{21}'(0) + q_{22}'(0)\alpha &= -\frac{1}{ka^3}\left((ka\rho_{01}+2ac_{01}) + \left(ka\rho_{11}+2ac_{11}+2ka^2\right)\alpha\right). \end{aligned} \tag{3.163}$$

At $O(1)$ of α

$$q_{21}'' = \frac{1}{a}(2y^2+8y+4-\frac{2}{a}\rho_{01}), \tag{3.164}$$

and the boundary conditions are

$$q_{21}(-1) = \frac{1}{2a}, \tag{3.165}$$

$$q_{21}(0) = 0, \tag{3.166}$$

$$q'_{21}(-1) = 0, \tag{3.167}$$

$$q'_{21}(0) = -\frac{1}{ka^3}(ka\rho_{01} + 2ac_{01}). \tag{3.168}$$

Integration of equation (3.164) yields

$$q'_{21} = \frac{1}{a}\left(\frac{2}{3}y^3 + 4y^2 + \left(4 - \frac{2}{a}\rho_{01}\right)y\right) + A_{21},$$

and a further integration yields

$$q_{21} = \frac{1}{a}\left(\frac{1}{6}y^4 + \frac{4}{3}y^3 + \left(2 - \frac{1}{a}\rho_{01}\right)y^2\right) + A_{21}y + B_{21}, \tag{3.169}$$

where A_{21} and B_{21} are integration constants.

Application of boundary conditions (3.166) yields

$$B_{21} = 0,$$

application of boundary condition (3.167) yields, after rearrangement,

$$A_{21} = \frac{1}{a}\left(\frac{2}{3} - \frac{2}{a}\rho_{01}\right), \tag{3.170}$$

and application of boundary condition (3.165) yields, after rearrangement,

$$A_{21} = \frac{1}{a}\left(\frac{1}{3} - \frac{1}{a}\rho_{01}\right). \tag{3.171}$$

Equating equation (3.170) with equation (3.171) yields

$$\frac{2}{3} - \frac{2}{a}\rho_{01} = \frac{1}{3} - \frac{1}{a}\rho_{01},$$

hence

$$\rho_{01} = \frac{1}{3}a. \tag{3.172}$$

Substituting ρ_{01} from equation (3.172) into equation (3.171) yields

$$A_{21} = 0.$$

From boundary condition (3.168) we obtain

$$0 = -\frac{1}{ka^3}(ka\rho_{01} + 2ac_{01}).$$

Substuiting for ρ_{01} and rearranging yields

$$c_{01} = -\frac{1}{6}ka. \tag{3.173}$$

At O(α)

$$q''_{22} = \frac{1}{a}\left(-4y^2 - 16y - 10 + \frac{\rho_{01}}{a} - \frac{2}{a}\rho_{11}\right), \tag{3.174}$$

and the boundary conditions are

$$q_{22}(-1) = 0, \tag{3.175}$$

$$q_{22}(0) = \frac{c_{01}}{ka^2}, \tag{3.176}$$

$$q'_{22}(-1) = 0, \tag{3.177}$$

$$q'_{22}(0) = -\frac{1}{ka^3}\left(ka\rho_{11} + 2ac_{11} + 2ka^2\right). \tag{3.178}$$

Substitution for ρ_{01} from equation (3.172) and integration of equation (3.174) yields

$$q'_{22} = \frac{1}{a}\left(-\frac{4}{3}y^3 - 8y^2 - (\frac{29}{3} + \frac{2}{a}\rho_{11})y\right) + A_{22}.$$

The general solution to equation (3.174) is

$$q_{22} = -\frac{1}{a}\left(\frac{1}{3}y^4 + \frac{8}{3}y^3 + \left(\frac{29}{6} + \frac{1}{a}\rho_{11}\right)y^2\right) + A_{22}y + B_{22}, \tag{3.179}$$

where A_{22} and B_{22} are integration constants.

Application of boundary condition (3.176) yields

$$B_{22} = -\frac{1}{6a},$$

Substituting for B_{22} and application of boundary condition (3.175) yields

$$A_{22} = -\frac{1}{a}\left(\frac{8}{3} + \frac{1}{a}\rho_{11}\right), \tag{3.180}$$

and application of boundary conditions (3.177) yields

$$A_{22} = -\frac{1}{a}\left(3 + \frac{2}{a}\rho_{11}\right). \tag{3.181}$$

Equating equation (3.180) with (3.181) yields

$$\rho_{11} = -\frac{1}{3}a.$$

Hence

$$A_{22} = -\frac{7}{3a}.$$

Application of boundary condition (3.178) yields

$$A_{22} = -\frac{1}{ka^3}\left(ka\rho_{11} + 2ac_{11} + 2ka^2\right).$$

Substituting for A_{22} and ρ_{11} yields

$$c_{11} = \frac{1}{3}ak.$$

Hence the solution is

$$q_{22}(y) = -\frac{1}{a}\left(\frac{1}{3}y^4 + \frac{8}{3}y^3 + \frac{27}{6}y^2 + \frac{7}{3}y + \frac{1}{6}\right). \tag{3.182}$$

The general solution to equation (3.158) is therefore

$$\begin{aligned} q_2(y) &= \frac{1}{a}\left(y^2\left(\frac{1}{6}y^2 + \frac{4}{3}y + \frac{5}{3}\right) - \alpha\left(\frac{1}{3}y^4 + \frac{8}{3}y^3 + \frac{27}{6}y^2 + \frac{7}{3}y + \frac{1}{6}\right)\right) + O(\alpha^2), \\ \rho_1 &= \frac{a}{3\alpha}\left((1-\alpha) + O(\alpha)\right) \quad \text{and} \quad c_1 = -\alpha\frac{ak}{6}\left(1 - 2\alpha + O(\alpha^2)\right). \end{aligned}$$

The full asymptotic solutions take the form

$$\begin{aligned} \rho &= \frac{a}{\alpha}\left(2(1 - \frac{\alpha}{2} + O(\alpha^2)) + \varepsilon\frac{1}{3}(1 - \alpha + O(\alpha^2))\right) + O(\varepsilon^2), \\ c &= ka\alpha\left((1 - \frac{\alpha}{2} + O(\alpha^2))\varepsilon - \frac{\varepsilon^2}{6}(1 - 2\alpha + O(\alpha^2))\right) + O(\varepsilon^3), \\ q(y) &= \frac{1}{a}(1 + \left(-(1 - \alpha + O(\alpha^2))y(y+2) + \alpha(1 - \frac{\alpha}{2} + O(\alpha^2))\right)\varepsilon + \\ &\quad \left(y^2\left(\frac{1}{6}y^2 + \frac{4}{3}y + \frac{5}{3}\right) - \alpha\left(\frac{1}{3}y^4 + \frac{8}{3}y^3 + \frac{27}{6}y^2 + \frac{7}{3}y + \frac{1}{6}\right) + O(\alpha^2)\right)\varepsilon^2 + O(\varepsilon^3). \end{aligned} \tag{3.183}$$

In Figure 3.9 there is an excellent agreement between asymptotic and numerical investigations. The solution in the second approximation at $O(\varepsilon)$ shows improved accuracy of asymptotic solution.

3.3 Discussion

In this chapter we have considered a linearised version of the model presented in equations (1.2)-(1.6). After numerically exploring the solution we performed a travelling wave analysis and obtained a linear ODE in the travelling wave frame that has an exact solution. Application of the boundary conditions yields a transcendental equation that can be solved only after identification of a small parameter ε, the log of the ratio of the proliferation threshold density to the equilibrium density. Hence we obtain asymptotic expressions for wavespeed, c, and proliferating rim width, ρ, that show excellent agreement with numerical estimates of the wave speed computed using a shooting method. It is also notable that the density profile at leading order is a parabolic.

However, a limitation of this technique is that it requires the availability of an explicit solution which may not be available for more general problems. As a result, we computed the problem using perturbation theory and obtained the same results obtain in exact solution. Subsequently, we reintroduced the Robin boundary condition and used perturbation theory to again construct asymptotic approximations to the wave speed and proliferating rim width. To solve the Robin problem we introduce a second small parameter, α, which can be justified by noting that the mechanical time scale is much shorter than the proliferative time scale. We note that other techniques, such as gearing, could be used to simplify the structure of the solutions and express relevant quantities as a function of a single parameter.

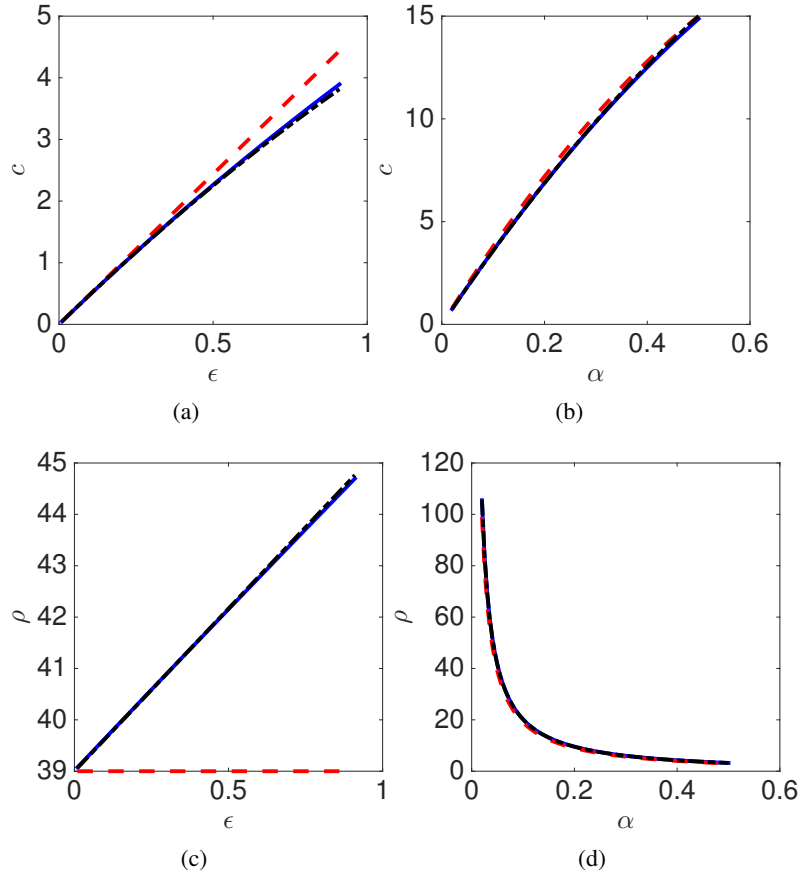

Figure 3.9: Comparing numerical and asymptotic approximations to the wave speed. (a) The wave speed, c, is plotted against ε ($\alpha = 0.05$). (b) The wave speed, c, is plotted against α ($\varepsilon = 0.4$). (c) The proliferation width, ρ, is plotted against ε ($\alpha = 0.05$). (d) The proliferation width, ρ, is plotted against α ($\varepsilon = 0.4$). Numerical solutions (blue solid lines) are computed using a shooting method (see equations (3.111)–(3.114)). Leading order asymptotic solution (dashed red lines) and corrections (dashed black lines) are given by equations (3.157) and (3.183), respectively. Parameter values as in Table 3 unless otherwise stated.

It is notable that taking the Robin problem we obtain the solution at leading order of the Dirichlet problem. In previous work Murray et al. assumed a Dirichlet boundary condition on a moving front and showed excellent agreement between discrete simulations and continuum model. In this work we show that this approximation is reasonable so long as the parameter α is small.

In this chapter, note that by simplifying the problem allowed the identification of a small parameter and asymptotic expansions for tissue-scale quantities where the density profile is a parabola. The results its new in computing the wave speed rather than approximate minimum wave speed as other research did. Notably, the wave speed is less than a wave speed obtained

It is worth comparing the work in this chapter with the travelling wave solution of the Fisher-KPP equation [22]. Importantly, the boundary conditions in the fisher-KPP equations are usually applied at $\pm\infty$. In the present work the domain is semi-infinite and the density is non-zero on the boundary. Hence the condition typically assumed in the Fisher-KPP equation that the origin is not a spiral that yields the minimum wave speed result is not relevant to the current study. In the proposed model the wavespeed is bounded above by $2\sqrt{rD}$.

Chapter 4

A model for generalised linear spring

In this chapter we consider the problem defined by equations (1.2)-(1.6) in the case of a nonlinear diffusion coefficient. As introduced in the literature review, Murray [49] introduced a force law of the form

$$F(x) = k(a-x), \tag{4.1}$$

where x is inter-cell separation distance, k is the linear spring constant and a is resting spring length. In one spatial dimensional a corresponding diffusion coefficient is

$$D(q) = \frac{k}{q^2}. \tag{4.2}$$

Following the approach in Chapter 3, the first challenge in this chapter is to explore what the effect of the non-linearity in diffusion coefficient has on the front speed of a proliferating cell population.

Subsequently we generalise the result by considering a nonlinear diffusion coefficient

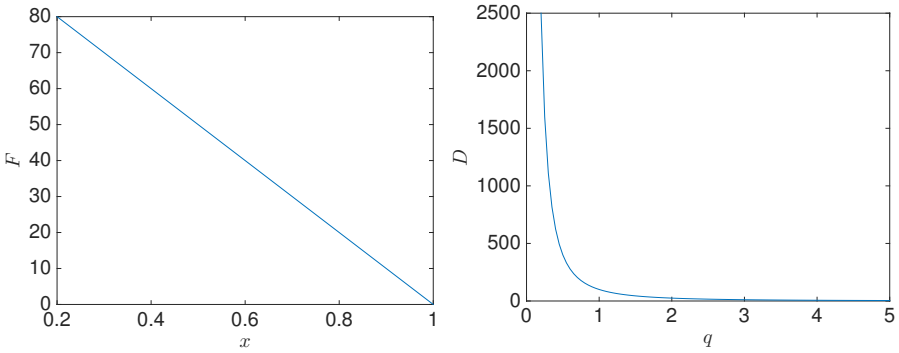

(a) (b)

Figure 4.1: A linear force law and its corresponding diffusion coefficient. (a) The force law, $F(x)$, is plotted against separation distance, x (equation (4.1)). (b) The diffusion coefficient, $D(q)$, is plotted against cell density, q (equation (4.2)). Here $k = 100$, $a = 1$.

parameter	value	description
k	100	spring constant
r	$\log(2)/14$	growth rate
q_c	1.4	threshold proliferation density
a	1	resting spring length
s_0	50	initial domain length

Table 4.1: A table with model parameters.

of the form

$$\frac{a^2 k}{(aq)^n}. \tag{4.3}$$

The layout as follows: in Section 4.1 we consider the case of a nonlinear diffusion (4.2) corresponding to a linear force law; in Section 4.2 we consider the generalised diffusion coefficient given by (4.3); and, finally, in Section 4.3 we conclude with a discussion.

Case number	diffusion $D(q)$	Boundary at $z=0$	Section
(1)	$\frac{k}{q^2}$	$\frac{1}{a}$	4.1.1
(2)	$\frac{k}{q^2}$	$\frac{1}{a(1-\frac{c}{ak})}$	4.1.2
(3)	$\frac{a^2k}{(aq)^n}$	$\frac{1}{a}$	4.2.1
(4)	$\frac{a^2k}{(aq)^n}$	$\frac{1}{a(1-\frac{c}{ak})}$	4.2.2
(5)	$\frac{a^2k}{(aq)^n}$	$\frac{1}{a(1-\frac{c(n-1)}{ak})^{1/(n-1)}}$	4.2.3

Table 4.2: A table illustrating the different cases considered in Chapter 4.

4.1 Nonlinear diffusion model

Here we consider the diffusion coefficient

$$D(q) = \frac{k}{q^2}, \tag{4.4}$$

proposed by Murray et al. [49]. Following the approach taken in Chapter 3, we consider simplifying cases for the boundary condition before tackling the problem given by equations (1.2).

4.1.1 Linear spring with a Dirichlet boundary condition

Substituting for the diffusion coefficient (4.4) in equation (1.2) we obtain

$$\frac{\partial q}{\partial t} = \frac{\partial}{\partial x}\left(\frac{k}{q^2}\frac{\partial q}{\partial x}\right) + rqH(q_c - q). \tag{4.5}$$

Considering a Dirichlet boundary condition yields

$$\left.\frac{\partial q}{\partial x}\right|_{x=0} = 0, \quad q(s(t),t) = \frac{1}{a} \quad \text{and} \quad \frac{ds}{dt} = -ka^3\left.\frac{\partial q}{\partial x}\right|_{x=s(t)}, \tag{4.6}$$

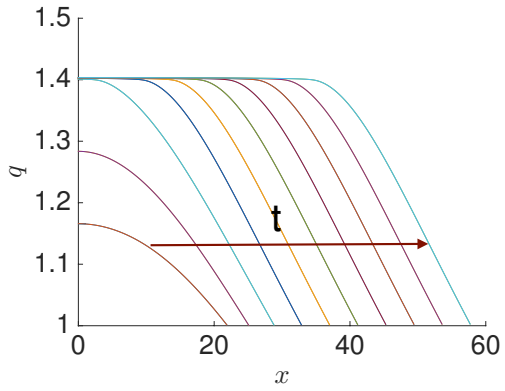

Figure 4.2: Numerical solution of equations (4.5) -(4.7). The cell density, q, is plotted against spatial position, x, at different times, t. See Table 3 for parameters values.

and the initial conditions satisfy

$$q(x,0) = f(x) \quad \text{and} \quad s(0) = s_0. \tag{4.7}$$

4.1.1.1 Numerical solution

To investigate the behaviour of equations (4.5) -(4.7), we computed a numerical solution using the Method of Lines (see Section 2.3.3). In Figure 4.2 we present illustrative results which suggest a travelling wave solution.

4.1.1.2 Phase plane solution

We define the travelling wave coordinate $z = x - ct$ where c is the wave speed. Transforming equations (4.5)-(4.7) yields

$$-cq' = \frac{k}{q^2}q'' - \frac{2k}{q^3}q'^2 + rqH(q_c - q), \tag{4.8}$$

and

$$\left.\frac{dq}{dz}\right|_{z\to-\infty} = 0, \quad q(0) = \frac{1}{a} \quad \text{and} \quad \left.\frac{dq}{dz}\right|_{z=0} = -\frac{c}{a^3 k}. \tag{4.9}$$

Translating independent variable so that the initial condition is applied at the origin

$$\bar{z} = z - \rho,$$

and

$$u = q \quad \text{and} \quad v = \frac{dq}{d\bar{z}}. \tag{4.10}$$

Equation (4.8) transforms to

$$\begin{aligned} \frac{du}{d\bar{z}} &= v, \\ \frac{dv}{d\bar{z}} &= -\frac{u^2}{k}\left(2\frac{k}{u^3}v^2 + cv + ru\right). \end{aligned} \tag{4.11}$$

The initial conditions are

$$u(0) = q_c \quad \text{and} \quad v(0) = 0. \tag{4.12}$$

For a given initial guess for c we numerically identify ρ such that

$$u(\rho) = \frac{1}{a}. \tag{4.13}$$

We then seek a solution that satisfies

$$v(\rho) = -\frac{c}{a^3 k}, \tag{4.14}$$

by minimising the function

$$E(c) = \left(v(\rho) + \frac{c}{a^3 k} \right)^2. \tag{4.15}$$

Using the shooting method defined in Section 3.1.2, we identified a unique value of the wave speed, c, that minimises the error defined in equation (4.15) (see Figure 4.3). We then performed parameter sweeps and computed the wave speed c. Note that for parameter values sampled, the wave speed is an increasing function of the proliferation rate, r, and the proliferation threshold density, q_c.

4.1.1.3 Perturbation solution

We make a change of independent variable

$$y = \frac{z}{\rho}.$$

Equations (4.8) transforms to

$$-c\rho \frac{dq}{dy} = \frac{k}{q^2} \frac{d^2 q}{dy^2} - \frac{2k}{q^3} \left(\frac{dq}{dy} \right)^2 + r\rho^2 q, \tag{4.16}$$

and the boundary conditions (4.9) transform to

$$q(-1) = q_c, \tag{4.17}$$

$$q'(-1) = 0, \tag{4.18}$$

$$q(0) = \frac{1}{a}, \tag{4.19}$$

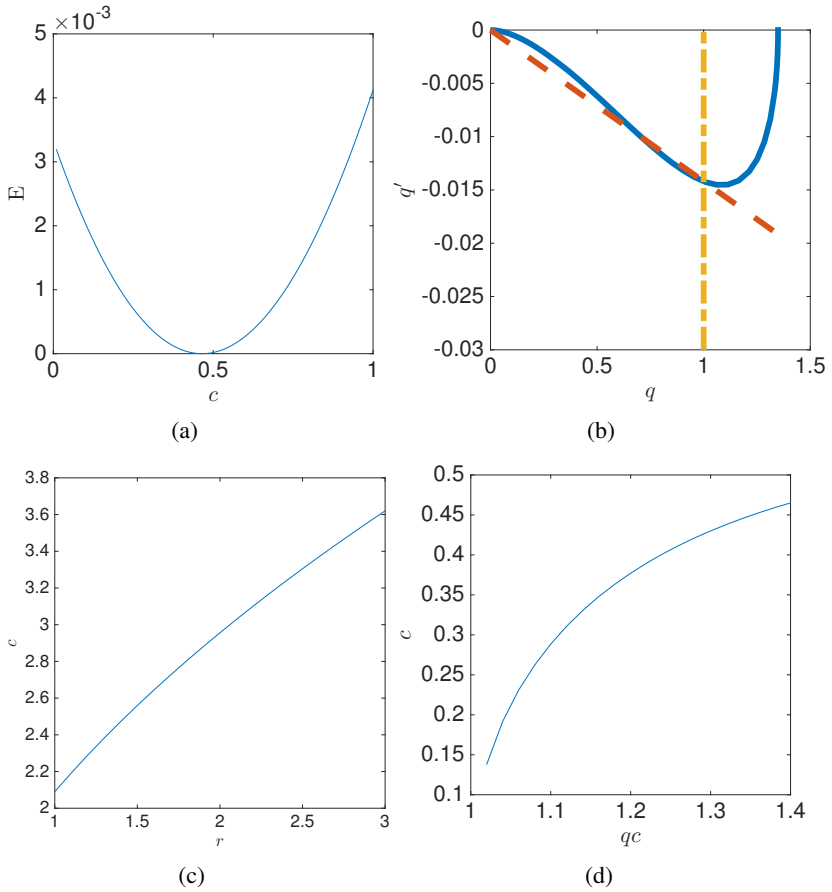

Figure 4.3: Using a shooting method to compute wave speed, c. (a) A unique wave speed, c^*, is identified using a shooting method. Error, $E(c)$, is plotted against wave speed, c (see equation (4.15)). (b) A representative phase plane trajectory is presented for wave speed $c = c^*$. q' is plotted against q. Equations (4.11) were solved numerically (blue lines). Red and yellow lines represent boundary conditions (4.13) and (4.14), respectively. (c) The wave speed, c, is plotted against the proliferation rate, r. (d) The wave speed, c, is plotted against the proliferation threshold density, q_c. Other parameter values as in Table 4.

and

$$q'(0) = -\frac{c\rho}{a^3 k}. \tag{4.20}$$

We follow a similar argument to that proposed in Section 3.2.3.

Assuming that

$$q_c = \frac{1}{a}e^{\varepsilon}, \tag{4.21}$$

where ε is a small parameter, and expanding boundary condition (4.17) yields

$$q(-1) = \frac{1}{a}e^{\varepsilon} = \frac{1}{a}\left(1 + \varepsilon + \frac{1}{2}\varepsilon^2 + O(\varepsilon^3)\right). \tag{4.22}$$

Hence we propose that q is an expansion in integer powers of ε, i.e

$$q = q_0 + \varepsilon q_1 + \varepsilon^2 q_2 + O(\varepsilon^3).$$

Substituting the proposed expansion for q in boundary condition (4.20) and rearranging, we obtain that c and ρ must also be expansions in powers of ε, i.e.

$$c = c_0\varepsilon + \varepsilon^2 c_1 + O(\varepsilon^3)$$
$$\rho = \rho_0 + \varepsilon\rho_1 + O(\varepsilon^2).$$

Finally, balancing diffusion and proliferation terms at leading order yields

$$\frac{k}{q^2}q'' \sim rq\rho. \tag{4.23}$$

Substituting for the proposed form for q and ρ and rearranging yields

$$\frac{k}{q_0^2} q_1'' \varepsilon = r q_0 \rho_0.$$

Hence

$$\frac{r}{k} \propto \varepsilon.$$

As the proliferation timescale $(\frac{1}{r})$ is much longer than the diffusion timescale is $\frac{1}{k}$, we assume that

$$r = \frac{\alpha^2 \varepsilon k}{2},$$

where $\alpha \ll 1$.

In summary we seek asymptotic solution of equations (4.25) of the form

$$\begin{aligned} c &= c_0 \varepsilon + c_1 \varepsilon^2 + O(\varepsilon^3), \\ \rho &= \rho_0 + \rho_1 \varepsilon + O(\varepsilon^2), \\ q &= q_0(y) + q_1(y)\varepsilon + q_2(y)\varepsilon^2 + O(\varepsilon^3). \end{aligned} \tag{4.24}$$

Substituting r into equation (4.16) yields

$$-c\rho \frac{dq}{dy} = \frac{k}{q^2}\frac{d^2q}{dy^2} - \frac{2k}{q^3}\left(\frac{dq}{dy}\right)^2 + \frac{\alpha^2 \varepsilon k}{2}\rho^2 q(y). \tag{4.25}$$

After substituting the series equations (4.24) into equation (4.25) and using the binomial expansion

$$\begin{aligned} &-(c_0\varepsilon + c_1\varepsilon^2)(\rho_0 + \rho_1\varepsilon^2)(q_0'(y) + q_1'(y)\varepsilon) = \\ &\frac{-2k}{q_0^3}\left(1 - 3\varepsilon\frac{q_1}{q_0}\right)(q_0(y)' + \varepsilon q_1'(y))^2 \\ &+\frac{k}{q_0^2}\left(1 - 2\varepsilon\frac{q_1}{q_0}\right)(q_0''(y) + q_1''(y)\varepsilon) + \frac{k\alpha^2\varepsilon}{2}\left(q_0(y) + \varepsilon q_1(y)\right)(\rho_0 + \varepsilon\rho_1)^2, \end{aligned} \tag{4.26}$$

and the boundary conditions are

$$\begin{aligned}
q_0(-1)+q_1(-1)\varepsilon+q_2(-1)\varepsilon^2 &= \frac{1}{a}e^{\varepsilon} = \frac{1}{a}\left(1+\varepsilon+\frac{1}{2}\varepsilon^2\right)\\
q_0'(-1)+q_1'(-1)\varepsilon+q_2'(-1)\varepsilon^2 &= 0\\
q_0(0)+q_1(0)\varepsilon+q_2(0)\varepsilon^2 &= \frac{1}{a}\\
q_0'(0)+q_1'(0)\varepsilon+q_2'(0)\varepsilon^2 &= -\frac{1}{a^3k}\Big(c_0\rho_0\varepsilon+(\rho_0c_1+\rho_1c_0)\varepsilon^2\Big).
\end{aligned} \tag{4.27}$$

Balancing terms at different orders of ε and applied the boundary condition, we can analyse the solution as described below.

At O(1)

$$\left(\frac{k}{q_0^2}q_0'\right)' = 0, \tag{4.28}$$

and the boundary conditions are

$$q_0(-1)=\frac{1}{a}, \quad q_0(0)=\frac{1}{a} \quad q_0'(-1)=0 \quad \text{and} \quad q_0'(0)=0. \tag{4.29}$$

Integrating equation (4.28) yields

$$\frac{k}{q_0^2}q_0' = A_0. \tag{4.30}$$

A further integration yields

$$-\frac{1}{q_0} = \hat{A}_0 y + \hat{B}_0. \tag{4.31}$$

Rearranging

$$q_0 = -\frac{1}{\hat{A_0}y + \hat{B_0}}. \tag{4.32}$$

Application of boundary conditions (4.29) yields

$$\hat{A_0} = 0 \quad \text{and} \quad \hat{B_0} = a. \tag{4.33}$$

Hence

$$q_0(y) = \frac{1}{a}. \tag{4.34}$$

At $O(\varepsilon)$

$$q_1''(y) = -\frac{\alpha^2 \rho_0^2}{2a^3}, \tag{4.35}$$

with boundary conditions

$$q_1(0) = 0, \tag{4.36}$$

$$q_1(-1) = \frac{1}{a}, \tag{4.37}$$

$$q_1'(-1) = 0, \tag{4.38}$$

$$q_1'(0) = -\frac{c_0 \rho_0}{a^3 k}. \tag{4.39}$$

Integrating equation (4.35) yields

$$q_1'(y) = -\frac{\alpha^2\rho_0^2}{2a^3}y + A_1, \tag{4.40}$$

and a further integration yields

$$q_1(y) = -\frac{\alpha^2\rho_0^2}{4a^3}y^2 + A_1 y + B_1, \tag{4.41}$$

where A_1 and B_1 are integration constants.

Applying boundary condition equation (4.36) yields

$$B_1 = 0.$$

Applying boundary condition equation (4.37), substituting for B_1 and rearrangement yields

$$A_1 = -\left(\frac{1}{a} + \frac{\alpha^2\rho_0^2}{4a^3}\right). \tag{4.42}$$

Applying boundary condition equation (4.38) and rearranging yields

$$A_1 = -\frac{\alpha^2\rho_0^2}{2a^3}. \tag{4.43}$$

Application the boundary condition equation (4.39) yields

$$A_1 = -\frac{c_0\rho_0}{a^3 k}. \tag{4.44}$$

Equating equations (4.43) and (4.42) yields

$$-\frac{\alpha^2\rho_0^2}{2a^3} = -\left(\frac{1}{a} + \frac{\alpha^2\rho_0^2}{4a^3}\right).$$

Taking the positive solution and rearranging

$$\rho_0 = \frac{2a}{\alpha}. \tag{4.45}$$

Hence

$$A_1 = -\frac{2}{a}. \tag{4.46}$$

Substituting in equation (4.44) yields

$$c_0 = ak\alpha. \tag{4.47}$$

Hence the solution of equation (4.35) is

$$q_1(y) = -\frac{1}{a}\left(y(y+2)\right). \tag{4.48}$$

At O(ε^2)

$$-c_0\rho_0 q_1' = -\frac{2k}{q_0^3}q_1'^2 + \frac{k}{q_0^2}q_2'' - 2k\frac{q_1}{q_0^4}q_1'' + \frac{k\alpha^2}{2}q_1\rho_0^2 + k\alpha^2 q_0\rho_0\rho_1, \tag{4.49}$$

with boundary conditions

$$q_2(0) = 0, \tag{4.50}$$

$$q_2'(-1) = 0, \tag{4.51}$$

$$q_2(-1) = \frac{1}{2a}, \tag{4.52}$$

$$q_2'(0) = -\frac{1}{a^3 k}\left(c_0\rho_1 + c_1\rho_0 + 2ac_0\rho_0 q_1(0)\right). \tag{4.53}$$

Substituting for c_0, ρ_0 and q_1 from equations (4.47), (4.45) and (4.48), respectively, into (4.49) yields

$$q_2'' = \frac{1}{a}\left(14y^2 + 32y + 12 - 2\alpha\frac{\rho_1}{a}\right). \tag{4.54}$$

Integration of equation (4.54) yields

$$q_2' = \frac{1}{a}\left(\frac{14}{3}y^3 + 16y^2 + (12 - 2\alpha\frac{\rho_1}{a})y\right) + A_{21}, \tag{4.55}$$

and a further integration yields

$$q_2 = \frac{1}{a}\left(\frac{7}{6}y^4 + \frac{16}{3}y^3 + (6 - \alpha\frac{\rho_1}{a})y^2\right) + A_{21}y + B_{21}, \tag{4.56}$$

where A_{21} and B_{21} are integration constants.

Applying boundary condition (4.50) yields

$$B_{21} = 0.$$

Applying boundary condition (4.51) yields

$$A_{21} = \frac{1}{a}\left(\frac{2}{3} - 2\alpha\frac{\rho_1}{a}\right). \tag{4.57}$$

Applying boundary condition (4.52) and rearranging yields

$$A_{21} = \frac{1}{a}\left(\frac{4}{3} - \alpha\frac{\rho_1}{a}\right). \tag{4.58}$$

Applying boundary condition (4.53) yields

$$A_{21} = -\frac{1}{a^3 k}\left(c_0\rho_1 + c_1\rho_0 + 2ac_0\rho_0 q_1(0)\right). \tag{4.59}$$

Hence solving for A_{21}, ρ_1 and c_1 we obtain

$$\rho_1 = -\frac{2a}{3\alpha}, \quad c_1 = -\frac{2a}{3}\alpha k \quad \text{and} \quad A_{21} = -\frac{2}{a}. \tag{4.60}$$

The full solution is given by

$$\begin{aligned}
\rho &= \frac{a}{\alpha}\left(2 - \frac{2}{3}\varepsilon + O(\varepsilon^2)\right), \\
c &= ak\alpha\left(\varepsilon - \frac{2}{3}\varepsilon^2 + O(\varepsilon^3)\right), \\
q &= \frac{1}{a}\left(1 - y(y+2)\varepsilon + \left(\frac{7}{6}y^4 + \frac{16}{3}y^3 + \frac{20}{3}y^2 + 2\right)\varepsilon^2 + O(\varepsilon^3)\right).
\end{aligned} \tag{4.61}$$

In Figure 4.4 we compare numerical and asymptotic solutions for the wave speed, c, and proliferating width, ρ. Note the improved accuracy of the asymptotic method for higher order correction.

Substituting for α into equation (4.61) we obtain

$$\begin{aligned}
\rho &= a\sqrt{\frac{2k\varepsilon}{r}}\left(1 - \frac{1}{3}\varepsilon + O(\varepsilon^2)\right), \\
c &= a\sqrt{2rk\varepsilon}\left(1 - \frac{2}{3}\varepsilon + O(\varepsilon^2)\right).
\end{aligned} \tag{4.62}$$

In Chapter 3 we considered the case of a constant diffusion coefficient and obtained an expression for the wave speed, c, and proliferation width, ρ, given by

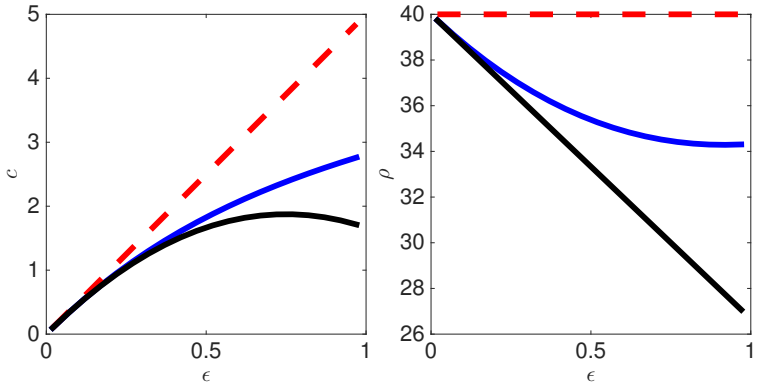

(a) (b)

Figure 4.4: Comparing numerical and asymptotic approximations to the wave speed. (a) The wave speed, c, is plotted against ε. (b) The proliferation width, ρ, is plotted against ε. Numerical solution was computed using shooting method (blue lines). Leading order asymptotic solution (dashed lines) and corrections (black solid lines) are given by equations (4.48) and (4.61), respectively. $\alpha = 0.05$, other parameter values as in Table 4.

$$c = \sqrt{2rk\varepsilon}\left(1 - \frac{1}{6}\varepsilon + O(\varepsilon^2)\right),$$
$$\rho = \sqrt{\frac{2k\varepsilon}{r}}\left(1 + \frac{1}{6}\varepsilon + O(\varepsilon^2)\right). \tag{4.63}$$

Hence here we show that the effect of nonlinear diffusion coefficient given by equation (4.62) is not present at leading order. In Figure 4.5 we compare an asymptotic expressions and numerical results which showed in Figure 3.6 and Figure 4.4 for the nonlinear model and constant diffusion case. We observed good results between constant D and nonlinear diffusion with Dirichlet boundary condition.

In Figure 4.5 we show that the main effect of the nonlinear diffusion is seen at $O(\varepsilon)$ and results in both a smaller wave speed, c, and proliferating rim width, ρ.

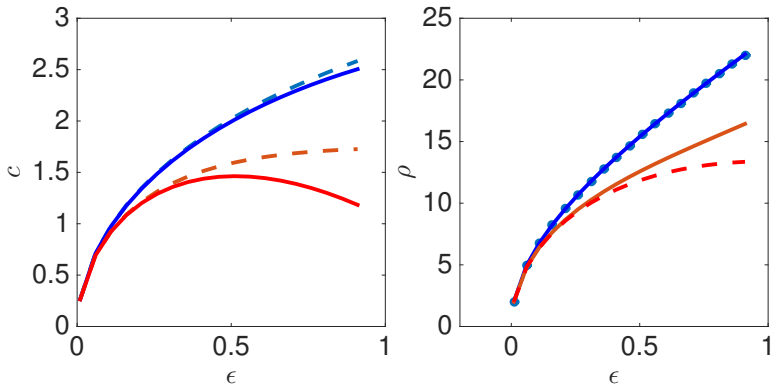

(a) (b)

Figure 4.5: Comparing numerical (solid lines) and asymptotic approximations (dashed line) for constant (equation (4.63), blue) and nonlinear diffusion (equation (4.62), red). (a) The wave speed, c, is plotted against ε. (b) The proliferation width, ρ, is plotted against ε.

4.1.2 Linear spring with a Robin boundary condition

In the case of the nonlinear diffusion coefficient

$$D(q) = \frac{k}{q^2}, \tag{4.64}$$

and a Robin boundary condition, equations (1.2) take the form

$$\frac{\partial q}{\partial t} = \frac{\partial}{\partial x}\left(\frac{k}{q^2}\frac{\partial q}{\partial x}\right) + rqH(q_c - q), \tag{4.65}$$

the boundary conditions are

$$\left.\frac{\partial q}{\partial x}\right|_{x=0} = 0, \quad \left.\frac{\partial q}{\partial x}\right|_{x=s(t)} = -\frac{ds}{dt}\frac{q(s(t),t)^3}{k} \quad \text{and} \quad \frac{ds}{dt} = ka\left(1 - \frac{1}{aq(s(t),t)}\right), \tag{4.66}$$

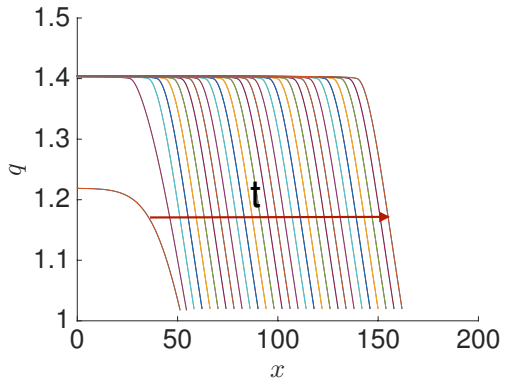

Figure 4.6: Numerical solution of equations (4.65)-(4.67). The cell density, q, is plotted against spatial position, x, at different times, t. See Table 4 for parameter values.

and initial conditions

$$q(x,0) = f(x) \quad \text{and} \quad s(0) = s_0. \tag{4.67}$$

In this section we explore that the nonlinear diffusion coefficient given by equation (4.64) modifies the solution behaviour at leading order in the case of a Robin boundary condition.

4.1.2.1 Numerical solution

To investigate the behaviour of equations (4.65)-(4.67), we computed a numerical solution using the Method of Lines, (see section 2.3.3 for implementation details). In Figure 4.6 the numerical solution appears to have a travelling wave solution. We observed there is a non-proliferating core of cells at density q_c, and that, as expected, the density is no longer constant on the moving boundary.

4.1.2.2 Phase plane solution

We define the travelling wave coordinate $z = x - ct$, where c is the wave speed. Transforming equations (4.65) yields

$$-cq' = \frac{k}{q^2}q'' - \frac{2k}{q^3}q'^2 + rqH(q_c - q), \tag{4.68}$$

with the boundary conditions given by

$$\left.\frac{dq}{dz}\right|_{z\to-\infty} = 0, \quad q(0) = \frac{1}{a(1-\frac{c}{ak})} \quad \text{and} \quad \left.\frac{dq}{dz}\right|_{z=0} = -\frac{cq(0)^3}{k} \tag{4.69}$$

Again I define

$$\bar{z} = z - \rho,$$

and

$$u = q \quad \text{and} \quad v = \frac{dq}{d\bar{z}}. \tag{4.70}$$

Qquations (4.68)–(4.69) transform to

$$\begin{aligned} \frac{du}{d\bar{z}} &= v, \\ \frac{dv}{d\bar{z}} &= \frac{u^2}{k}\left(-2\frac{k}{u^3}v^2 - cv - ru\right). \end{aligned} \tag{4.71}$$

The initial conditions are

$$u(0) = q_c \quad \text{and} \quad v(0) = 0. \tag{4.72}$$

For a given initial guess for c we numerically identify ρ such that

$$u(\rho) = \frac{1}{a(1-\frac{c}{ak})}. \tag{4.73}$$

We then seek a solution that satisfies

$$v(\rho) = -\frac{c}{k}\left(\frac{1}{a(1-\frac{c}{ak})}\right)^3, \tag{4.74}$$

by minimising the function

$$E(c) = \left(v(\rho) + \frac{c}{k}\left(\frac{1}{a(1-\frac{c}{ak})}\right)^3\right)^2. \tag{4.75}$$

Using a shooting method, Figure 4.7 (a) we plot the solution of equations (4.71) in the phase plane. In Figure 4.7 (b) we plot the error defined in equation (4.75) against a range of values for the unknown wave speed c. In Figure 4.7 (c) and (d) we show that the wave speed is an increasing function of the proliferation threshold density, q_c and proliferation rate, r.

4.1.2.3 Perturbation solution

Making the change of independent variable

$$y = \frac{z}{\rho},$$

equation (4.68) transforms to

$$-c\rho\frac{dq}{dy} = \frac{k}{q^2}\frac{d^2q}{dy^2} - \frac{2k}{q^3}\left(\frac{dq}{dy}\right)^2 + r\rho^2 q. \tag{4.76}$$

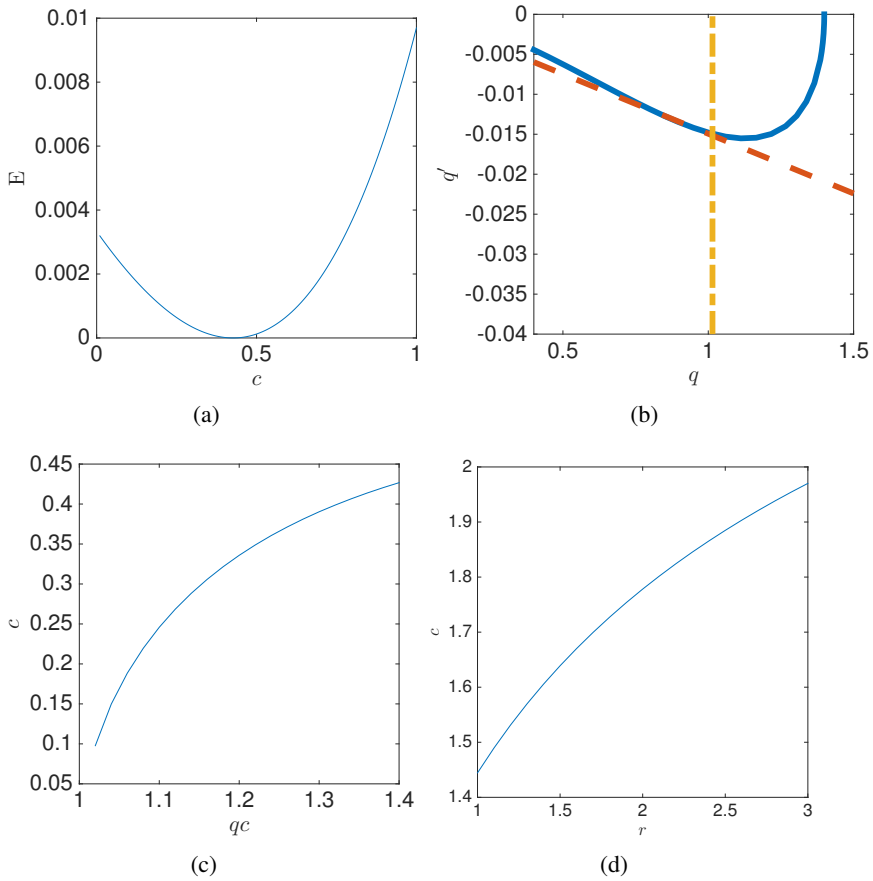

Figure 4.7: Using a shooting method to compute wave speed, c. (a) A unique wave speed, c^*, is identified using a shooting method. Error, $E(c)$, is plotted against wave speed, c (see equation (4.75)). (b) A representative phase plane trajectory is presented for wave speed $c = c^*$. q' is plotted against q. Equations (4.71) were solved numerically (blue line). Red and yellow lines represent boundary conditions (4.73) and (4.74), respectively. (c) The wave speed, c, is plotted against the proliferation threshold density, q_c. (d) The wave speed, c, is plotted against proliferation rate, r. Other parameter values as in Table 4.

The boundary conditions (4.69) transform to

$$q(-1) = \frac{1}{a}e^{\varepsilon}, \tag{4.77}$$

$$q'(-1) = 0, \tag{4.78}$$

$$q(0) = \frac{1}{a\left(1-\frac{c}{ak}\right)}, \tag{4.79}$$

$$q'(0) = -\frac{c\rho}{k}q(0)^3. \tag{4.80}$$

To proceed we follow a similar argument to that proposed in Section 3.2.3.

Assuming that

$$q_c = \frac{1}{a}e^{\varepsilon}, \tag{4.81}$$

where ε is a small parameter, and expanding boundary condition (4.77) yields

$$q(-1) = \frac{1}{a}e^{\varepsilon} = \frac{1}{a}\left(1+\varepsilon+\frac{1}{2}\varepsilon^2+O(\varepsilon^3)\right). \tag{4.82}$$

Hence we propose that q is an expansion in integer powers of ε, i.e

$$q = q_0 + \varepsilon q_1 + \varepsilon^2 q_2 + O(\varepsilon^3). \tag{4.83}$$

Substituting the proposed expansion for q in boundary condition (4.79) and rearranging, we obtain that c must also be an expansion in powers of ε, i.e.

$$c = c_0\varepsilon + c_1\varepsilon^2 + O(\varepsilon^3).$$

Substituting the proposed expansions for c and q in boundary condition (4.80) and rearranging, we find that ρ must be an expansion of the form

$$\rho = \rho_0 + \varepsilon\rho_1 + O(\varepsilon^2). \tag{4.84}$$

Finally, balancing diffusion and proliferation terms at leading order yields

$$\frac{k}{q^2}q'' \sim rq\rho. \tag{4.85}$$

Substituting for q and ρ from equations (4.83) and (4.84), respectively, and rearranging yields the scaling relationship

$$\frac{k}{q_0^2}q_1''\varepsilon = rq_0\rho_0.$$

Hence

$$\frac{r}{k} \propto \varepsilon,$$

As the proliferation timescale $(\frac{1}{r})$ is much longer than the diffusion timescale is $(\frac{1}{k})$, we assume that

$$r = \frac{\alpha^2\varepsilon k}{2},$$

where $\alpha \ll 1$.

Substituting for r in equation (4.76) yields

$$-c\rho\frac{dq}{dy} = \frac{k}{q^2}\frac{d^2q}{dy^2} - \frac{2k}{q^3}\left(\frac{dq}{dy}\right)^2 + \frac{\alpha^2\varepsilon k}{2}\rho^2 q. \tag{4.86}$$

In summary, we propose asymptotic solutions of equation (4.76) of the form

$$\begin{aligned} c &= c_0\varepsilon + c_1\varepsilon^2 + O(\varepsilon^3), \\ \rho &= \rho_0 + \rho_1\varepsilon + O(\varepsilon^2), \\ q &= q_0(y) + q_1(y)\varepsilon + q_2(y)\varepsilon^2 + O(\varepsilon^3). \end{aligned} \tag{4.87}$$

Substituting equation (4.87) in equation (4.86) and expanding yields

$$\begin{aligned} -(c_0\varepsilon + c_1\varepsilon^2)(\rho_0 + \rho_1\varepsilon^2)(q_0' + q_1'\varepsilon + q_2'\varepsilon^2) &= -\frac{2k}{q_0^3}(1 - 3\varepsilon\frac{q_1}{q_0})(q_0' + q_1'\varepsilon + q_2'\varepsilon^2)^2 \\ +\frac{k}{q_0^2}(1 - 2\varepsilon\frac{q_1}{q_0})(q_0'' + q_1''\varepsilon + q_2''\varepsilon^2) &+ \frac{k\alpha^2\varepsilon}{2}(q_0 + q_1\varepsilon + q_2\varepsilon^2)(\rho_0 + \varepsilon\rho_1)^2. \end{aligned} \tag{4.88}$$

Substituting the series (4.87) in the boundary conditions and expanding yields

$$\begin{aligned} q_0(-1) + q_1(-1)\varepsilon + q_2(-1)\varepsilon^2 &= \frac{1}{a}\left(1 + \varepsilon + \frac{1}{2}\varepsilon^2\right) \\ q_0'(-1) + q_1'(-1)\varepsilon + q_2'(-1)\varepsilon^2 &= 0 \\ q_0(0) + q_1(0)\varepsilon + q_2(0)\varepsilon^2 &= \frac{1}{a}\left(1 + \frac{c_0}{ak}\varepsilon + \left(\frac{c_1}{ak} + \frac{c_0^2}{a^2k^2}\right)\varepsilon^2\right) \\ q_0'(0) + q_1'(0)\varepsilon + q_2'(0)\varepsilon^2 &= \\ -\frac{1}{k}(q(0)^3 c_0\rho_0\varepsilon + \left(q(0)^3 c_1\rho_0 + q(0)^3\rho_1 c_0 + 3q(0)^2 c_0\rho_0 q_1(0)\right)\varepsilon^2). \end{aligned} \tag{4.89}$$

Balancing the terms at different orders of ε, we obtain the following results.

At $O(1)$

$$\left(\frac{k}{q_0^2}q_0'\right)' = 0, \tag{4.90}$$

and the boundary conditions are

$$q_0(-1) = \frac{1}{a}, \quad q_0(0) = \frac{1}{a}, \quad q_0'(-1) = 0 \quad \text{and} \quad q_0'(0) = 0. \tag{4.91}$$

Integrating equation (4.90) yields

$$\frac{k}{q_0^2} q_0' = A_0.$$

A further integrating yields

$$-\frac{1}{q_0} = \hat{A_0} y + \hat{B_0}.$$

Hence

$$q_0 = -\frac{1}{\hat{A_0} y + \hat{B_0}}$$

where $\hat{A_0}$ and $\hat{B_0}$ are integration constants.

Application the boundary conditions (4.91) yields

$$\hat{A_0} = 0 \quad \text{and} \quad \hat{B_0} = a. \tag{4.92}$$

Hence the solution is

$$q_0(y) = \frac{1}{a}.$$

At $O(\varepsilon)$

$$q_1'' = -\frac{\alpha^2 \rho_0^2}{2a^3}, \tag{4.93}$$

and the boundary conditions are

$$q_1(0) = \frac{c_0}{a^2 k}, \tag{4.94}$$

$$q_1(-1) = \frac{1}{a}, \tag{4.95}$$

$$q_1'(-1) = 0, \tag{4.96}$$

$$q_1'(0) = -\frac{c_0\rho_0}{ak}. \tag{4.97}$$

Integration of equation (4.93) yields

$$q_1'(y) = -\frac{\alpha^2\rho_0^2}{2a^3}y + A_1. \tag{4.98}$$

The general solution to equation (4.93) is

$$q_1(y) = -\frac{\alpha^2\rho_0^2}{4a^3}y^2 + A_1y + B_1, \tag{4.99}$$

where A_1 and B_1 are integration constants.

Application of boundary condition (4.94) yields

$$B_1 = \frac{c_0}{a^2k}, \tag{4.100}$$

application of boundary condition (4.95) yields

$$A_1 = -\frac{1}{a}\left(\frac{\alpha^2\rho_0^2}{4a^2} + 1 - \frac{c_0}{ak}\right), \tag{4.101}$$

application of boundary condition (4.96) yields

$$A_1 = -\frac{\alpha^2\rho_0^2}{2a^3}, \tag{4.102}$$

and application of boundary condition (4.97) yields

$$A_1 = -\frac{c_0\rho_0}{ak}. \tag{4.103}$$

Equating equations (4.102) and (4.103) yields

$$c_0 = \frac{\rho_0\alpha^2 k}{2}. \tag{4.104}$$

Equating equations (4.101) and (4.102) yields a quadratic equation in ρ_0 given by

$$\rho_0^2 + 2a\rho_0 - \frac{4a^2}{\alpha^2} = 0. \tag{4.105}$$

The positive solution is

$$\rho_0 = \frac{-2a + \sqrt{4a^2 + \frac{16a^2}{\alpha^2}}}{2}. \tag{4.106}$$

Simplifying yields

$$\rho_0 = -a + \frac{2a}{\alpha}(1 + \frac{\alpha^2}{4})^{\frac{1}{2}}. \tag{4.107}$$

As $\alpha \ll 1$, applying the binomial expansion yields

$$\rho_0 = -a + \frac{2a}{\alpha}(1 + \frac{1}{8}\alpha^2 + O(\alpha^3)). \tag{4.108}$$

Hence

$$\rho_0 = \frac{2a}{\alpha}\left(1 - \frac{\alpha}{2} + O(\alpha^2)\right). \tag{4.109}$$

Substituting ρ_0 from equation (4.109) into equation (4.104) yields

$$c_0 = ka\alpha\left(1-\frac{\alpha}{2}+O(\alpha^2)\right). \tag{4.110}$$

Hence

$$A_1 = -\frac{2}{a}\left(1-\alpha+O(\alpha^2)\right) \quad \text{and} \quad B_1 = \frac{\alpha}{a}\left(1-\frac{\alpha}{2}+O(\alpha^2)\right). \tag{4.111}$$

The first order solution is given by

$$\begin{aligned} c_0 &= \alpha ak(1-\frac{\alpha}{2}+O(\alpha^2)), \quad \rho_0 = \frac{2a}{\alpha}(1-\frac{\alpha}{2}+O(\alpha^2)), \\ q_1(y) &= \frac{1}{a}\left(-(1-\alpha+O(\alpha^2))(y^2+2y)+\alpha(1-\frac{\alpha}{2}+O(\alpha^2))\right). \end{aligned} \tag{4.112}$$

At O(ε^2)

$$-c_0\rho_0 q_1' = -\frac{2k}{q_0^3}q_1'^2+\frac{k}{q_0^2}q_2''-2k\frac{q_1}{q_0}q_1''+\frac{k\alpha^2}{2}q_1\rho_0^2+k\alpha^2 q_0\rho_0\rho_1, \tag{4.113}$$

with boundary condition

$$\begin{aligned} q_2'(-1) = 0, \quad q_2(0) &= \frac{c_1}{a^2k}+\frac{c_0^2}{a^3k^2}, \quad q_2(-1) = \frac{1}{2a}, \\ q_2'(0) &= -\frac{1}{ka^3}\left(c_0\rho_1+c_1\rho_0+3ac_0\rho_0 q_1(0)\right). \end{aligned} \tag{4.114}$$

To proceed, we seek asymptotic solution of equations (4.113)-(4.114) by writing as a series in α

$$\begin{aligned} q_2 &= q_{21}+\alpha q_{22}+O(\alpha^2), \\ c_1 &= c_{01}\alpha+c_{11}\alpha^2+O(\alpha^3), \\ \rho_1 &= \frac{1}{\alpha}\left(\rho_{01}+\alpha\rho_{11}+O(\alpha^2)\right). \end{aligned} \tag{4.115}$$

Substituting for $q_1(y)$, c_0 and ρ_0 from equations (4.115) and (4.112), respectively, yields

$$\begin{aligned} q_{21}'' + \alpha q_{22}'' &= (4-8\alpha)(y+1) + 8(1-2\alpha)\left(y^2+2y+1\right) \\ &\quad +2(-y(y+2)+\alpha y(y+2)+\alpha\left(1-\frac{\alpha}{2}\right))(-2+\alpha) \\ &\quad -2(1-\alpha)(-(1-\alpha)y(y+2)+\alpha\left(1-\frac{\alpha}{2}\right)) - 2\alpha\left(1-\frac{\alpha}{2}\right)\left(\frac{1}{\alpha}\rho_{01}+\rho_{11}\right), \\ &= \frac{1}{a}\left(\left(14y^2+32y+12-2\rho_{01}\right)+\alpha\left(-26y^2-60y-\frac{92}{3}-2\rho_{11}\right)\right). \end{aligned} \tag{4.116}$$

Simplifying yields

$$q_{21}'' + \alpha q_{22}'' = \frac{1}{a}\left(\left(14y^2+32y+12-2\rho_{01}\right)+\alpha\left(-26y^2-60y-\frac{92}{3}-2\rho_{11}\right)\right). \tag{4.117}$$

The boundary conditions are

$$\begin{aligned} &q_{21}'(-1) + \alpha q_{22}'(-1) = 0, \\ &q_{21}(0) + \alpha q_{22}(0) = \frac{c_{01}}{k}\alpha, \\ &q_{21}(-1) + \alpha q_{22}(-1) = 0 \\ &q_{21}'(0) + \alpha q_{22}'(0) = -\frac{1}{a^3 k}\left((ak\rho_{01}+2ac_{01})+\alpha\left(ak\rho_{11}-\frac{1}{2}k\rho_{01}+2ac_{11}-c_{01}+a^2 6k\right)\right). \end{aligned} \tag{4.118}$$

At $O(1)$

$$q_{21}'' = \frac{1}{a}(14y^2+32y+12-2\rho_{01}), \tag{4.119}$$

and the boundary conditions are

$$q_{21}(0) = 0, \tag{4.120}$$

$$q_{21}(-1) = \frac{1}{2a}, \tag{4.121}$$

$$q'_{21}(-1) = 0, \tag{4.122}$$

$$q'_{21}(0) = -\frac{1}{a^3 k}(ak\rho_{01} + 2ac_{01}). \tag{4.123}$$

Integration of equation (4.119) yields

$$q'_{21}(y) = \frac{14}{3}y^3 + 16y^2 + \left(12 - 2\frac{\rho_{01}}{a}\right)y + A_{21}. \tag{4.124}$$

A further integration gives

$$q_{21}(y) = \frac{1}{a}\left(\frac{7}{6}y^4 + \frac{16}{3}y^3 + (6 - \frac{\rho_{01}}{a})y^2\right) + A_{21}y + B_{21}, \tag{4.125}$$

where A_{21} and B_{21} are integration constants.

Application of boundary condition (4.120) yields

$$B_{21} = 0. \tag{4.126}$$

Application of boundary condition (4.121) and substituting for B_{21} yields

$$A_{21} = \frac{1}{a}\left(\frac{4}{3} - \frac{\rho_0}{a}\right). \tag{4.127}$$

Application of boundary condition (4.122) yields

$$A_{21} = \frac{1}{a}\left(\frac{2}{3} - 2\frac{\rho_{01}}{a}\right). \tag{4.128}$$

Application of boundary condition (4.123) yields

$$A_{21} = -\frac{1}{a^3 k}(ak\rho_{01} + 2ac_{01}). \tag{4.129}$$

Hence

$$A_{21} = \frac{2}{a}, \quad B_{21} = 0, \quad \rho_{01} = -\frac{2}{3}a \quad \text{and} \quad c_{01} = -\frac{2}{3}ka. \tag{4.130}$$

Hence the solution is

$$q_{21}(y) = \frac{y}{a}\left(\frac{7}{6}y^3 + \frac{16}{3}y^2 + \frac{11}{3}y + 2\right).$$

At O(α)

$$q''_{22}(y) = \frac{1}{a}\left(-26y^2 - 60y - \frac{92}{3} - 2\rho_{11}\right), \tag{4.131}$$

and the boundary conditions are

$$q_{22}(0) = \frac{c_{01}}{k}, \tag{4.132}$$

$$q_{22}(-1) = 0, \tag{4.133}$$

$$q'_{22}(-1) = 0, \tag{4.134}$$

$$q'_{22}(0) = -\frac{1}{a^3 k}\left(ak\rho_{11} - \frac{1}{2}k\rho_{01} + 2ac_{11} - c_{01} + 6a^2 k\right). \tag{4.135}$$

Integration of equation (4.131) yields

$$q'_{22}(y) = \frac{1}{a}\left(\frac{26}{3}y^3 - 30y^2 - y\left(\frac{92}{3} + 2\frac{\rho_{11}}{a}\right)\right) + A_{22}.$$

A further integration yields

$$q_{22} = \frac{1}{a}\left(-\frac{13}{6}y^4 - \frac{30}{3}y^3 - \left(\frac{92}{6} + \frac{\rho_{11}}{a}\right)y^2\right) + A_{22}y + B_{22}, \tag{4.136}$$

where A_{22} and B_{22} are integration constants.

Application of boundary conditions (4.132) yields

$$B_{22} = \frac{c_{01}}{k}. \tag{4.137}$$

Substituting B_{22} and applying the boundary condition (4.133) yields

$$A_{22} = -\frac{1}{a}\left(\frac{51}{6} - \frac{\rho_{11}}{a}\right). \tag{4.138}$$

Application of boundary condition (4.134) yields

$$A_{22} = -\frac{1}{a}\left(\frac{28}{3} - 2\frac{\rho_{11}}{a}\right). \tag{4.139}$$

Application of boundary condition (4.135) yields

$$A_{22} = -\frac{1}{a^3 k}\left(ak\rho_{11} - \frac{1}{2}k\rho_{01} + 2ac_{11} - c_{01} + 6a^2 k\right). \tag{4.140}$$

Solving for A_{22}, B_{22}, ρ_{11} and c_{11} yields

$$A_{22} = -\frac{7}{a}, \quad B_{22} = -\frac{2}{3a}, \quad \rho_{11} = -\frac{7a}{6} \quad \text{and} \quad c_{11} = \frac{7a}{12}k, \tag{4.141}$$

and the solution is

$$q_{22}(y) = -\frac{1}{a}\left(\frac{13}{6}y^4 + \frac{30}{3}y^3 + \frac{85}{3}y^2 + 7y + \frac{2}{3}\right).$$

Hence the solution to equation (4.113) and (4.114) is

$$\begin{aligned} q_2(y) &= \frac{1}{a}\left(y\left(\frac{7}{6}y^3 + \frac{16}{3}y^2 + \frac{11}{3}y + 2\right) - \alpha\left(\frac{13}{6}y^4 + \frac{30}{3}y^3 + \frac{85}{3}y^2 + 7y + \frac{2}{3}\right) + O(\alpha^2)\right) \\ \rho_1 &= -\frac{a}{3\alpha}\left(2 + \frac{7}{2}\alpha + O(\alpha^2)\right) \quad \text{and} \quad c_1 = -\frac{a\alpha k}{3}\left(2 - \frac{7}{4}\alpha + O(\alpha^2)\right). \end{aligned} \tag{4.142}$$

The full asymptotic solutions of equations (4.86)- (4.80) take the form

$$\begin{aligned} \rho &= \frac{a}{\alpha}\left(2(1 - \frac{\alpha}{2} + O(\alpha^2)) - \varepsilon\frac{1}{3}(2 + \frac{7}{2}\alpha + O(\alpha^2))\right) + O(\varepsilon^2), \\ c &= k\alpha a\left((1 - \frac{\alpha}{2} + O(\alpha^2))\varepsilon - \frac{\varepsilon^2}{3}(2 - \frac{7}{4}\alpha + O(\alpha^2))\right) + O(\varepsilon^3), \\ q(y) &= \frac{1}{a}(1 + \left(-(1 - \alpha + O(\alpha^2)\right)y(y+2) + \alpha\left(1 - \frac{\alpha}{2} + O(\alpha^2)\right)\varepsilon + (y(\frac{7}{6}y^3 \\ &+ \frac{16}{3}y^2 + \frac{11}{3}y + 2) + \alpha\left(-\frac{13}{6}y^4 - \frac{30}{3}y^3 - \frac{85}{3}y^2 - 7y - \frac{2}{3}\right) + O(\alpha^2))\varepsilon^2 + O(\varepsilon^3)). \end{aligned} \tag{4.143}$$

In Figure 4.8 we compare numerical solutions computed using the shooting method and asymptotic approximations. Note excellent agreement for biologically relevant parameter values. Recall that the asymptotic solutions of the corresponding model in

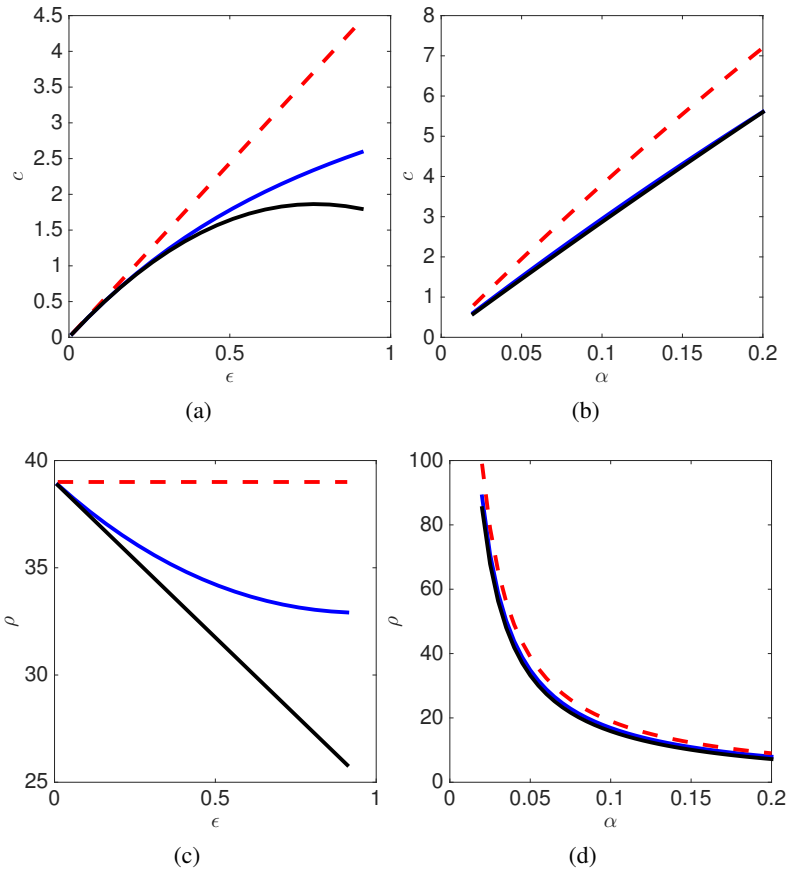

Figure 4.8: Comparing numerical and asymptotic approximations to the wave speed. (a) The wave speed, c, is plotted against ε ($\alpha = 0.05$). (b) The wave speed, c, is plotted against α ($\varepsilon = 0.3$). (c) The proliferation width, ρ, is plotted against ε ($\alpha = 0.05$). (d) The proliferation width, ρ, is plotted against α ($\varepsilon = 0.4$). Numerical solutions (blue solid lines) are computed using a shooting method. Leading order asymptotic solution (dashed lines) and corrections (black solid lines) are given by equations (4.112) and (4.143), respectively. Parameter values as in Table 4 unless otherwise stated.

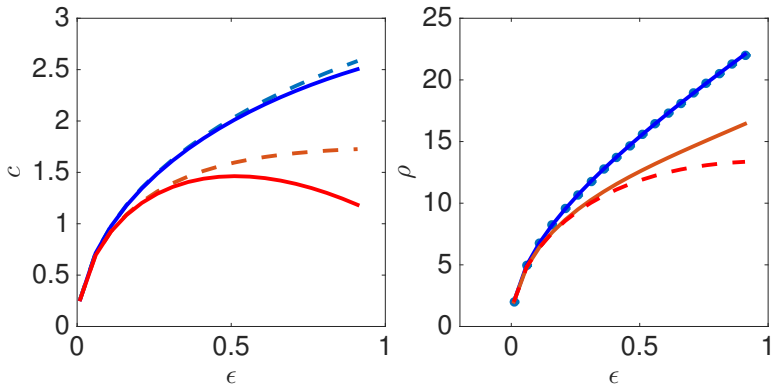

(a) (b)

Figure 4.9: Comparing numerical (dash lines) and asymptotic approximations (solid lines) in the case of constant (equation (4.144), blue) and nonlinear diffusion (equation (4.143), red). (a) The wave speed, c, is plotted against ε. (b) The proliferation width, ρ, is plotted against ε.

in Chapter 3 take the form

$$\rho = \frac{a}{\alpha}\left(2(1-\frac{\alpha}{2}+O(\alpha^2))+\varepsilon\frac{1}{3}(1-\alpha+O(\alpha^2))\right),$$
$$c = ka\alpha\left((1-\frac{\alpha}{2}+O(\alpha^2))\varepsilon-\frac{\varepsilon^2}{6}(1-2\alpha+O(\alpha^2))\right),$$
$$q(y) = \frac{1}{a}(1+\left(-(1-\alpha+O(\alpha^2))y(y+2)+\alpha\left(1-\frac{\alpha}{2}+O(\alpha^2)\right)\right)\varepsilon+(y^2\left(\frac{1}{6}y^2+\frac{4}{3}y+\frac{5}{3}\right)$$
$$-\alpha\frac{1}{3}\left(y^4+8y^3+\frac{27}{2}y^2+7y+\frac{1}{2}\right)+O(\alpha^2))\varepsilon^2)+O(\varepsilon^3). \qquad (4.144)$$

In Figure 4.9, we compare the asymptotic result (4.143) with (4.144). Note that the effect of nonlinear diffusion coefficient in the case of the Robin boundary condition is to reduce the wave speed and the proliferating rim width.

We return the value of α from equation (4.2.2.3)

$$\alpha = \sqrt{\frac{2r}{\varepsilon k}}.$$

Hence the leading order in equation (4.143) for the wave speed, c and proliferation width ρ are

$$\rho = a\sqrt{\frac{2k\varepsilon}{r}}\left(1-\frac{1}{3}\varepsilon\right),$$
$$c = a\sqrt{2rk\varepsilon}\left(1-\frac{2}{3}\varepsilon\right). \tag{4.145}$$

It is worth pointing out the differences of the results between constant diffusion and non linear diffusion model. Note that the results show that at leading order the more complicated model (nonlinear diffusion and nonlinear Robin boundary condition) has the same solution as the simpler model (constant diffusion with Dirichlet boundary condition), however the effects become obvious in higher order of ε. The same results are obtained for leading order approximation with some associated errors.

4.2 General nonlinear diffusion model

In this section we generalise the problem by considering a diffusion coefficient of the form

$$D(q) = \frac{a^2 k}{(aq)^n}. \tag{4.146}$$

We consider three sub cases; the first two allow direct comparison with the previous sections whilst the third satisfies the general form given by equations (1.2)-(1.6).

4.2.1 General nonlinear diffusion with a Dirichlet boundary condition

For the diffusion coefficient given by equation (4.146), equation (1.2) transforms to

$$\frac{\partial q}{\partial t} = \frac{\partial}{\partial x}\left(\frac{a^2 k}{(aq)^n}\frac{\partial q}{\partial x}\right) + rqH(q_c - q), \tag{4.147}$$

and the boundary conditions are

$$\left.\frac{\partial q}{\partial x}\right|_{x=0} = 0, \quad q(s(t),t) = \frac{1}{a} \quad \text{and} \quad \frac{ds}{dt} = -\frac{ka^2}{a^n q^{n+1}(0)}\left.\frac{\partial q}{\partial x}\right|_{x=s(t)}. \tag{4.148}$$

The main questions addressed in this section is what is the effect of changing n in solution approximation.

4.2.1.1 Numerical solution

To investigate the behaviour of equations (4.147)-(4.148), we computed a numerical solution using the Method of Lines (see Section 2.3.3 for implementation details). In Figures 4.10 the numerical solution appears to have a travelling wave solution. We observed there is a non-proliferating core of cells at density q_c. We observed that for increasing n doesn't have effect in the numerical solution, the wave front doesn't change much

.

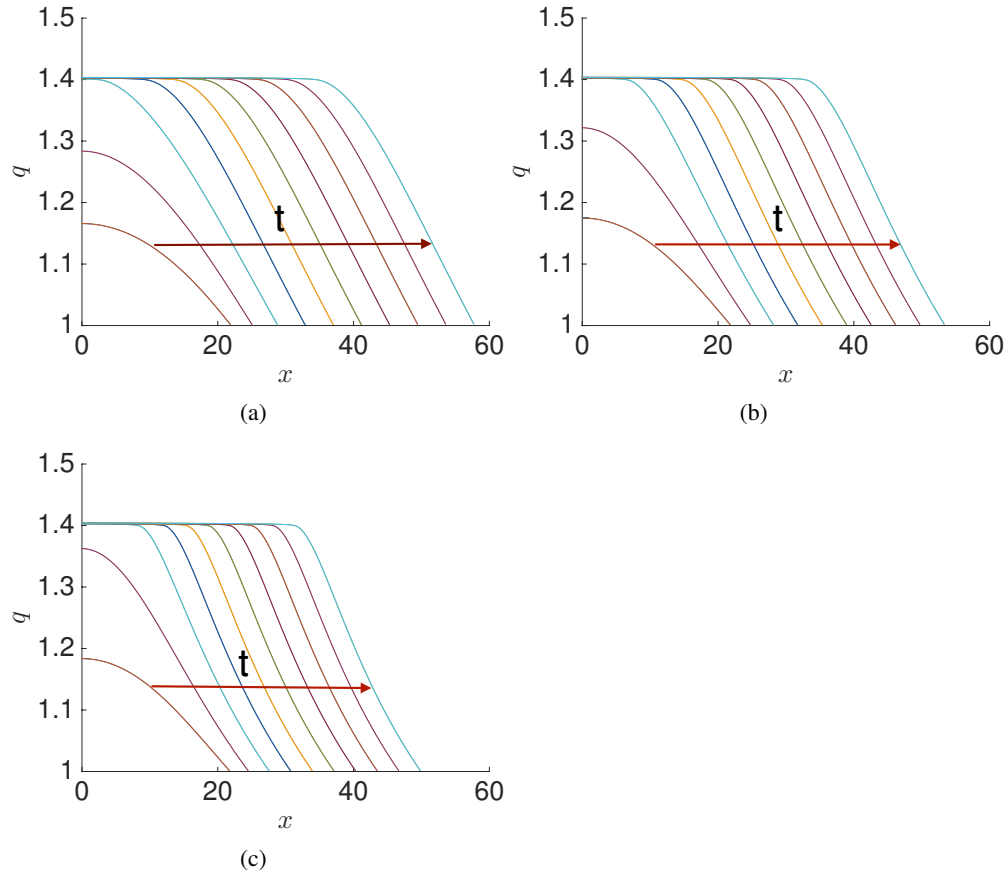

Figure 4.10: Numerical solution of equations (4.147)–(4.148). The cell density, q, is plotted against spatial position, x, at different times, t. (a) $n = 2$, (b) $n = 4$ and (c) $n = 6$. For other parameters see Table 4 .

4.2.1.2 Phase plane solution

We define the travelling wave coordinate $z = x - ct$, where c is the wave speed. Transforming equations (4.147) yields

$$-cq' = \frac{a^2k}{(aq)^n}q'' - \frac{na^2k}{a^n q^{n+1}}q'^2 + rqH(q_c - q), \tag{4.149}$$

with the boundary conditions given by

$$\left.\frac{dq}{dz}\right|_{z\to-\infty} = 0, \quad q(0) = \frac{1}{a} \quad \text{and} \quad \left.\frac{dq}{dz}\right|_{z=0} = -\frac{ca^n q(0)^{n+1}}{a^2k}. \tag{4.150}$$

Again, I define

$$\bar{z} = z - \rho,$$

and

$$u = q \quad \text{and} \quad v = \frac{dq}{d\bar{z}}, \tag{4.151}$$

equations (4.149)–(4.150) transform to

$$\begin{aligned} \frac{du}{d\bar{z}} &= v \\ \frac{dv}{d\bar{z}} &= -\frac{(au)^n}{a^2k}\left(n\frac{a^{2-n}k}{u^{n+1}}v^2 + cv + ru\right). \end{aligned} \tag{4.152}$$

The initial conditions are

$$u(0) = q_c \quad \text{and} \quad v(0) = 0. \tag{4.153}$$

For a given initial guess for c, we numerically identify ρ such that

$$u(\rho) = \frac{1}{a}. \tag{4.154}$$

We then seek a solution that satisfies

$$v(\rho) = -\frac{c\rho a^n u(\rho)^{n+1}}{a^2 k} = -\frac{c\rho}{a^3 k}, \tag{4.155}$$

by minimising the function

$$E(c) = \left(v(\rho) + \frac{c\rho a^n u(\rho)^{n+1}}{a^2 k} \right)^2. \tag{4.156}$$

Figure 4.11 shows numerically that there is unique wave speed, c^*, with a representative solution trajectory in the phase plane. We can clearly see that the wave speed, c increase over a range of parameter values. Note that wave speed approches zero as $n \to \infty$. The goal of the rest of this section is to derive approximate expressions for the wave speed and proliferating rim width using perturbation methods.

4.2.1.3 Perturbation method

Following a similar argument to that proposed in Section 3.2.3, we make change of independent variable

$$y = \frac{z}{\rho}. \tag{4.157}$$

Substituting (4.157) in equations (4.149)-(4.150) yields

$$-c\rho \frac{dq}{dy} = \frac{a^2 k}{(aq)^n} \frac{d^2 q}{dy^2} - \frac{n a^2 k}{a^n q^{(n+1)}} \left(\frac{dq}{dy} \right)^2 + r\rho^2 q, \tag{4.158}$$

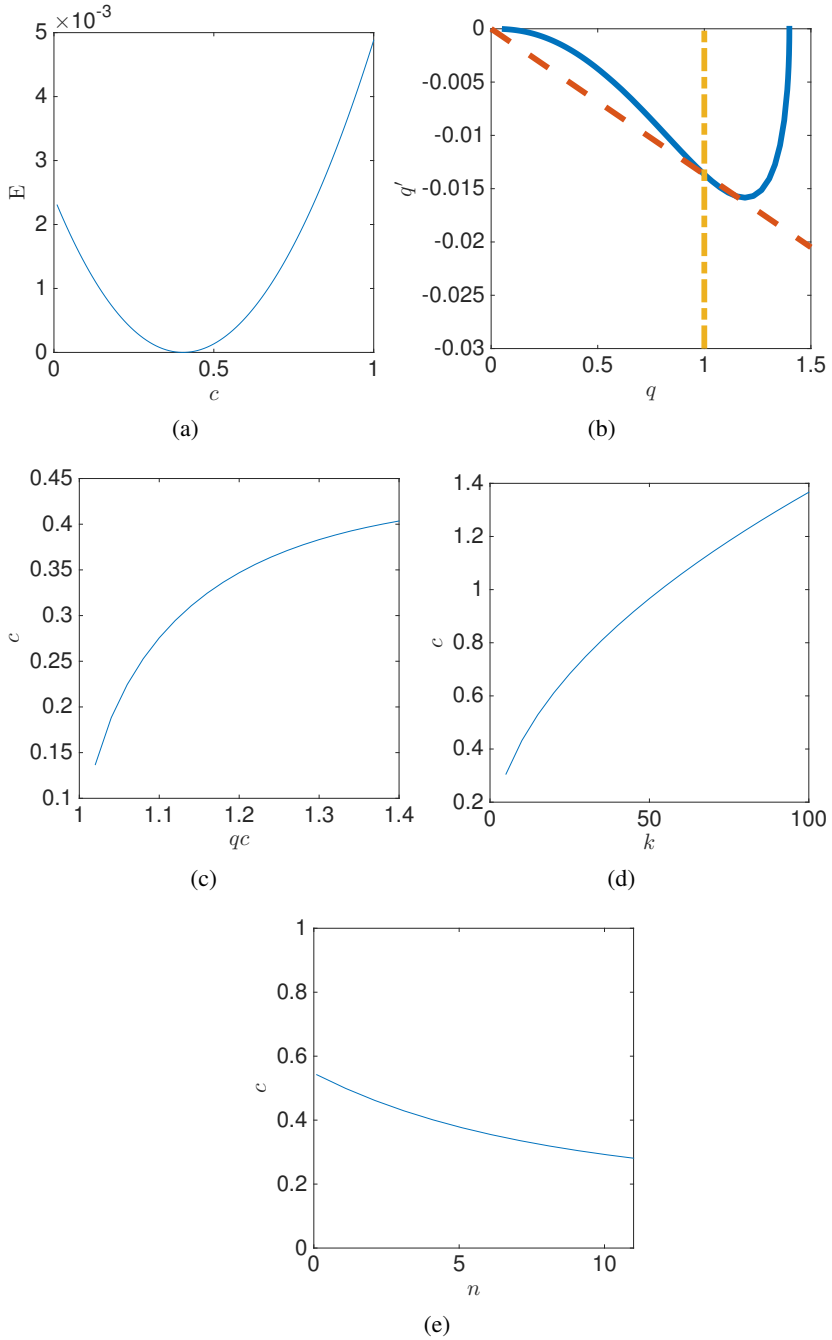

Figure 4.11: Using a shooting method to compute wave speed, c. (a) A unique wave speed, c^*, is identified using a shooting method. Error, $E(c)$, is plotted against wave speed, c (equation (4.156)). (b) A representative phase plane trajectory is presented for wave speed $c = c^*$. q' is plotted against q. Equations (4.152) were solved numerically (blue lines) with boundary condition (4.154)-(4.155). (c) The wave speed, c, is plotted against the proliferation threshold, q_c. (d) The wave speed, c, plotted against k. (e) The wave speed, c, is plotted against n. Other parameter values as in Table 4.

with boundary conditions

$$q(-1) = q_c, \tag{4.159}$$

$$q'(-1) = 0, \tag{4.160}$$

$$q(0) = \frac{1}{a}, \tag{4.161}$$

$$q'(0) = -\frac{c\rho a^n q(0)^{n+1}}{a^2 k}. \tag{4.162}$$

Motivated by the exact solution derived in Section 3.1.3 we define

$$q_c = \frac{1}{a} e^{\varepsilon}, \tag{4.163}$$

where ε is a small parameter.

Expand boundary condition (4.159) yields

$$q(-1) = \frac{1}{a} e^{\varepsilon} = \frac{1}{a} \left(1 + \varepsilon + \frac{1}{2}\varepsilon^2 + O(\varepsilon^3) \right). \tag{4.164}$$

Hence we seek an expansion in integer powers of epsilon, i.e.

$$q = q_0 + \varepsilon q_1 + \varepsilon^2 q_2 + O(\varepsilon^3).$$

Substituting the proposed expansion for q in boundary condition (4.162) and rearranging, we obtain that c and ρ must also be expansions in powers of ε, i.e.

$$c = c_0 \varepsilon + \varepsilon^2 c_1 + O(\varepsilon^3).$$

$$\rho = \rho_0 + \varepsilon\rho_1 + O(\varepsilon^2).$$

Finally, balancing diffusion and proliferation terms at leading order

$$\frac{a^2k}{(aq)^n}\left(\frac{d^2q}{dy^2}\right) \sim rq\rho. \tag{4.165}$$

Substituting for q and ρ and rearranging yields the scaling relationship

$$\frac{r}{k} \propto \varepsilon.$$

Following a similar argument that proposed in Section 4.1.1.3,

$$r = \frac{\alpha^2\varepsilon k}{2}, \tag{4.166}$$

where $\alpha \ll 1$.

Substituting equation (4.166) in equation (4.158) where $\alpha \ll 1$ yields

$$-c\rho\frac{dq}{dy} = \frac{a^{2-n}k}{q^n}\frac{d^2q}{dy^2} - \frac{na^{2-n}k}{q^{n+1}}\left(\frac{dq}{dy}\right)^2 + \frac{\alpha^2\varepsilon k}{2}\rho^2 q. \tag{4.167}$$

We propose asymptotic solutions to equation (4.167) of the form

$$\begin{aligned} c &= c_0\varepsilon + c_1\varepsilon^2 + O(\varepsilon^3), \\ \rho &= \rho_0 + \rho_1\varepsilon + O(\varepsilon^2), \\ q &= q_0(y) + q_1(y)\varepsilon + q_2(y)\varepsilon^2 + O(\varepsilon^3). \end{aligned} \tag{4.168}$$

Substituting equation (4.168) into equation (4.167) yields

$$\begin{aligned}
&-(c_0\varepsilon + c_1\varepsilon^2)(\rho_0 + \rho_1\varepsilon^2)(q_0'(y) + q_1'(y)\varepsilon + q_2'(y)\varepsilon^2) = \\
&-\frac{na^{2-n}k}{q_0^{n+1}}(1-(n+1)\varepsilon\frac{q_1}{aq_0})(q_0(y)' + \varepsilon q_1'(y) + \varepsilon^2 q_2'(y))^2 \\
&+\frac{a^2k}{(aq_0)^n}(1-n\varepsilon\frac{q_1}{aq_0})(q_0''(y) + q_1''(y)\varepsilon + q_2''(y)\varepsilon^2) \\
&+\frac{k\alpha^2\varepsilon}{2}(q_0(y) + \varepsilon q_1(y) + q_2\varepsilon^2)(\rho_0 + \varepsilon\rho_1)^2. \qquad (4.169)
\end{aligned}$$

Substituting equation (4.168) into boundary conditions (4.159)-(4.162), and expanding the right-hand sides, yields

$$\begin{aligned}
&q_0(-1) + q_1(-1)\varepsilon + q_2(-1)\varepsilon^2 = \frac{1}{a}e^{\varepsilon} = \frac{1}{a}\left(1 + \varepsilon + \frac{1}{2}\varepsilon^2\right), \\
&q_0'(-1) + q_1'(-1)\varepsilon + q_2'(-1)\varepsilon^2 = 0, \\
&q_0(0) + q_1(0)\varepsilon + q_2(0)\varepsilon^2 = \frac{1}{a} \quad \text{and} \\
&q_0'(0) + q_1'(0)\varepsilon + q_2'(0)\varepsilon^2 = -\frac{\left(c_0\rho_0\varepsilon + (\rho_0 c_1 + \rho_1 c_0)\,\varepsilon^2\right)}{a^3k}. \qquad (4.170)
\end{aligned}$$

At O(1)

$$\left(\frac{a^2k}{(aq_0)^n}q_0'\right)' = 0, \qquad (4.171)$$

and the boundary conditions are

$$q_0(-1) = \frac{1}{a}, \quad q_0(0) = \frac{1}{a} \quad q_0'(-1) = 0 \quad \text{and} \quad q_0'(0) = 0. \qquad (4.172)$$

Integration of equation (4.171) yields

$$\frac{a^2k}{(aq_0)^n}q_0'(y) = \hat{A}_0. \qquad (4.173)$$

Hence

$$q_0' = \frac{\hat{A_0} a^n q_0^n}{a^2 k},$$

Integrating yields

$$-\frac{1}{n+1} q_0^{-n+1} = \frac{\hat{A_0} a^{n-2}}{k} y + \hat{B_0},$$

where $\hat{A_0}$ and B_0 are integration constants.

Hence

$$q_0(y) = \left(-(1+n) \frac{\hat{A_0} a^{n-2}}{k} y + \hat{B_0} \right)^{\frac{1}{1-n}}. \tag{4.174}$$

Application of boundary conditions (4.172) yields

$$\hat{A_0} = 0 \quad \text{and} \quad \hat{B_0} = \frac{1}{a}. \tag{4.175}$$

Hence

$$q_0(y) = \frac{1}{a}.$$

At $O(\varepsilon)$ we obtain

$$q_1''(y) = -\frac{\alpha^2 \rho_0^2}{2a^3}, \tag{4.176}$$

with boundary conditions

$$q_1(0) = 0, \tag{4.177}$$

$$q_1(-1) = \frac{1}{a}, \tag{4.178}$$

$$q_1'(-1) = 0, \tag{4.179}$$

$$q_1'(0) = -\frac{c_0\rho_0}{a^3k}. \tag{4.180}$$

The general solution to equation (4.176) is

$$q_1(y) = -\frac{\alpha^2\rho_0^2}{4a^3}y^2 + A_1y + B_1, \tag{4.181}$$

where A_1 and B_1 are integration constants.

Applying boundary conditions (4.177) yields

$$B_1 = 0. \tag{4.182}$$

Applying boundary condition (4.178) yields

$$A_1 = -\left(\frac{1}{a} + \frac{\alpha^2\rho_0^2}{4a^3}\right). \tag{4.183}$$

Applying boundary condition (4.179) yields

$$A_1 = -\frac{\alpha^2\rho_0^2}{2a^3}. \tag{4.184}$$

Applying boundary condition (4.180) yields

$$A_1 = -\frac{c_0\rho_0}{a^3k}. \tag{4.185}$$

Hence

$$A_1 = -\frac{2}{a}, \quad \rho_0 = \frac{2}{\alpha}a, \quad c_0 = ka\alpha, \quad \text{and} \quad q_1 = -\frac{1}{a}\left(y^2 + 2y\right). \tag{4.186}$$

At O(ε^2) we obtain

$$-c_0\rho_0 q_1' = \frac{-na^2k}{a^n q_0^{n+1}} q_1'^2 + \frac{a^2k}{(aq_0)^n} q_2'' - nka^{2-n}\frac{q_1}{q_0^{2n}} q_1'' + \frac{k\alpha^2}{2} q_1\rho_0^2 + k\alpha^2 q_0\rho_0\rho_1, \tag{4.187}$$

with boundary conditions

$$q_2'(-1) = 0, \tag{4.188}$$

$$q_2(0) = 0, \tag{4.189}$$

$$q_2(-1) = \frac{1}{2a}, \tag{4.190}$$

$$q_2'(0) = -\frac{1}{a^3k}(c_0\rho_1 + c_1\rho_0). \tag{4.191}$$

Substituting for c_0, ρ_0 and q_1 from equations (4.186) into equation (4.187) yields

$$q_2'' = \frac{1}{a}\left(4(y+1) + n(2y+2)^2 + 2n(y^2+2y) + 2(y^2+2y) - 2\alpha\rho_1\right). \tag{4.192}$$

Rearranging

$$q_2'' = \frac{1}{a}\left((6n+2)\,y^2 + (8+12n)\,y + (4n+4) - 2\alpha\frac{\rho_1}{a}\right).$$

Integration of equation (4.192) yields

$$q_2' = \frac{1}{a}\left((6n+2)\,\frac{y^3}{3} + (8+12n)\,\frac{y^2}{2} + \left((4n+4) - 2\alpha\frac{\rho_1}{a}\right)y\right) + A.$$

A further integration yields

$$q_2 = \frac{1}{a}\left(\frac{(6n+2)}{12}y^4 + \frac{(8+12n)}{6}y^3 + \left(4n+4-2\alpha\frac{\rho_1}{a}\right)\frac{y^2}{2}\right) + Ay + B,$$

where A and B integration constants.

Applying boundary condition (4.189)

$$B = 0. \tag{4.193}$$

Applying boundary condition (4.190) yields

$$A = \frac{1}{a}\left(\frac{1}{2}n + \frac{1}{3} - \alpha\frac{\rho_1}{a}\right). \tag{4.194}$$

Applying boundary condition (4.188) yields

$$A = \frac{1}{a}\left(\frac{2}{3} - 2\alpha\frac{\rho_1}{a}\right). \tag{4.195}$$

Equating equations (4.194) and (4.195) yields

$$\rho_1 = \frac{(\frac{1}{3} - \frac{1}{2}n)}{\alpha}a.$$

Applying boundary condition (4.191)

$$A = -\frac{1}{a^3 k}\left(ka^2\left(\frac{1}{3} - \frac{1}{2}\right) + c_1\frac{2a}{\alpha}\right). \tag{4.196}$$

Rearranging yields

$$c_1 = -\frac{a\alpha k}{2}\left(\frac{1}{3} + \frac{n}{2}\right).$$

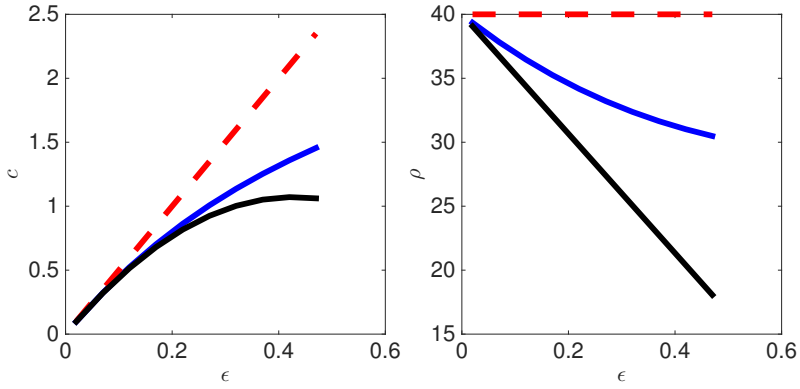

(a) (b)

Figure 4.12: Comparing numerical and asymptotic approximations to the wave speed. (a) The wave speed, c, is plotted against ε. (b) The proliferation width, ρ, is plotted against ε. Numerical solution-blue solid line. Leading order asymptotic solution (dash lines) and corrections (black solid lines) are given by equations (4.186) and (4.197), respectively. $\alpha = 0.05$ and $n = 4$, other parameter values as in Table 4.

Hence the asymptotic solution for the case of a the general nonlinear diffusion coefficient and a Dirichlet boundary condition is given by

$$\rho = \frac{a}{\alpha}\left(2 - \left(\frac{1}{3}+\frac{1}{2}n\right)\varepsilon + O(\varepsilon^2)\right),$$
$$c = a\alpha k\left(\varepsilon - \frac{1}{2}\left(\frac{1}{3}+\frac{1}{2}n\right)\varepsilon^2 + O(\varepsilon^3)\right),$$
$$q(y) = \frac{1}{a}\left(1 - y(y+2)\varepsilon + y\left(\frac{6n+2}{12}y^3 + \frac{8+12n}{6}y^2 + \left(\frac{10}{3}+5n\right)\frac{y}{2} + n\right)\varepsilon^2 + O(\varepsilon^3)\right). \tag{4.197}$$

In Figure 4.12, we compare shooting method solution in phase plane and asymptotic approximations for a wave speed c. We observe a good agreement between asymptotic solution approximation and numerical solution.

In Figure 4.13, we compare shooting method and asymptotic approximations for the

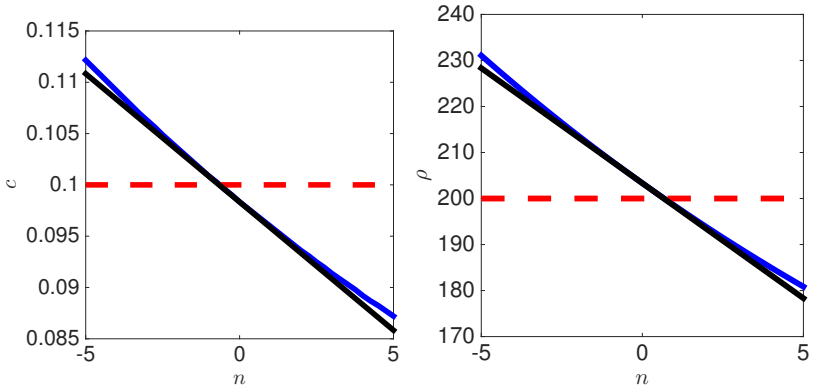

Figure 4.13: Comparing numerical and asymptotic approximations to the wave speed, c, and proliferation width, ρ. (a) The wave speed, c, is plotted against n. (b) The proliferation width, ρ, is plotted against n. Leading order asymptotic solution (dashed lines) and corrections (black solid lines) are given by equations (4.186) and (4.197), respectively. $\varepsilon = 0.1$ and $\alpha = 0.01$, other parameter values as in Table 4.

wave speed, c, and proliferation width, ρ, with different value of n. Note that equation (4.197) yields the result obtained in nonlinear spring modle in the spacial case where $n = 2$.

Note that we observe slower wave fronts with smaller proliferating rims with increasing n. However, the effect is not apparent at leading order.

Return (4.197) to original parameters the solution at leading order

$$\rho = a\sqrt{\frac{k\varepsilon}{2r}} \quad c = a\sqrt{2rk\varepsilon}.$$

4.2.2 A general nonlinear diffusion with a Robin boundary condition

Here we consider the case of the generalised diffusion coefficient with a Robin boundary condition. Substituting for diffusion coefficient (4.146) in equation (1.2) yields

$$\frac{\partial q}{\partial t} = \frac{\partial}{\partial x}\left(\frac{a^2 k}{(aq)^n}\frac{\partial q}{\partial x}\right) + rqH(q_c - q). \tag{4.198}$$

The boundary conditions are

$$\left.\frac{\partial q}{\partial x}\right|_{x=0} = 0, \quad \left.\frac{\partial q}{\partial x}\right|_{x=s(t)} = -\frac{ds}{dt}\frac{a^n q(s(t),t)^{n+1}}{a^2 k} \quad \text{and} \quad \frac{ds}{dt} = k\left(a - \frac{1}{q(s(t),t)}\right). \tag{4.199}$$

and the initial conditions satisfy

$$q(x,0) = f(x) \quad \text{and} \quad s(0) = s_0. \tag{4.200}$$

4.2.2.1 Numerical solution

The numerical solutions of equations (4.198)–(4.200) was computed using the Method of Lines (see Section 2.3.3). Representative results are plotted in Figure 4.14. The numerical analysis suggests a travelling wave solution with a constant front speed. Behind the wave front, there is a non-proliferating core of cells at density, q_c. At the front there is a proliferating rim of fixed width that propagates with a constant wave speed. Note that the wave speed decreses with the parameter n.

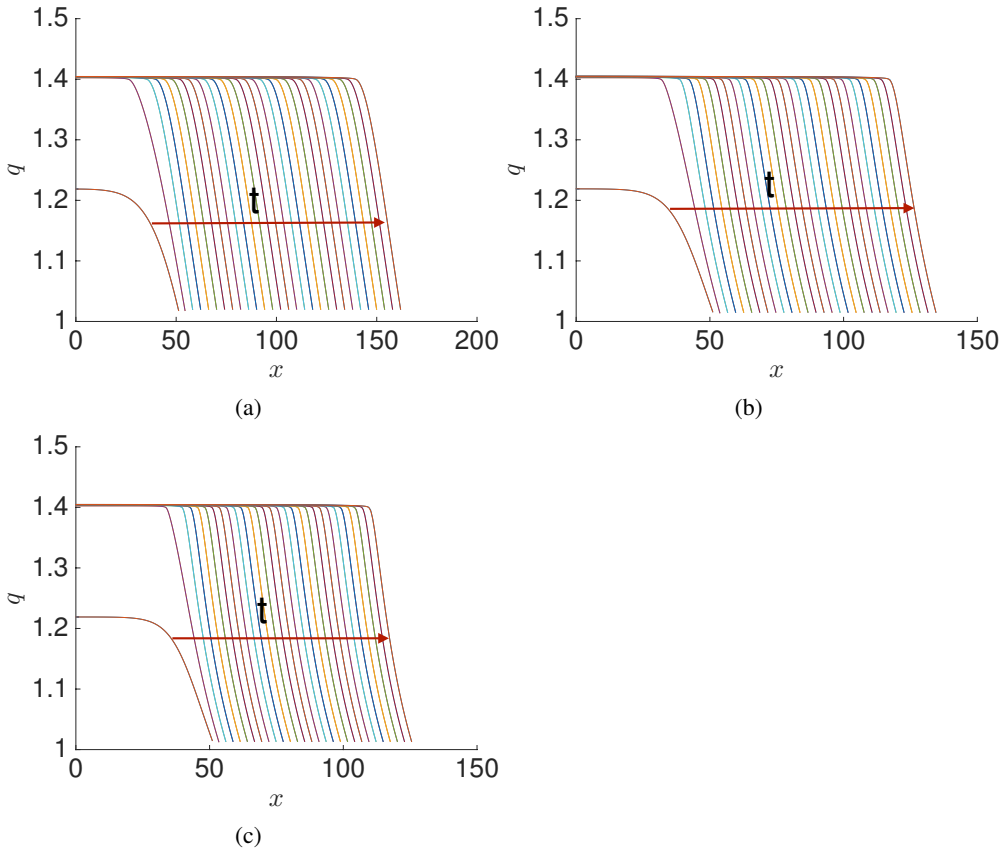

Figure 4.14: Numerical solution of equations (4.198)–(4.200). The cell density, q, is plotted against spatial position, x, at different times, t. (a) $n = 2$, (b) $n = 6$ and (c) $n = 10$, other parameters values in Table 4.

4.2.2.2 Phase plane solution

We define the travelling wave coordinate $z = x - ct$, where c is the wave speed. Transforming equations (4.198)

$$-cq' = \frac{a^2 k}{(aq)^n} q'' - \frac{n a^{2-n} k}{q^{n+1}} q'^2 + rqH(q_c - q), \tag{4.201}$$

and the boundary conditions (4.199) are given by

$$\left.\frac{dq}{dz}\right|_{z\to-\infty} = 0, \quad q(0) = \frac{1}{a(1-\frac{c}{ak})} \quad \text{and} \quad \left.\frac{dq}{dz}\right|_{z=0} = -\frac{ca^n}{a^2 k}\left(\frac{1}{a(1-\frac{c}{ak})}\right)^{n+1}. \tag{4.202}$$

Again, I define

$$\bar{z} = z - \rho,$$

and

$$u = q \quad \text{and} \quad v = \frac{dq}{d\bar{z}}, \tag{4.203}$$

equations (4.201)–(4.202) transform to

$$\begin{aligned} \frac{du}{d\bar{z}} &= v, \\ \frac{dv}{d\bar{z}} &= -\frac{(au)^n}{a^2 k}\left(n\frac{a^{2-n}k}{u^{n+1}}v^2 + cv + ru\right). \end{aligned} \tag{4.204}$$

The initial conditions are

$$u(0) = q_c \quad \text{and} \quad v(0) = 0. \tag{4.205}$$

For a given initial guess for c we numerically identify ρ such that

$$u(\rho) = \frac{1}{a(1-\frac{c}{ak})}. \tag{4.206}$$

We then seek a solution that satisfies

$$v(\rho) = -\frac{ca^n}{a^2k}\left(\frac{1}{a(1-\frac{c}{ak})}\right)^{n+1}, \tag{4.207}$$

by minimising the function

$$E(c) = \left(v(\rho) + \frac{ca^n}{a^2k}\left(\frac{1}{a(1-\frac{c}{ak})}\right)^{n+1}\right)^2. \tag{4.208}$$

In Figure 4.15 we plot representative results from the shooting method. In Figure 4.15 (a) we plot the error defined in equation (4.208) against a range of values for the unknown wave speed c. Note that there is a unique minimum. In Figure 4.15 (b)a solution of equations (4.204) in the phase plane. Note that solution trajectories originate at point $(q_c, 0)$. In Figure 4.15 (c) and (d) we plot the computed wave speed as a function of the model parameters q_c and n. Note that the wave speed does not change very much with the parameter n.

4.2.2.3 Perturbation method

Making a change of independent variable

$$y = \frac{z}{\rho},$$

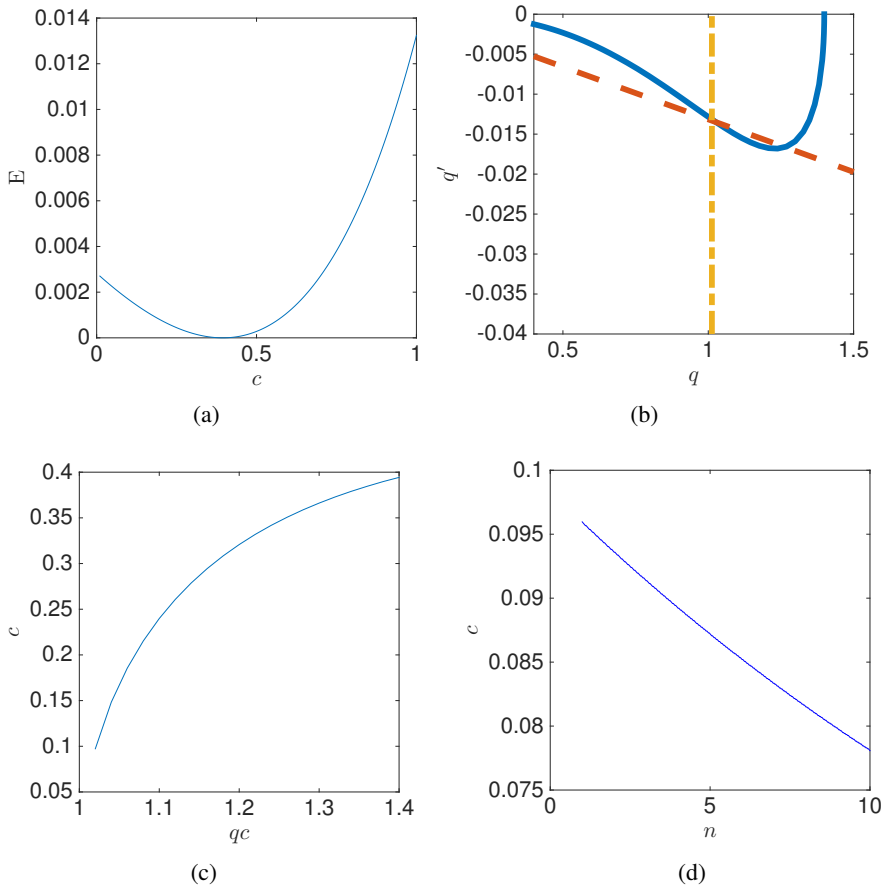

Figure 4.15: Using a shooting method to compute wave speed, c. (a) A unique wave speed, c^*, is identified using a shooting method. Error, $E(c)$, is plotted against wave speed, c (see equation (4.208)). (b) A representative phase plane trajectory is presented for wave speed $c = c^*$. q' is plotted against q. Equations (4.204) were solved numerically (blue line). Red and yellow lines represent boundary conditions (4.206) and (4.207), respectively. (c) The wave speed, c, is plotted against the proliferation threshold density, q_c. (d) The wave speed, c, is plotted against n. Other parameter values as in Table 4.

equation (4.201) transforms to

$$-c\rho\frac{dq}{dy} = \frac{a^2k}{(aq)^n}\frac{d^2q}{dy^2} - \frac{na^2k}{a^nq^{n+1}}\left(\frac{dq}{dy}\right)^2 + r\rho^2q. \tag{4.209}$$

The boundary conditions (4.202) transform to

$$q(-1) = \frac{1}{a}e^{\varepsilon}, \tag{4.210}$$

$$q'(-1) = 0, \tag{4.211}$$

$$q(0) = \frac{1}{a\left(1-\frac{c}{ak}\right)}, \tag{4.212}$$

$$q'(0) = -\frac{a^nc\rho}{a^2k}q^{n+1}(0). \tag{4.213}$$

We follow a similar argument to that proposed in Section 3.2.3.

Assuming that

$$q_c = \frac{1}{a}e^{\varepsilon}, \tag{4.214}$$

where ε is a small parameter and expanding boundary condition (4.77) yields

$$q(-1) = \frac{1}{a}e^{\varepsilon} = \frac{1}{a}(1+\varepsilon+\frac{1}{2}\varepsilon^2+O(\varepsilon^3)). \tag{4.215}$$

Hence we propose that q is an expansion in integer powers of ε, i.e

$$q = q_0 + \varepsilon q_1 + \varepsilon^2 q_2 + O(\varepsilon^3).$$

Substituting the proposed expansion for q in boundary condition (4.212) and rearranging, we obtain that c must also be an expansion in powers of ε, i.e.

$$c = c_0\varepsilon + \varepsilon^2 c_1 + O(\varepsilon^3).$$

Substituting the proposed expansions for c and q in boundary condition (4.213) and rearranging, we find that ρ must be an expansion of the form

$$\rho = \rho_0 + \varepsilon\rho_1 + O(\varepsilon^2).$$

Finally, balancing diffusion and proliferation terms at leading order we obtain

$$\frac{a^{2-n}k}{q^n} q'' \sim rq\rho. \tag{4.216}$$

Substituting for q and ρ and $D(q)$ and rearranging yields

$$\frac{r}{k} \propto \varepsilon.$$

Assuming that the proliferation timescale $\left(\frac{1}{r}\right)$ is much longer than the diffusion timescale is $\left(\frac{1}{k}\right)$, we assume

$$r = \frac{\alpha^2 \varepsilon k}{2},$$

where $\alpha \ll 1$.

In summary, we propose asymptotic solutions of equation (4.76)

$$\begin{aligned} c &= c_0\varepsilon + c_1\varepsilon^2 + O(\varepsilon^3), \\ \rho &= \rho_0 + \rho_1\varepsilon + O(\varepsilon^2), \\ q &= q_0(y) + q_1(y)\varepsilon + q_2(y)\varepsilon^2 + O(\varepsilon^3). \end{aligned} \tag{4.217}$$

Substituting r in (4.209) yields

$$-c\rho q' = \frac{a^2k}{(aq)^n}q'' - \frac{na^2k}{a^n q^{n+1}}q'^2 + \frac{\alpha^2\varepsilon k}{2}\rho^2 q. \tag{4.218}$$

Substituting equation (4.217) into equation (4.218) yield and expanding

$$\begin{aligned} -(c_0\varepsilon + c_1\varepsilon^2)(\rho_0 + \rho_1\varepsilon^2)(q_0'(y) + q_1'(y)\varepsilon + ..) = \\ -\frac{na^{2-n}k}{q_0^{n+1}}(1-(n+1)\varepsilon\frac{q_1}{q_0})(q_0(y)' + \varepsilon q_1'(y))^2 \\ +\frac{a^{2-n}k}{q_0^n}(1-n\varepsilon\frac{q_1}{q_0})(q_0''(y) + q_1''(y)\varepsilon + ..) + \frac{k\alpha^2\varepsilon}{2}(q_0(y) + \varepsilon q_1(y))(\rho_0 + \varepsilon\rho_1)^2. \end{aligned} \tag{4.219}$$

Substituting the series (4.217) in the boundary conditions (4.210)-(4.213) yields

$$\begin{aligned} q_0(-1) + q_1(-1)\varepsilon + q_2(-1)\varepsilon^2 &= \frac{1}{a}\left(1 + \varepsilon + \frac{1}{2}\varepsilon^2\right) \\ q_0'(-1) + q_1'(-1)\varepsilon + q_2'(-1)\varepsilon^2 &= 0 \\ q_0(0) + q_1(0)\varepsilon + q_2(0)\varepsilon^2 &= \frac{1}{a}\left(1 + \frac{c_0}{ak}\varepsilon + \left(\frac{c_1}{ak} + \frac{c_0^2}{a^2k^2}\right)\varepsilon^2\right) \\ q_0'(0) + q_1'(0)\varepsilon + q_2'(0)\varepsilon^2 &= -\frac{a^{n-2}}{k}q_0(0)^{n+1} \\ &\quad \left(c_0\rho_0\varepsilon + \left(c_1\rho_0 + \rho_1 c_0 + \frac{(n+1)}{q_0(0)}c_0\rho_0 q_1(0)\right)\varepsilon^2\right). \end{aligned} \tag{4.220}$$

At $O(1)$ and $O(\varepsilon)$ we have the solution obtained in Section 4.1.2.3 i.e .

$$\rho_0 = \frac{a}{\alpha}\left(2(1-\frac{\alpha}{2}+O(\alpha^2))\right), \quad c_0 = ka\alpha\left((1-\frac{\alpha}{2}+O(\alpha^2)\right),$$
$$q_0(y) = \frac{1}{a} \qquad \text{and} \qquad q_1(y) = \frac{1}{a}\left(-(1-\alpha+O(\alpha^2)\right)y(y+2)+\alpha(1-\frac{\alpha}{2}+O(\alpha^2)). \tag{4.221}$$

At O(ε^2) the governing equation is

$$-c_0\rho_0 q_1' = -\frac{na^{2-n}k}{q_0^{n+1}}q_1'^2 + \frac{a^2k}{(a^nq_0)^n}q_2'' - na^{2-n}k\frac{q_1}{q_0}q_1'' + \frac{k\alpha^2}{2}q_1\rho_0^2 + k\alpha^2 q_0\rho_0\rho_1, \tag{4.222}$$

with boundary conditions given by

$$q_2'(-1) = 0, \quad q_2(0) = \frac{c_1}{a^2k} + \frac{c_0^2}{a^3k^2}, \quad q_2(-1) = \frac{1}{2a},$$
$$q_2'(0) = -\frac{1}{a^3k}\left(c_1\rho_0 + \rho_1 c_0 + a(n+1)c_0\rho_0 q_1(0)\right). \tag{4.223}$$

Following Section 4.2.1.3, we seek series solution of the form

$$q_2 = q_{21} + \alpha q_{22} + O(\alpha^2),$$
$$c_1 = c_{01}\alpha + c_{11}\alpha^2 + O(\alpha^3),$$
$$\rho_1 = \frac{1}{\alpha}\left(\rho_{01} + \alpha\rho_{11} + O(\alpha^2)\right). \tag{4.224}$$

We substitute the series in α equation (4.224) in equations (4.222)- (4.223).

$$q_{21}'' + q_{22}''\alpha = \frac{1}{a}\left((6n+2)y^2 + (12n+8)y + (4+4n-2\rho_{01})\right) + \frac{\alpha}{a}\left(-(11n+4)y^2 - (22n+16)y - \left(\frac{21}{2} + \frac{29}{3} + 2\rho_{11}\right)\right). \tag{4.225}$$

The boundary conditions are

$$\begin{aligned} q_{21}(0) + q_{22}(0)\alpha &= \frac{c_{01}}{a^2 k}\alpha, \\ q_{2!}(-1) + q_{22}(-1)\alpha &= \frac{1}{2a}, \\ q_{21}(-1)' + q_{22}(-1)'\alpha &= 0, \\ q_{21}(0)' + q_{22}(0)'\alpha &= \\ -\frac{1}{a^3 k}&\left((ak\rho_{01} + 2ac_{01}) + \alpha\left(ak\rho_{11} - \frac{1}{2}k\rho_{01} + 2ac_{11} - c_{01} + (2n+2)\,a^2 k\right)\right). \end{aligned} \tag{4.226}$$

At $O(1)$

$$q_{21}'' = \frac{1}{a}\left((6n+2)y^2 + (12n+8)y + (4+4n-2\rho_{01})\right). \tag{4.227}$$

The boundary conditions are

$$q_{21}(0) = 0, \tag{4.228}$$

$$q_{21}(-1) = \frac{1}{2a}, \tag{4.229}$$

$$q_{21}'(-1) = 0, \tag{4.230}$$

$$q'_{21}(0) = -\frac{1}{a^3 k}(ak\rho_{01} + 2ac_{01}). \tag{4.231}$$

Integration of equation (4.227) yields

$$q'_{21}(y) = \frac{1}{a}\left(\frac{(6n+2)}{3}y^3 + (4+6n)y^2 + (4+4n-2\rho_{01})y\right) + A_{21}. \tag{4.232}$$

A further integration of equation (4.227) yields

$$q_{21}(y) = \frac{1}{a}\left(\frac{(6n+2)}{12}y^4 + \frac{(4+6n)}{3}y^3 + (2+2n-\rho_{01})y^2\right) + A_{21}y + B_{21}, \tag{4.233}$$

where A_{21} and B_{21} are integration constants.

Application of boundary condition (4.228) yields

$$B_{21} = 0.$$

Application of boundary condition (4.230) yields

$$A_{21} = \frac{1}{a}\left(\frac{2}{3} - 2\frac{\rho_{01}}{a}\right). \tag{4.234}$$

Application of boundary condition (4.229) yields

$$A_{21} = \frac{1}{a}\left(\frac{1}{2}n + \frac{1}{3} - \frac{\rho_{01}}{a}\right). \tag{4.235}$$

Application of boundary condition (4.231) yields

$$A_{21} = -\frac{1}{a^3 k}(ak\rho_{01} + 2ac_{01}).$$

Solving for A_{21}, B_{21}, ρ_{01} and c_{01} we find

$$A_{21} = \frac{n}{a}, \quad B_{21} = 0, \quad \rho_{01} = a\left(\frac{1}{3} - \frac{1}{2}n\right) \quad \text{and} \quad c_{01} = -\frac{1}{2}\left(\frac{1}{3} + \frac{1}{2}n\right)ak. \tag{4.236}$$

The solution for $q_{21}(y)$ is

$$q_{21}(y) = \frac{1}{a}y\left(\frac{3n+1}{6}y^3 + \frac{4+6n}{3}y^2 + 5\left(\frac{1}{3} + \frac{1}{2}n\right)y + n\right).$$

At O(α):

$$q''_{22}(y) = \frac{1}{a}\left(-(11n+4)y^2 - (22n+16)y - \left(\frac{21}{2} + \frac{29}{3} + 2\rho_{11}\right)\right). \tag{4.237}$$

The boundary conditions are

$$q_{22}(0) = \frac{c_{01}}{a^2k}, \tag{4.238}$$

$$q_{22}(-1) = 0, \tag{4.239}$$

$$q'_{22}(-1) = 0, \tag{4.240}$$

$$q'_{22}(0) = -\frac{1}{a^3k}\left(ak\rho_{11} - \frac{1}{2}k\rho_{01} + 2ac_{11} - c_{01} + (2n+2)a^2k\right). \tag{4.241}$$

Integration of equation (4.237) yields

$$q'_{22}(y) = \frac{1}{a}\left(-\frac{(11n+4)}{3}y^3 - (11n+8)y^2 - y\left(\frac{21}{2}n - \frac{29}{3} + 2\rho_{11}\right)\right) + A_{22}.$$

A further integration yields the general solution to equation (4.237)

$$q_{22} = \frac{1}{a}\left(-\frac{(11n+4)}{12}y^4 - \frac{(11n+8)}{3}y^3 - \left(\frac{21}{4}n + \frac{29}{6} + \rho_{11}\right)y^2\right) + A_{22}y + B_{22}, \tag{4.242}$$

where A_{22} and B_{22} are integration constants.

Application of boundary condition (4.238) yields

$$B_{22} = \frac{1}{2a}\left(\frac{1}{3} + \frac{1}{2}n\right). \tag{4.243}$$

Application of boundary condition (4.240) yields

$$A_{22} = \frac{1}{a}\left(-\frac{11}{4}n - \frac{8}{3} - \frac{\rho_{11}}{a}\right). \tag{4.244}$$

Application of boundary condition (4.239) yields

$$A_{22} = -\frac{1}{a}\left(\frac{19}{6}n + 3 + 2\frac{\rho_{11}}{a}\right). \tag{4.245}$$

Application of boundary condition (4.241) yields

$$A_{22} = -\frac{1}{a^3 k}\left(ak\rho_{11} - \frac{1}{2}k\rho_{01} + 2ac_{11} - c_{01} + (2n+2)a^2 k\right). \tag{4.246}$$

Solving for A_{22}, B_{22}, ρ_{11} and c_{11} yields

$$\begin{aligned} A_{22} &= -\frac{1}{a}\left(\frac{7}{3}n - \frac{7}{3}\right), \quad B_{22} = -\frac{1}{2a}\left(\frac{1}{3} + \frac{1}{2}n\right), \\ \rho_{11} &= a\left(\frac{5}{12}n + \frac{1}{3}\right), \quad c_{11} = \frac{ak}{2}\left(\frac{3}{12}n + \frac{2}{3}\right). \end{aligned} \tag{4.247}$$

Hence the solution is

$$q_{22}(y) = \frac{1}{a}\left(-\frac{(11n+4)}{12}y^4 - \frac{(11n+8)}{3}y^3 - \left(\frac{58}{12}n+\frac{27}{6}\right)y^2 - \frac{7}{3}(n+1)y - \frac{1}{2}\left(\frac{1}{3}+\frac{1}{2}n\right)\right).$$

Hence the asymptotic solution for the case of a general nonlinear diffusion coefficient and a Robin boundary condition is given by

$$\begin{aligned}
c &= a\alpha k\left(\left(1-\frac{\alpha}{2}\right)\varepsilon + \left(\frac{1}{2}\left(\frac{3}{12}n+\frac{2}{3}\right)+\frac{\alpha}{2}\left(\frac{1}{3}+\frac{1}{2}n\right)\right)\varepsilon^2\right) + O(\varepsilon^3),\\
\rho &= \frac{a}{\alpha}\left(2\left(1-\frac{\alpha}{2}\right)+\left(\left(\frac{1}{3}-\frac{1}{2}n\right)-\alpha\left(\frac{5}{12}n+\frac{1}{3}\right)\right)\varepsilon\right) + O(\varepsilon^2),\\
q &= \frac{1}{a}(1-((1-\alpha)y(y+2)+\alpha(1-\frac{\alpha}{2}))\varepsilon+\varepsilon^2(y(\frac{3n+1}{6}y^3+\frac{4+6n}{3}y^2+,\\
&5(\frac{1}{3}+\frac{1}{2}n)y+n)-\alpha(\frac{11n+4}{12}y^4+\frac{11n+8}{3}y^3+(\frac{58}{12}n+\frac{27}{6})y^2+\\
&\frac{7}{3}(n+1)y+\frac{1}{2}(\frac{1}{3}+\frac{1}{2}n))+O(\varepsilon^3).
\end{aligned} \tag{4.248}$$

In Figure 4.16, we compare numerical solution in phase plane and asymptotic approximations results from perturbation method for wave speed c. However, the effect is rather small. We had a good agreement between the numerical and asymptotic solution especially at leading order approximation.

In Figure 4.17, we compare numerical and asymptotic approximations for the wave speed, c, and proliferation width, ρ, with different value of n. Note that as n increases, the wave speed and proliferation rim width are smaller. However, this is not a leading order effect.

Return (4.248) to original parameters the solution at leading order

$$\rho = a\sqrt{\frac{k\varepsilon}{2r}} \quad c = a\sqrt{2rk\varepsilon}.$$

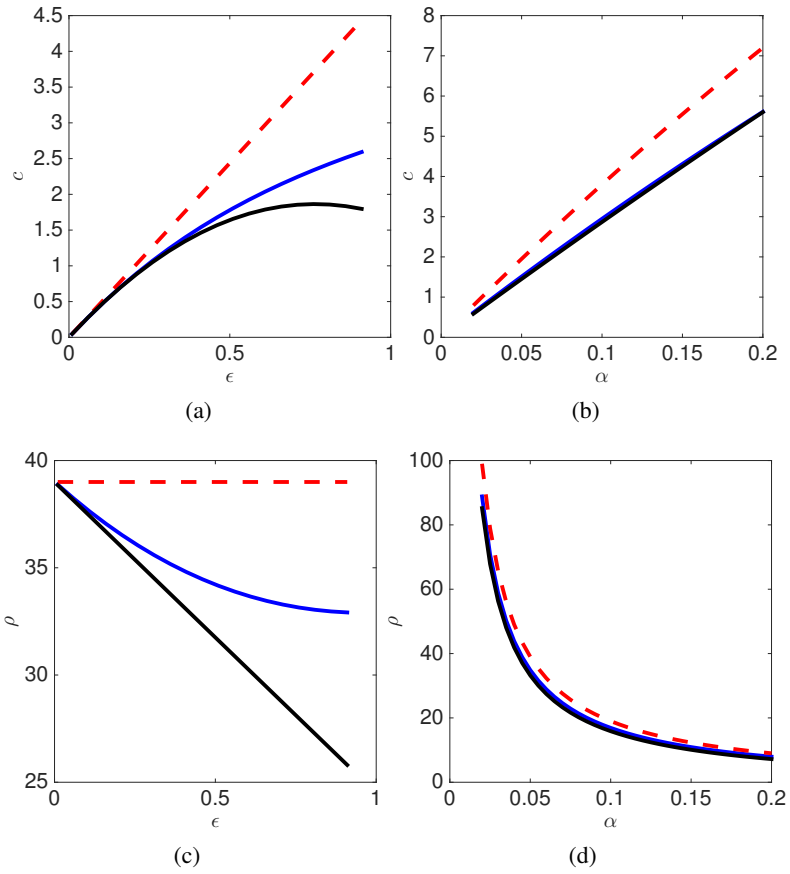

Figure 4.16: Comparing numerical and asymptotic approximations to the wave speed. (a) The wave speed, c, is plotted against ε ($\alpha = 0.05$). (b) The wave speed, c, is plotted against α ($\varepsilon = 0.3$). (c) The proliferation width, ρ, is plotted against ε ($\alpha = 0.05$). (d) The proliferation width, ρ, is plotted against α ($\varepsilon = 0.4$). Numerical solutions (red solid line) are computed using a shooting method. Leading order asymptotic solution (dashed lines) and corrections (black solid lines) are given by equations (4.221) and (4.248), respectively. Parameter values as in Table 4 unless otherwise stated.

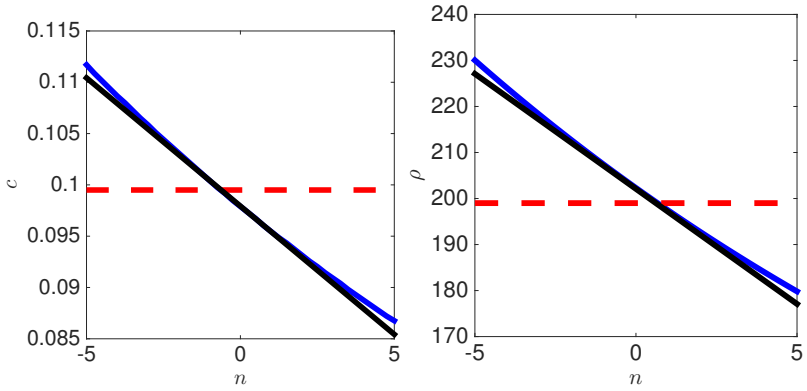

Figure 4.17: Comparing numerical and asymptotic approximations to the wave speed, c, and proliferation width, ρ. (a) The wave speed, c, is plotted against n. (b) The proliferation width, ρ, is plotted against n. Leading order asymptotic solution (blue solid lines) and corrections (black solid lines) are given by equations (4.221) and (4.248), respectively. $\varepsilon = 0.1$ and $\alpha = 0.01$. Other parameter values as in Table 4.

4.2.3 A general nonlinear model

Murray [49] derived a relationship between diffusion coefficient and force given by

$$D(q) = -\frac{F'(\frac{1}{q})}{\eta q^2}, \tag{4.249}$$

where $F(\frac{1}{q})$ force law and μ the over damping constant. Hence we consider the diffusion coefficient of the form

$$D(q) = \frac{a^2 k}{(aq)^n}, \tag{4.250}$$

where it is assumed that n is $O(1)$

. Substituting equation (4.250) into equation (4.249),

$$\frac{a^2 k}{(aq)^n} = -\frac{F'(\frac{1}{q})}{\eta q^2},$$

rearranging

$$F'(\frac{1}{q}) = a^{2-n}k\left(\frac{1}{q}\right)^{n-2}. \tag{4.251}$$

Integration equation 4.251, hence the corresponding force law is

$$F\left(\frac{1}{q}\right) = \frac{ka}{n-1}\left(1-\left(\frac{1}{aq}\right)^{n-1}\right). \tag{4.252}$$

Hence a particular case of the general form introduced in equations (1.2) is

$$\frac{\partial q}{\partial t} = \frac{\partial}{\partial x}\left(\frac{a^2k}{(aq)^n}\frac{\partial q}{\partial x}\right) + rqH(q_c - q), \tag{4.253}$$

with boundary conditions

$$\left.\frac{\partial q}{\partial x}\right|_{x=0} = 0, \quad \left.\frac{\partial q}{\partial x}\right|_{x=s(t)} = -\frac{ds}{dt}\frac{a^n q^{n+1}(0)}{a^2k} \quad \text{and} \quad \frac{ds}{dt} = \frac{ka}{n-1}\left(1-\left(\frac{1}{aq(s(t),t)}\right)^{n-1}\right). \tag{4.254}$$

and the initial conditions

$$q(x,0) = f(x) \quad \text{and} \quad s(0) = s_0. \tag{4.255}$$

4.2.3.1 Numerical solution

Equations (4.253)-(4.254) were solved numerically using the Method of Lines, (see Section 2.3.3). Figure 4.18 indicates the solution of the model (4.253) that is suggestive of travelling wave. The solution does not appear to change qualitatively upon changing the parameter n.

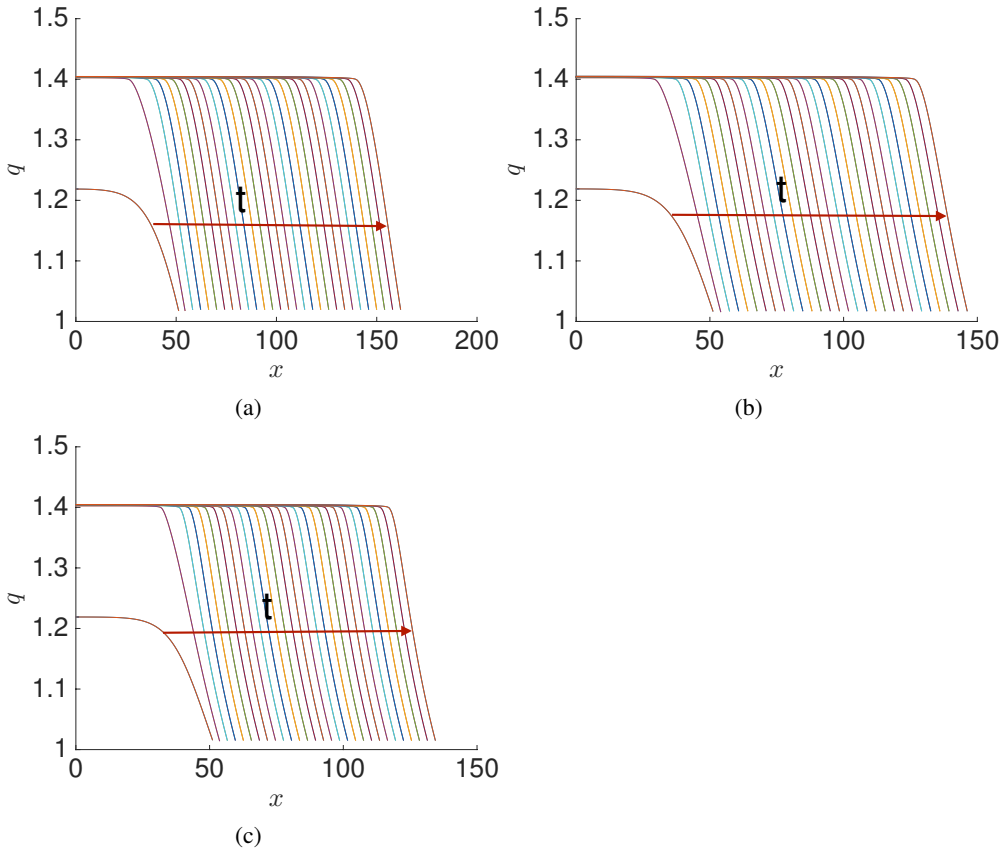

Figure 4.18: Numerical solution of equations (4.253)-(4.254). The cell density, q, is plotted against spatial position, x, at different times. (a) $n = 2$, (b) $n = 4$ and (c) $n = 6$. See Table 4 for parameter values.

4.2.3.2 Phase plane solution

We define the travelling wave coordinate

$$z = x - ct,$$

where c is the wave speed. Transforming equations (4.253)-(4.254) yields

$$-cq' = \frac{a^2k}{(aq)^n}q'' - \frac{na^2k}{a^nq^{n+1}}q'^2 + rqH(q_c - q), \tag{4.256}$$

with the boundary conditions given by

$$\begin{aligned} \left.\frac{dq}{dz}\right|_{z\to-\infty} &= 0, \\ q(0) &= \frac{1}{a\left(1-\frac{c(n-1)}{ak}\right)^{\frac{1}{n-1}}}, \\ \text{and} \quad \left.\frac{dq}{dz}\right|_{z=0} &= -\frac{c(aq(0))^n}{a^2k}\frac{1}{a\left(1-\frac{c(n-1)}{ak}\right)^{\frac{1}{n-1}}}. \end{aligned} \tag{4.257}$$

Again, making the coordinate transformation

$$\bar{z} = z - \rho,$$

and

$$u = q \quad \text{and} \quad v = \frac{dq}{d\bar{z}}, \tag{4.258}$$

equations (4.256)–(4.257) transform to

$$\begin{aligned}\frac{du}{d\bar{z}} &= v,\\ \frac{dv}{d\bar{z}} &= -\frac{a^{n-2}u^n}{k}\left(n\frac{a^{2-n}k}{u^{n+1}}v^2+cv+ru\right).\end{aligned} \tag{4.259}$$

The initial conditions are

$$u(0)=q_c \quad \text{and} \quad v(0)=0. \tag{4.260}$$

For a given initial guess for c, we find a solution that satisfies

$$u(\rho)=\frac{1}{a\left(1-\frac{c(n-1)}{ak}\right)^{\frac{1}{n-1}}}. \tag{4.261}$$

We then seek a solution that satisfies

$$v(\rho)=-\frac{c}{a^2k}\left(\frac{1}{a\left(1-\frac{c(n-1)}{ak}\right)^{\frac{1}{n-1}}}\right)^{n+1}, \tag{4.262}$$

by minimising the function

$$E(c)=\left(v(\rho)+\frac{c}{a^2k}\left(\frac{1}{a\left(1-\frac{c(n-1)}{ak}\right)^{\frac{1}{n-1}}}\right)^{n+1}\right)^2. \tag{4.263}$$

In Figure 4.19 we plot the error given by equation (4.263) and minimised giving a unique wave speed c. In Figure 4.19 (a) we plot the solution trajectory of equations (4.259) in the phase plane start .

Note that there is a unique minimum. In Figure 4.19 (c) and (d) we computed wave

speed as a function of the model parameters q_c and k.

4.2.3.3 Perturbation method

We will begin by making a change of dependent variable that rescales the width of the proliferating region.

Letting

$$y = \frac{z}{\rho},$$

equation (4.256) transforms to

$$-c\rho\frac{dq}{dy} = \frac{a^2k}{(aq)^n}\frac{d^2q}{dy^2} - \frac{na^2k}{a^nq^{n+1}}\left(\frac{dq}{dy}\right)^2 + r\rho^2 q. \tag{4.264}$$

The boundary conditions (4.257) transform to

$$\begin{aligned} &q(-1) = e^{\varepsilon}, \quad q'(-1) = 0, \\ &q(0) = \frac{1}{a\left(1-\frac{c(n-1)}{ak}\right)^{\frac{1}{n-1}}}, \quad \text{and} \quad q'(0) = -\frac{c\rho}{a^2k}a^n q(0)^{n+1}. \end{aligned} \tag{4.265}$$

Following the argument in Section 4.2.1.3, we assume that the parameter r scales like

$$r = \frac{\alpha^2\varepsilon k}{2}, \quad \text{where} \quad \alpha \ll 1,$$

such that diffusion balances proliferation at leading order

$$\frac{a^2k}{(aq)^n}q'' = rq\rho^2.$$

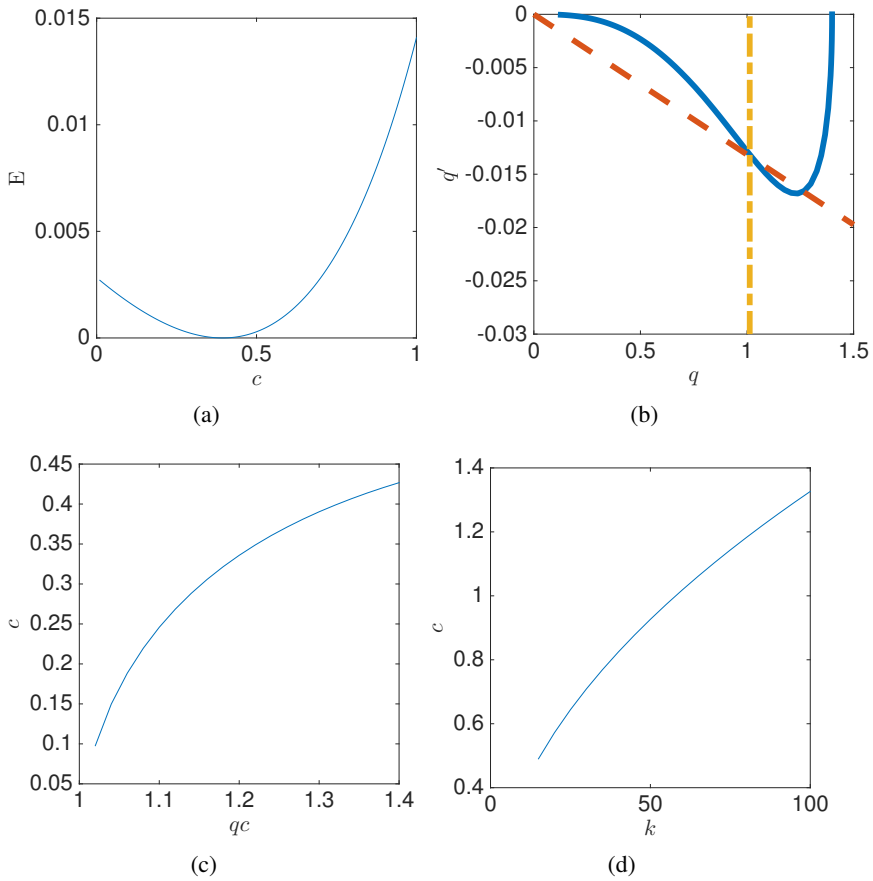

Figure 4.19: Using a shooting method to compute wave speed, c. (a) A unique wave speed, c^*, is identified using a shooting method. Error, $E(c)$, is plotted against wave speed, c (see equation (4.263)). (b) A representative phase plane trajectory is presented for wave speed $c = c^*$. q' is plotted against q. Equations (4.259) were solved numerically (blue line). Red and yellow lines represent boundary conditions (4.261) and (4.262), respectively. (c) The wave speed, c, is plotted against the proliferation threshold density, q_c. (d) The wave speed, c, is plotted against k , ($n = 4$). Other parameter values as in Table 4.

Hence equation (4.264) transforms to

$$-c\rho\frac{dq}{dy}=\frac{a^2k}{(aq)^n}\frac{d^2q}{dy^2}-\frac{na^2k}{a^nq^{n+1}}\left(\frac{dq}{dy}\right)^2+\frac{\alpha^2\varepsilon k}{2}\rho^2q. \tag{4.266}$$

We propose asymptotic solutions to equation (4.266) of the form

$$\begin{aligned}
c &= c_0\varepsilon+c_1\varepsilon^2+O(\varepsilon^3),\\
\rho &= \rho_0+\rho_1\varepsilon+O(\varepsilon^2),\\
q &= q_0(y)+q_1(y)\varepsilon+q_2(y)\varepsilon^2+O(\varepsilon^3).
\end{aligned} \tag{4.267}$$

Substituting equations (4.267) into equation (4.266) and applying binomial expansion yields

$$\begin{aligned}
&-(c_0\varepsilon+c_1\varepsilon^2)(\rho_0+\rho_1\varepsilon^2)(q_0'(y)+q_1'(y)\varepsilon+..)=\\
&\frac{-na^2k}{a^nq_0^{n+1}}(1-(n+1)\varepsilon\frac{q_1}{a^nq_0})(q_0(y)'+\varepsilon q_1'(y))^2\\
&+\frac{a^2k}{a^nq_0^n}(1-n\varepsilon\frac{q_1}{q_0})(q_0''(y)+q_1''(y)\varepsilon+..)+\frac{k\alpha^2\varepsilon}{2}(q_0(y)+\varepsilon q_1(y))(\rho_0+\varepsilon\rho_1)^2.
\end{aligned} \tag{4.268}$$

The boundary conditions are

$$
\begin{aligned}
q_0(-1)+q_1(-1)\varepsilon+q_2(-1)\varepsilon^2 &= \frac{1}{a}\left(1+\varepsilon+\frac{1}{2}\varepsilon^2\right)\\
q_0'(-1)+q_1'(-1)\varepsilon+q_2'(-1)\varepsilon^2 &= 0\\
q_0(0)+q_1(0)\varepsilon+q_2(0)\varepsilon^2 &= \frac{1}{a}\left(1+\frac{c_0}{ak}\varepsilon+\left(\frac{c_1}{ak}+\frac{c_0^2}{a^2k^2}\right)\varepsilon^2\right)\\
q_0'(0)+q_1'(0)\varepsilon+q_2'(0)\varepsilon^2 &= -\frac{a^{n-2}}{k}q_0(0)^{n+1}\\
&\quad\left(c_0\rho_0\varepsilon+\left(c_1\rho_0+\rho_1c_0+\frac{(n+1)}{q_0(0)}c_0\rho_0q_1(0)\right)\varepsilon^2\right).
\end{aligned}
\tag{4.269}
$$

At $O(1)$ and $O(\varepsilon)$ we find the solution defined in Section 4.2.2.3, i.e

$$
\begin{aligned}
c_0 &= a\alpha k(1-\frac{\alpha}{2a}),\quad \rho_0=\frac{2a}{\alpha}(1-\frac{\alpha}{2a}),\\
q_0(y) &= \frac{1}{a},\quad \text{and}\quad q_1(y)=\frac{1}{a}\left(-(1-\alpha+O(\alpha^2))y(y+2)+\alpha(1-\frac{\alpha}{2}+O(\alpha^2))\right).
\end{aligned}
\tag{4.270}
$$

At O(ε^2)

$$
-c_0\rho_0q_1' = \frac{-na^{2-n}k}{q_0^{n+1}}q_1'^2+\frac{a^{2-n}k}{q_0^n}q_2''-nk\frac{q_1}{q_0}q_1''+\frac{k\alpha^2}{2}q_1\rho_0^2+k\alpha^2q_0\rho_0\rho_1, \tag{4.271}
$$

with boundary conditions

$$
\begin{aligned}
q_2'(-1)=0,\quad q_2(0)&=\frac{c_1}{a^2k}+\frac{c_0^2}{a^3k^2},\quad q_2(-1)=\frac{1}{2a},\\
q_2'(0)&=-\frac{1}{a^3k}\left(c_0\rho_1+c_1\rho_0+(n+1)q_0(0)c_0\rho_0q_1(0)\right)
\end{aligned}
\tag{4.272}
$$

Following Section 4.2.2.3 we seek a series solution in α of the form

$$\begin{aligned} q_2 &= q_{21} + \alpha q_{22} + O(\alpha^2), \\ c_1 &= c_{01}\alpha + c_{11}\alpha^2 + O(\alpha^3), \\ \rho_1 &= \frac{1}{\alpha}(\rho_{01} + \alpha\rho_{11}) + O(\alpha). \end{aligned} \tag{4.273}$$

We find that the solution is the same as that presented in equation (4.248) up to $O(\alpha)$ yields

$$\begin{aligned} c &= \alpha a k \left((1-\frac{\alpha}{2})\varepsilon + \left(\frac{1}{2}\left(\frac{3}{12}n + \frac{2}{3} \right) + \frac{\alpha}{2}\left(\frac{1}{3} + \frac{1}{2}n \right) \right) \varepsilon^2 \right), \\ \rho &= \frac{a}{\alpha}\left(2\left(1-\frac{\alpha}{2} \right) + \left(\frac{1}{3} - \frac{1}{2}n \right) - \alpha\left(\frac{5}{12}n + \frac{1}{3} \right)\varepsilon \right), \\ q &= \frac{1}{a}(1 + \left(-(1-\alpha)y(y+2) + \alpha\left(1-\frac{\alpha}{2} \right) \right)\varepsilon \\ &\quad + \varepsilon^2(y\left(\frac{3n+1}{6}y^3 + \frac{4+6n}{3}y^2 + 5(\frac{1}{3} + \frac{1}{2}n)y + n \right) \\ &\quad - \alpha(\frac{11n+4}{12}y^4 + \frac{11n+8}{3}y^3 + \left(\frac{58}{12}n + \frac{27}{6} \right)y^2 + \frac{7}{3}(n+1)y + \frac{1}{2}\left(\frac{1}{3} + \frac{1}{2}n \right))) + O(\varepsilon^3)). \end{aligned} \tag{4.274}$$

The effect of the modify boundary condition can be seen at $O(\alpha^2)$. In Figure 4.20 show the asymptotic agreement with shooting method. At leading order the solution is similar to solution Chapter 3 where the diffusion coefficient is constant. These results suggest that the effect of changing the boundary condition from (4.199) to (4.257) is not important. In Figure 4.21 we plot numerical solution and asymptotic results for different value of n. We observe that there are no significant change with increasing n. Return to original parameters at leading order

$$\rho = a\sqrt{\frac{k\varepsilon}{2r}} \quad c = a\sqrt{2rk\varepsilon}.$$

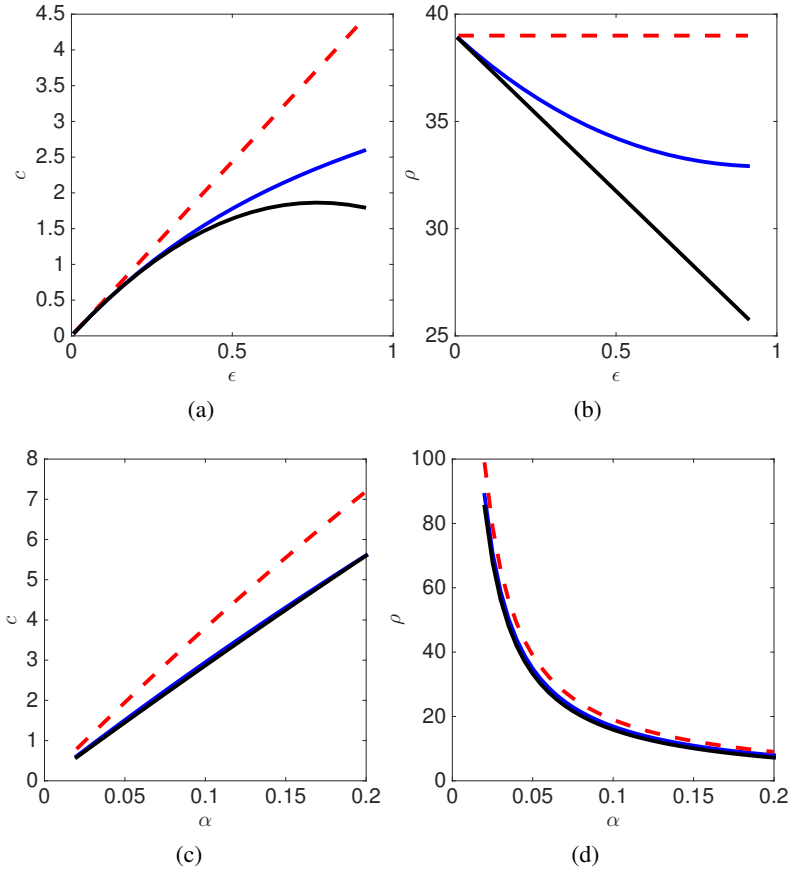

Figure 4.20: Comparing numerical and asymptotic approximations to the wave speed. (a) The wave speed, c, is plotted against ε ($\alpha = 0.05$). (b) The proliferation width, ρ, is plotted against ε ($\alpha = 0.05$). (c) The wave speed, c, is plotted against α ($\varepsilon = 0.4$). (d) The proliferation width, ρ, is plotted against α ($\varepsilon = 0.4$). Numerical solutions (red solid line) are computed using a shooting method. Leading order asymptotic solution (dashed line) and corrections (black solid) line are given by equations (4.270) and (4.274), respectively $n = 4$. Other parameter values as in Table 4 unless otherwise stated.

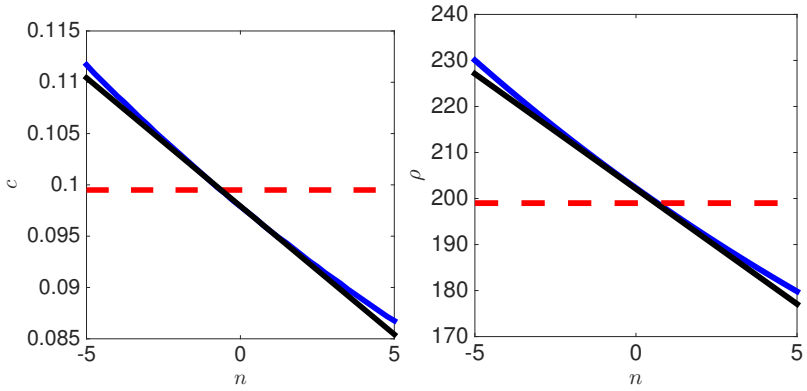

Figure 4.21: Comparing numerical and asymptotic approximations to the wave speed, c, and proliferation width, ρ. (a) The wave speed, c, is plotted against n. (b) The proliferation width, ρ, is plotted against n. Leading order asymptotic solution (blue solid lines) and corrections (black solid lines) are given by equations (4.270) and (4.274), respectively. Here $\varepsilon = 0.1$ and $\alpha = 0.01$. Other parameter values as in Table 4.

4.3 Discussion

In previous work Murray and coworkers showed that a certain class of discrete cell-based models could be represented by nonlinear diffusion equations [49, 53, 50, 52]. Here we consider the case of a linear force law with contact-inhibited cell proliferating cell population, a model that be described as a Stefan problem with a nonlinear boundary condition and nonlinear diffusion coefficient

$$D(q) = \frac{k}{q^2}. \tag{4.275}$$

The major question addressed are: (i) whether the techniques developed in the previous chapter can be used to derive expressions for the wavespeed and proliferating rim width; (ii) whether the nonlinearity in the diffusion coefficient affects the wavespeed and proliferating rim width. Using numerical approximations, we show that the solutions are characterised by a central non-proliferating region with density equal to the proliferation threshold density and a propagating front of proliferating cells. Applying

techniques developed in the previous chapter we construct asymptotic solutions for the case of Dirichlet and Robin boundary conditions and show excellent agreement with numerical solutions. The major conclusion is that in the case of a linear force law the effect of the nonlinearity in the diffusion coefficient is not seen at leading order. These results suggest that for many practical purposes the system could be approximated by a constant diffusion coefficient.

To further explore this result we considered a generalised form of the force law given by

$$F\left(\frac{1}{q}\right) = \frac{ka}{n-1}\left(1-\left(\frac{1}{aq}\right)^{n-1}\right).$$

which has corresponding nonlinear diffusion coefficient

$$D(q) = \frac{a^2 k}{(aq)^n}. \tag{4.276}$$

For this family of force laws, the exponent n does not affect the solution at leading order.

We again note that in Murray et al. [49] the case of a linear force and Dirchlet boundary condition showed excellent agreement with discrete model simulations. Here we show that the correct boundary condition, which is a Robin condition, is well approximated by the Dirichlet condition in the limiting case where $\alpha \ll 1$.

Chapter 5

General model with nonlinear diffusion

5.1 Introduction

As described in Section 2.2.3.6 Murray et al. [53] showed that a cell-cell interaction force law of the form

$$F(x) = ka\left(1 - \frac{x}{a}\right)^n, \tag{5.1}$$

yielded a nonlinear diffusion coefficient of the form

$$D(q) = \frac{nk}{q^2}\left(1 - \frac{1}{aq}\right)^{n-1}. \tag{5.2}$$

Note that special cases $n = 1$ and $n = 3/2$ correspond to linear and Hertz force laws. The goal of this chapter is to consider the problem defined by equations (1.2)-(1.6) in the case of the diffusion coefficient given by equation (5.2).

Before addressing this case, note that

$$\lim_{q\to\frac{1}{a}} D(q) = 0,$$

which give a qualitatively different behaviour with previous cases. Note that as a result of boundary and initial conditions the limit is never realised in numerical solutions.

Consider the model

$$\frac{\partial q}{\partial t} = \frac{\partial}{\partial x}\left(\frac{nk}{q^2}\left(1-\frac{1}{aq}\right)^{n-1}\left(\frac{\partial q}{\partial x}\right)\right) + rqH(q_c - q), \tag{5.3}$$

where $q(x,t)$ is the cell density, x is the position variable, t is time, $D(q)$ is a diffusion coefficient, r is a proliferation rate, q_c is the threshold cell density at which cells stop proliferating.

The boundary conditions are given by:

$$\left.\frac{\partial q}{\partial x}\right|_{x=0} = 0, \tag{5.4}$$

and

$$\left.\frac{\partial q}{\partial x}\right|_{x=s(t)} = -\frac{q(s(t),t)}{D(q(s(t),t))}\frac{ds}{dt}, \tag{5.5}$$

where $s(t)$ represents the position of moving boundary that satisfies the ordinary differential equation

$$\frac{ds}{dt} = ka\left(1-\frac{1}{aq}\right)^n. \tag{5.6}$$

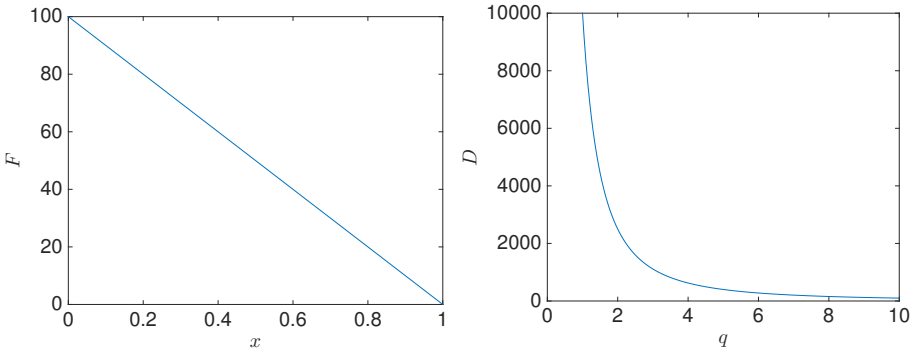

(a) (b)

Figure 5.1: A linear force law and its corresponding diffusion coefficient. (a) The force, F, is plotted against separation distance, x (equation (5.1)). (b) The nonlinear diffusion coefficient, $D(q)$, is plotted against cell density, q (equation (5.2)). $k = 100$, $a = 1$ and $n = 1$.

The initial conditions are

$$s(0) = s_0, \tag{5.7}$$

and

$$q(x,0) = f(x), \quad x \in [0, s_0]. \tag{5.8}$$

5.2 Numerical solution

Equations (5.3)-(5.8) were solved numerically using the Method of Lines (see section 2.3.3). In Figure 5.4 the solution is plotted for values of the parameter n representing linear, Hertz and cubic force laws. Note that, in contrast to Chapter 4, as n increases there is a marked increase in the front steepness and decrease in the front speed.

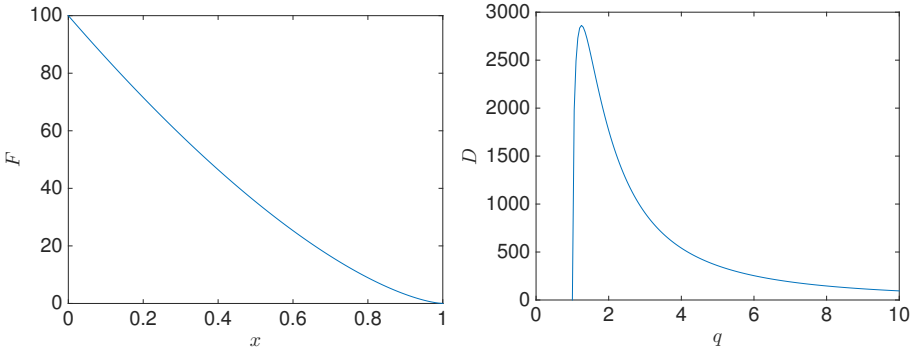

(a) (b)

Figure 5.2: The Hertz force law and its corresponding diffusion coefficient. (a) The force, F, is plotted against separation distance, x (equation (5.1)). (b) The diffusion coefficient, $D(q)$, is plotted against cell density q (equation (5.2)). $k = 100$, $a = 1$ and $n = \frac{3}{2}$.

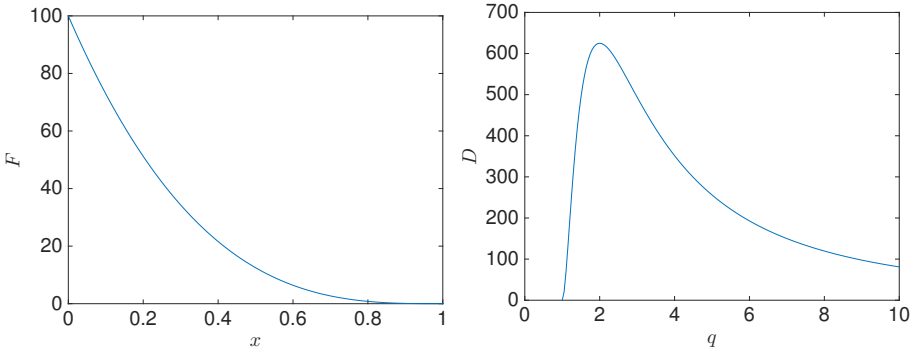

(a) (b)

Figure 5.3: A cubic force law and its corresponding diffusion coefficient. (a) The force, F, is plotted against separation distance, x (equation (5.1)). (b) The diffusion coefficient, $D(q)$, is plotted against cell density q (equation (5.2)). $k = 100$, $a = 1$ and $n = 3$.

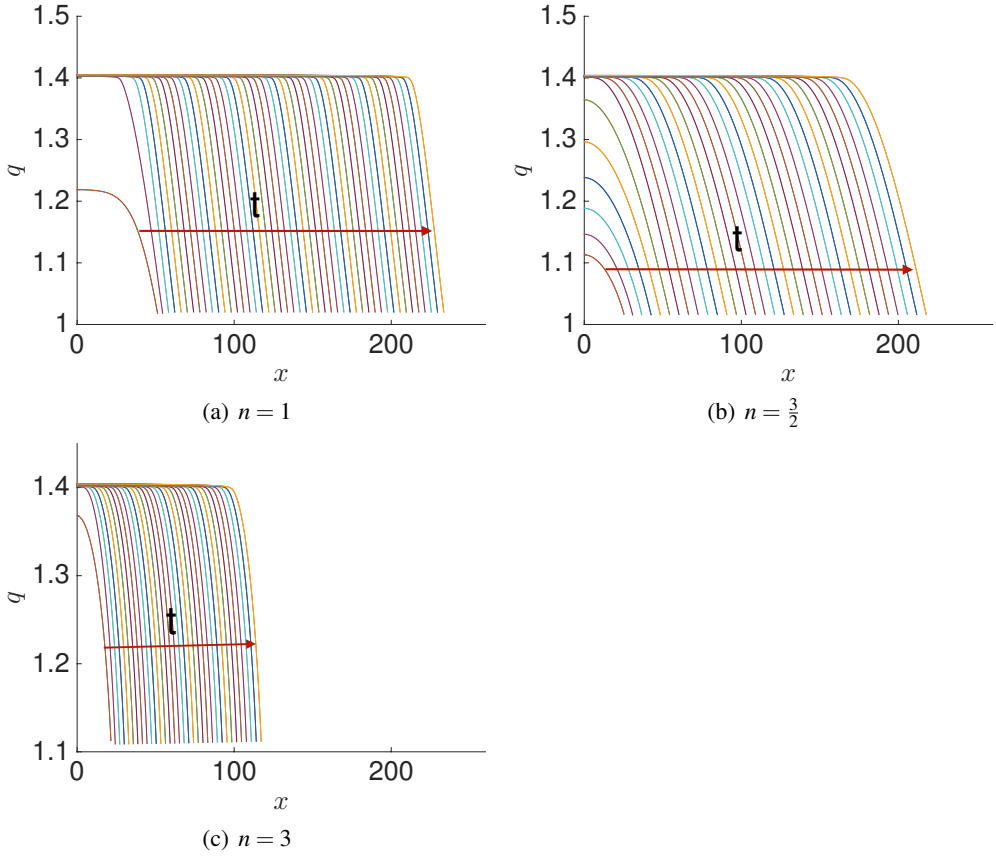

(a) $n = 1$

(b) $n = \frac{3}{2}$

(c) $n = 3$

Figure 5.4: Numerical solution of equations (5.3)-(5.8). The cell density, q, is plotted against spatial position, x, at different times, t. See Table 3 for parameters values. (a) $n = 1$, (b) $n = 3/2$ and (c) $n = 3$.

5.3 Phase plane solution

In order to explore travelling wave solutions, we employ a Shooting Method (see Section 3.1.2). We define

$$z = x - ct,$$

and equations (5.3)-(5.8) transform to

$$-cq' = D(q)q'' + D'(q)q'^2 + rq. \tag{5.9}$$

The boundary conditions become

$$\left.\frac{dq}{dz}\right|_{z\to-\infty} = 0, \tag{5.10}$$

$$q(0) = \frac{1}{a\left(1-\left(\frac{c}{ak}\right)^{\frac{1}{n}}\right)}, \tag{5.11}$$

$$\left.\frac{dq}{dz}\right|_{z\to-0} = -\frac{cq(0)}{D(q(0))}. \tag{5.12}$$

Differentiating equation (5.2) yields

$$D'(q) = \frac{nk}{q^4}\left(1-\frac{1}{qa}\right)^{n-2}\left(-q\left(1-\frac{1}{aq}\right)+\frac{(n-1)}{a}\right).$$

We assume that for some unknown ρ, $q = q_c$ where $z < -\rho$ and $q'(-\rho) = 0$.

Letting

$$u = q \quad \text{and} \quad v = \frac{dq}{dz}, \tag{5.13}$$

equations (5.9)-(5.12) transform to

$$\begin{aligned}
&\frac{du}{dz} = v,\\
&\frac{dv}{dz} = -\frac{1}{nk}u^2\left(1-\frac{1}{au}\right)^{\frac{1}{n-1}}\left(\left(\frac{nk}{u^4}(1-\frac{1}{ua})^{n-1}((n-1)(a-\frac{1}{u})^{-1}-2u)\right)v^2+cv+ru\right).
\end{aligned} \tag{5.14}$$

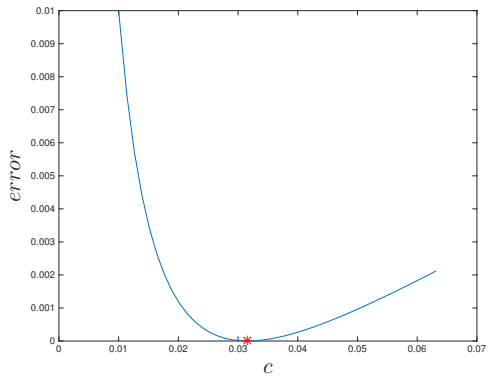

(a)

Figure 5.5: A unique wave speed, c, is identified. Error, E(c), is plotted against wave speed, c (equation (5.18)) and $n = 3$.

The initial conditions are

$$u(0) = q_c \qquad \text{and} \qquad v(0) = 0. \tag{5.15}$$

For a given initial guess for c, we numerically identify ρ such that

$$u(\rho) = \frac{1}{a\left(1 - \left(\frac{c}{ak}\right)^{\frac{1}{n}}\right)}. \tag{5.16}$$

We seek a solution that satisfies

$$v(\rho) = -\frac{cu(\rho)}{D(u(\rho))}, \tag{5.17}$$

by minimising the function

$$E(c) = \left(v(\rho) + \frac{cu(\rho)}{D(u(\rho))}\right)^2. \tag{5.18}$$

In Figure 5.5 (a) we plot the error defined in equation (5.18) against a range of values

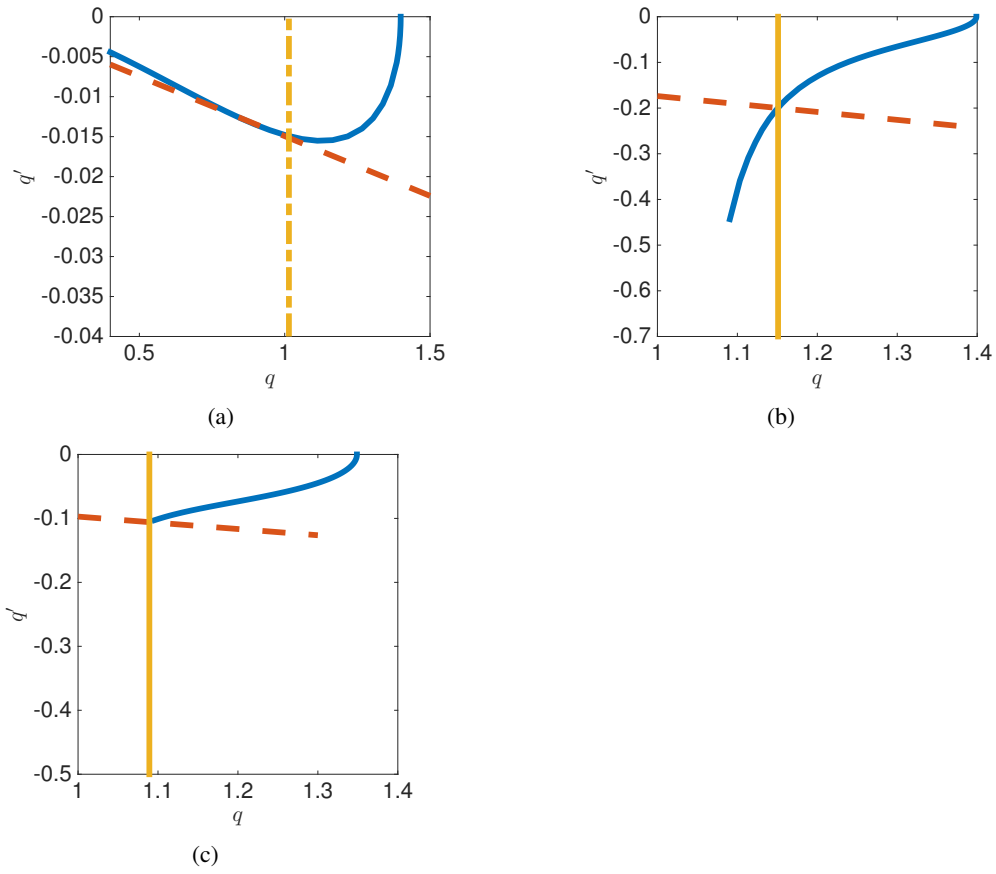

Figure 5.6: A representative phase plane trajectory is presented for wave speed $c = c^*$. q' is plotted against q. Equations (5.14) were solved numerically (blue line). Red and yellow lines represent boundary conditions (5.16) and (5.17), respectively. (a) $n = 1$. (b) $n = 3$. (c) $n = \frac{3}{2}$.

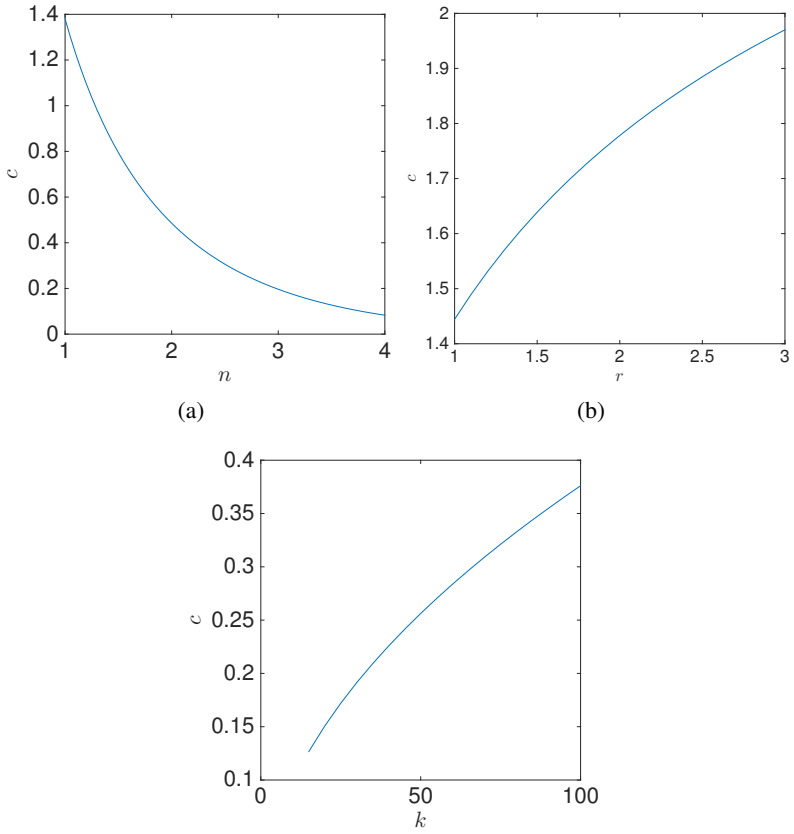

Figure 5.7: Computing the wave speed using a shooting method. (a) The wave speed, c, is plotted against n. (b) The wave speed, c, is plotted against the growth rate, r ($n = 3$). (c) The wave speed, c, is plotted against k ($n = 3$). Other parameter values as in Table 3.

for the unknown wave speed c. As we shown in Chapter 4 there is a unique minimum. In Figure 5.6 we show the results from the shooting method. In Figure 5.6 (a),(b) and (c) solution of equation (5.14) in the phase plane. Note that where $n = 1$ the solution return to Section 4.1.2 where we analyse the nonlinear diffusion $D(q) = \frac{k}{q^2}$ and Robin boundary condition.

In Figure 5.7 we plot the computed wave speed as a function of the model parameters n, r and k. Note that wave speed decreases as n increases. In addition the wave speed increases with proliferation r rate and spring constant k.

5.4 Asymptotic solution

Making the change of independent variable

$$y = \frac{z}{\rho}, \tag{5.19}$$

equations (5.9)-(5.12) transform to

$$-c\rho q' = D(q)q'' + D'(q)(q')^2 + r\rho^2 q, \tag{5.20}$$

with the boundary conditions

$$q(-1) = q_c \tag{5.21}$$

$$q'(-1) = 0, \tag{5.22}$$

$$q(0) = \frac{1}{a\left(1 - \left(\frac{c}{ak}\right)^{\frac{1}{n}}\right)}, \tag{5.23}$$

$$q'(0) = -\frac{c\rho q(0)}{D(q(0))}. \tag{5.24}$$

Note that in the limit $\varepsilon \to 0$, $D(q) \to 0$ the problem becomes singular. Hence we make the ansatz that at leading order

$$q_0 = \frac{1}{a}.$$

The right hand side of boundary condition (5.21) is expanded as a power series in ε yielding

$$q_c = \frac{1}{a}e^{\varepsilon} = \frac{1}{a}\left(1 + \varepsilon + \frac{1}{2}\varepsilon^2 + O(\varepsilon^3)\right).$$

Hence we propose that q can be written as as expansion of the form

$$q(y) = \frac{1}{a} + \varepsilon q_1(y) + \varepsilon^2 q_2(y) + O(\varepsilon^3). \tag{5.25}$$

From equation (5.6) we have

$$c = ka\left(1 - \frac{1}{aq}\right)^n. \tag{5.26}$$

Substuiting for q in equation (5.26) yields

$$c = ak\left(1 - \frac{1}{a\frac{1}{a}(1 + aq_1\varepsilon + aq_2\varepsilon^2)}\right)^n. \tag{5.27}$$

Applying a binomial expansion and rearranging yields

$$c = ak\left((aq_1)^n\varepsilon^n + O(\varepsilon^{n+1})\right). \tag{5.28}$$

Hence we consider expansion on c of the form

$$c = c_0\varepsilon^n + c_1\varepsilon^{n+1} + O(\varepsilon^{n+2}).$$

For boundary condition (5.24) we need first the expansion for the diffusion coefficient $D(q)$. Upon substituting for q in equation (5.25) and expanding yields

$$D(q) = \frac{nk}{q_0^2}\left(1 - 2\frac{q_1}{q_0}\varepsilon\right)\left(1 - \frac{1}{aq_0}\left(1 - \frac{q_1}{aq_0}\varepsilon + O(\varepsilon^2)\right)\right)^{n-1}. \tag{5.29}$$

Hence at leading order

$$D(q) = a^2 nk(aq_1)^{n-1}\varepsilon^{n-1} + O(\varepsilon^n). \tag{5.30}$$

Differentiating $D(q)$ yields

$$D'(q) = ka^3 n(n-1)(q_1 a)^{n-2} q_1' \varepsilon^{n-2} + O(\varepsilon^{n-1}). \tag{5.31}$$

Substituting for the expanded forms for $D(q)$, c and q in boundary condition (5.24) and rearranging yields

$$-(na^2 k)(aq_1)^{n-1}\varepsilon^{n-1}\left(q_1'\varepsilon\right) = \left(c_0\varepsilon^n + c_1\varepsilon^{n+1}\right)\left(\frac{1}{a} + \varepsilon q_1\right)\rho. \tag{5.32}$$

Hence we propose that ρ can be written as an expansion in the form

$$\rho = \rho_0 + \rho_1\varepsilon + O(\varepsilon^2).$$

Finally, substituting for q and ρ in equation (5.20) and imposing the constraint that at leading order diffusion balances proliferation,

$$D(q)q'' = rq\rho.$$

Substituting for q, $D(q)$ and ρ yields

$$a^2nk(aq_1)^{n-1}\varepsilon^n q_1'' = \frac{r\rho_0^2}{a}.$$

Balancing at leading order in epsilon we require that

$$\frac{r}{nk} \propto \varepsilon^n.$$

Following a similar argument to that made in previous chapters, we assume

$$r = \frac{n\alpha^2 k\varepsilon^n}{2},$$

where $\alpha \ll 1$.

Hence we seek asymptotic solutions to equation (5.20)-(5.24) of the form

$$\begin{aligned} c &= c_0\varepsilon^n + \varepsilon^{n+1}c_1 + O(\varepsilon^{n+2}), \\ \rho &= \rho_0 + \rho_1\varepsilon + O(\varepsilon^2), \\ q(y) &= \frac{1}{a} + q_1(y)\varepsilon + q_2(y)\varepsilon^2 + O(\varepsilon^2). \end{aligned} \tag{5.33}$$

Substituting the series expansion in equations of c, ρ, r, $D(q)$ and $D'(q)$ in equation (5.20) yields

$$\begin{aligned} &-(c_0\varepsilon^n + c_1\varepsilon^{n+1})(\rho_0 + \varepsilon\rho_1)(q_1'\varepsilon + q_2'\varepsilon^2) = a^2nk(aq_1)^{n-1}\varepsilon^{n-1}(q_1''\varepsilon + q_2''\varepsilon^2) \\ &+ka^3n(n-1)(q_1a)^{n-2}q_1'\varepsilon^{n-1}(q_1'\varepsilon)^2 + \frac{n\alpha^2k\varepsilon^n}{2}(\rho_0 + \varepsilon\rho_1)^2(\frac{1}{a} + \varepsilon q_1). \end{aligned} \tag{5.34}$$

Dividing by (ε^{n-1}) yields

$$-(c_0\varepsilon + c_1\varepsilon^2)(\rho_0 + \varepsilon\rho_1)(q_1'\varepsilon + q_2'\varepsilon^2) = a^2kn(aq_1)^{n-1}(q_1''\varepsilon + q_2''\varepsilon^2)$$
$$+ a^3kn(n-1)(q_1a)^{n-2}q_1'(q_1'\varepsilon)^2 + \frac{\alpha^2nk\varepsilon}{2}(\rho_0 + \varepsilon\rho_1)^2(\frac{1}{a} + \varepsilon q_1). \tag{5.35}$$

The boundary conditions (5.21) and (5.22) are

$$q_0(-1) + q_1(-1)\varepsilon = \frac{1}{a}\left(1 + \varepsilon + \frac{1}{2}\varepsilon^2\right),$$
$$q_0'(-1) + q_1'(-1)\varepsilon = 0. \tag{5.36}$$

Note that boundary condition (5.23) can be expanded as follows

$$\frac{1}{a} + q_1(0)\varepsilon + q_2(0)\varepsilon^2 = \frac{1}{a\left(1 - \left(\frac{c_0}{ak}\varepsilon^n + \frac{c_1}{ak}\varepsilon^{n+1}\right)^{\frac{1}{n}}\right)}, \tag{5.37}$$

Upon simplification, the right-hand side yields

$$= \frac{1}{a\left(1 - \left(\frac{c_0}{ak}\right)^{\frac{1}{n}}\varepsilon\left(1 + \frac{c_1}{c_0}\varepsilon + O(\varepsilon^2)\right)^{\frac{1}{n}}\right)}. \tag{5.38}$$

Applying the binomial expansion

$$\frac{1}{a} + q_1(0)\varepsilon = \frac{1}{a}\left(1 + \left(\frac{c_0}{ak}\right)^{\frac{1}{n}}\varepsilon\left(1 + \frac{c_1}{c_0}\varepsilon + O(\varepsilon^2)\right)\right).$$

Hence the boundary condition (5.24) transforms to

$$-(na^2k)(aq_1)^{n-1}\varepsilon^{n-1}\left(q_1'\varepsilon\right) = \left(c_0\varepsilon^n + c_1\varepsilon^{n+1}\right)\left(\frac{1}{a} + \varepsilon q_1\right)(\rho_0 + \varepsilon\rho_1). \tag{5.39}$$

Hence, at leading order

$$nka^2 q_1'(0)\varepsilon^n = -\frac{c_0\rho_0}{a}\left(\frac{1}{(aq_1(0))^{n-1}}\right)\varepsilon^n. \tag{5.40}$$

In summary, the series for boundary conditions (5.23) and (5.24) are

$$\begin{aligned} q_0(0) + q_1(0)\varepsilon &= \frac{1}{a}\left(1 + \left(\frac{c_0}{ak}\right)^{\frac{1}{n}}\varepsilon + O(\varepsilon^2)\right), \\ q_1'(0)\varepsilon &= -\frac{c_0\rho_0}{na^3k}\left(\frac{1}{(aq_1(0))^{n-1}}\right)\varepsilon. \end{aligned} \tag{5.41}$$

Solving at $O(\varepsilon)$ yields

$$(aq_1)^{n-1}q_1'' + a(n-1)(aq_1)^{n-2}q_1^{2\prime} = -\frac{\alpha^2\rho_0^2}{2a^3}, \tag{5.42}$$

After rearrangement we obtain

$$\left((aq_1)^{n-1}q_1'\right)' = -\frac{\alpha^2\rho_0^2}{2a^3}, \tag{5.43}$$

with boundary conditions

$$q_1(0) = \frac{1}{a}\left(\frac{c_0}{ak}\right)^{\frac{1}{n}}, \tag{5.44}$$

$$q_1'(-1) = 0, \tag{5.45}$$

$$q_1(-1) = \frac{1}{a}, \tag{5.46}$$

$$q_1'(0) = -\left(\frac{c_0\rho_0}{a^3 nk}\right)\left(\frac{1}{\left(aq_1(0)\right)^{n-1}}\right). \tag{5.47}$$

Integrating equation (5.43) yields

$$(aq_1)^{n-1}q_1' = -\frac{\alpha^2\rho_0^2}{2a^3}y + A.$$

A further integration, using separation of variables, yields

$$\int (aq_1)^{n-1}dq_1 = \int\left(-\frac{\alpha^2\rho_0^2}{2a^3}y + A\right)dy.$$

Hence

$$\frac{1}{n}a^{n-1}q_1^n = -\frac{\alpha^2\rho_0^2}{4a^3}y^2 + Ay + B.$$

$$q_1^n = -\frac{n\alpha^2\rho_0^2}{4a^{n+2}}y^2 + \hat{A}y + \hat{B}.$$

Hence the general solution to equation (5.42) is

$$q_1 = \left(-\frac{n\alpha^2\rho_0^2}{4a^{n+2}}y^2 + \hat{A}y + \hat{B}\right)^{\frac{1}{n}}, \tag{5.48}$$

where $\hat{A}$ and $\hat{B}$ are integration constants.

Differentiating equation (5.48) yields

$$q_1'(y) = \frac{1}{n}\left(-\frac{n\alpha^2\rho_0^2}{4a^{n+2}}y^2 + \hat{A}y + \hat{B}\right)^{\frac{1}{n}-1}\left(-\frac{n\alpha^2\rho_0^2}{2a^{n+2}}y + \hat{A}\right). \tag{5.49}$$

Applying boundary condition (5.44) yields

$$\left(\hat{B}\right)^{\frac{1}{n}} = \frac{1}{a}\left(\frac{c_0}{ak}\right)^{\frac{1}{n}},$$

hence

$$\hat{B} = \left(\frac{1}{a}\right)^n \frac{c_0}{ak}. \tag{5.50}$$

Applying boundary condition (5.45) yields

$$q_1'(-1) = \frac{1}{n}\left(-\frac{n\alpha^2\rho_0^2}{4a^{n+2}} - \hat{A} + \left(\frac{1}{a}\right)^n \frac{c_0}{ak}\right)^{\frac{1}{n}-1}\left(\frac{n\alpha^2\rho_0^2}{2a^{n+2}} + \hat{A}\right) = 0. \tag{5.51}$$

Hence, assuming $n > 1$,

$$\frac{n\alpha^2\rho_0^2}{2a^{n+2}} + \hat{A} = 0.$$

Rearranging,

$$\hat{A} = -\frac{n\alpha^2\rho_0^2}{2a^{n+2}}. \tag{5.52}$$

Applying boundary condition (5.46) yields

$$q_1(-1) = \left(-\frac{n\alpha^2\rho_0^2}{4a^{n+2}} + \frac{n\alpha^2\rho_0^2}{2a^{n+2}} + \left(\frac{1}{a}\right)^n \frac{c_0}{ak}\right)^{\frac{1}{n}} = \frac{1}{a}.$$

Simplifying yields

$$\frac{n}{4a^{n+2}}\alpha^2\rho_0^2 + \left(\frac{1}{a}\right)^n \frac{c_0}{ak} = \left(\frac{1}{a}\right)^n.$$

Multiplying by a^n yields

$$\frac{n}{4a^2}\alpha^2\rho_0^2 = 1 - \frac{c_0}{ak}. \tag{5.53}$$

Applying boundary condition (5.47) yields

$$\frac{1}{n}(\hat{B})^{\frac{1}{n}-1}\hat{A} = -\left(\frac{c_0\rho_0}{a^3nk}\right)\left(\frac{1}{a^{n-1}(\hat{B}^{\frac{1}{n}})^{n-1}}\right).$$

Upon simplification

$$\hat{A} = -\frac{c_0\rho_0}{a^3k}\left(\frac{1}{a^{n-1}}\right). \tag{5.54}$$

Equating equations (5.52) and (5.54)

$$-\frac{n\alpha^2\rho_0^2}{2a^{n+2}} = -\frac{c_0\rho_0}{a^3k}\left(\frac{1}{a^{n-1}}\right).$$

Hence

$$c_0 = \frac{n\alpha^2 k\rho_0}{2}. \tag{5.55}$$

Substituting for c_0 from equation (5.55) into equation (5.53) yields

$$\frac{n}{4a^2}\alpha^2\rho_0^2 + \frac{n\alpha^2\rho_0}{2a} - 1 = 0.$$

Hence

$$\rho_0^2 + 2a\rho_0 - \frac{4a^2}{n\alpha^2} = 0.$$

Solving the quadratic equation, the positive solution is

$$\rho_0 = \frac{-2a + \sqrt{4a^2 + \frac{16a^2}{n\alpha^2}}}{2}. \tag{5.56}$$

Application of a binomial expansion yields

$$\rho_0 = -a + \frac{2a}{\sqrt{n}\alpha}\left(1 + \frac{n}{8}\alpha^2 + O(\alpha^3)\right). \tag{5.57}$$

Hence ρ_0 can be written as

$$\rho_0 = \frac{2a}{\sqrt{n}\alpha}\left(1 - \frac{\sqrt{n}\alpha}{2} + O(\alpha^2)\right). \tag{5.58}$$

Substituting for ρ_0 from equation (5.58) into equation (5.55) yields

$$c_0 = k\alpha a\sqrt{n}\left(1 - \frac{\alpha\sqrt{n}}{2} + O(\alpha^2)\right). \tag{5.59}$$

Substituting for $\hat{A}$ from equation (5.52) yields

$$\hat{A} = -\frac{2}{a^n}\left(1 - \frac{\sqrt{n}\alpha}{2} + O(\alpha^2)\right)^2. \tag{5.60}$$

Substituting in $\hat{B}$ yields

$$\hat{B} = \alpha\left(1 - \frac{\sqrt{n}\alpha}{2} + O(\alpha^2)\right)\left(\frac{1}{a}\right)^n.$$

Hence the solution at leading order is

$$\begin{aligned}
c &= k\alpha a\sqrt{n}\left(1 - \frac{\sqrt{n}\alpha}{2} + O(\alpha^2)\right)\varepsilon^n + O(\varepsilon^{n+1}) \\
\rho &= \frac{2a}{\sqrt{n}\alpha}\left(1 - \frac{\sqrt{n}\alpha}{2} + O(\alpha^2)\right) + O(\varepsilon) \\
q &= \frac{1}{a}\left(1 + \left(1 - \frac{\alpha}{\sqrt{n}}\right)\left(-y(y+2) + \alpha + O(\alpha^2)\right)^{\frac{1}{n}}\varepsilon\right) + O(\varepsilon^2).
\end{aligned} \tag{5.61}$$

In Figure 5.8 we compare asymptotic expressions for the wave speed, c, with numerical values computing using the shooting method. Note that in contrast to Chapter 4, there is drastic change in wave speed as the parameter n is varied.

In Figure 5.9 we compare proliferation width, ρ, with shooting method solution as α, ε and n are varied.

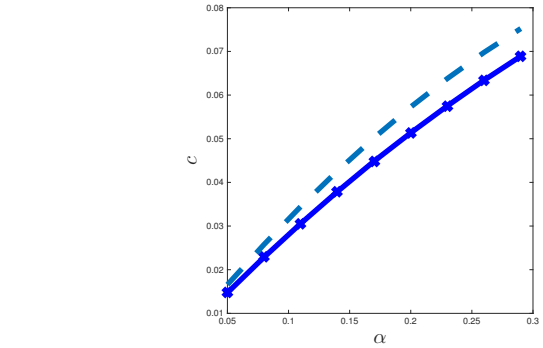

(a)

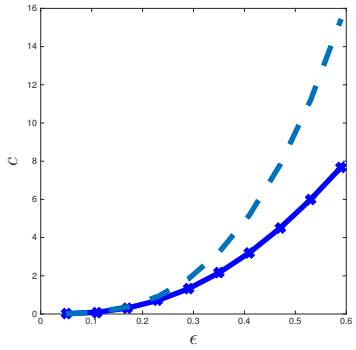

(b)

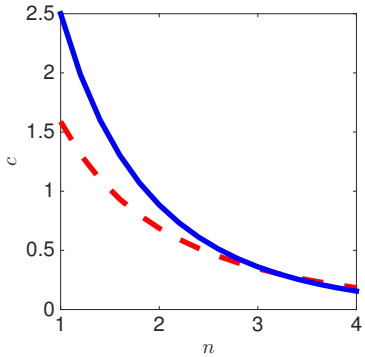

(c)

Figure 5.8: Comparing numerical and asymptotic approximations to the wave speed. (a) The wave speed, c, is plotted against α. ($n = 3$ and $\varepsilon = 0.15$). (b) The wave speed, c, is plotted against ε ($\alpha = 0.05$, $n = 3$). (c) The wave speed, c, is plotted against n. Numerical solutions are computed using a shooting method. Dash line-numerical solution, solid line-asymptotic solution.

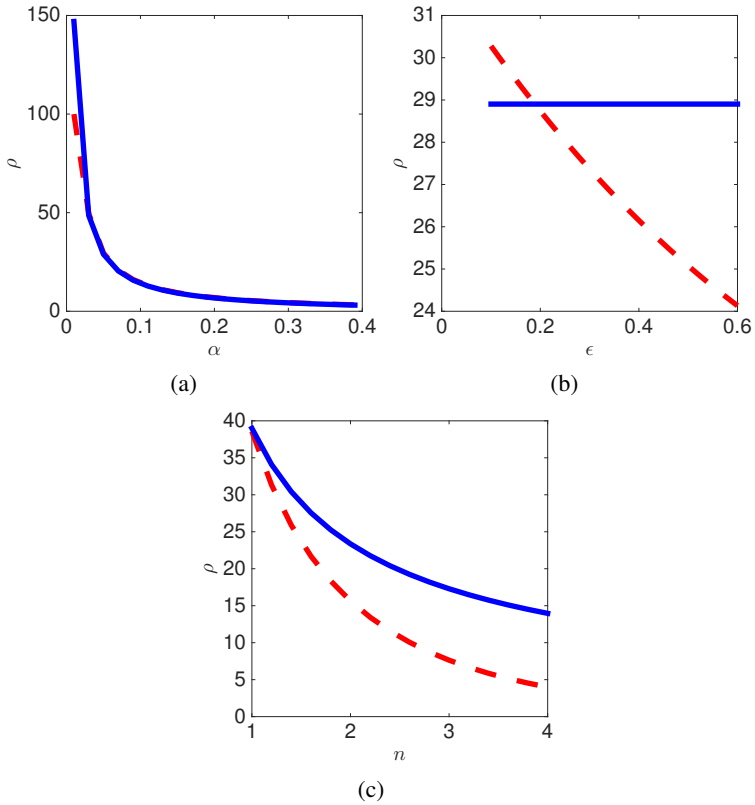

Figure 5.9: Comparing numerical and asymptotic solution to the proliferation width. (a) The proliferation width, ρ, is plotted against α ($n = 3$, $\varepsilon = 0.15$). (b) The proliferation width, ρ, is plotted against ε ($\alpha = 0.05$, $n = 3$). (c) The proliferation width, ρ, is plotted against n. Numerical solutions are computed using a shooting method. Dash line-numerical solution, solid line- asymptotic solution.

As we did in chapter 4, we emphasise that

$$\alpha = \sqrt{\frac{2r}{nk\varepsilon^n}},$$

hence we obtain the solution expression at leading order

$$\begin{aligned} c &= a\sqrt{2rk\varepsilon^n}, \\ \rho &= a\sqrt{\frac{2k\varepsilon^n}{r}}. \end{aligned} \tag{5.62}$$

Note that when $n = 1$ we return to the solution at leading order for the constant diffusion model Chapter 3 and nonlinear diffusion Chapter 4.

5.5 Interpreting parameter choices in discrete cell based model simulations

The results presented in equation (5.61) suggest that the type of force law chosen can have a profound effect, via the parameter n, on the wave speed and proliferating width.

Suppose, for example, that one wanted to make a multi scale simulation of a proliferating monolayer but was unsure whether to use a cubic or a linear force law. The results presented in Figures 5.8 and 5.9 suggest that the wave speed and proliferating rim width will vary depending on the choice of force law.

Here we use the results derived in Section 5.4 to deal with this problem. In a typical experimental simulation we might expect to measure the front speed, c, the threshold density, q_c and the proliferation rate, r. However, the spring constant, k, is typically difficult to measure.
As an example we consider simulations from Byrne and drasdo [14].
Here

$$c = \tilde{c} = 0.3 \quad c.d/h.$$

With the results of wave speed solution in this chapter,

$$\tilde{c} = ak\alpha\sqrt{n}\varepsilon^n. \tag{5.63}$$

parameter n	value of k
1	60
2	424
3	3464
4	30000

Table 5.1: Model parameters as k rescaling for increasing n in different values where $\alpha = 0.05$, $a = 1$ and $\varepsilon = 0.1$.

Hence

$$k \sim \frac{\tilde{c}}{a\alpha\sqrt{n}\varepsilon^n}. \tag{5.64}$$

Hence the effective spring constant inverses as n inverse power of n. Table (5.5) shows the results in some values of k and n where $\alpha = 0.05$ and $\varepsilon = 0.1$.

Murray et al claim that the coefficient in the Hertz force can be written in the form

$$\hat{k} = \frac{4E}{3\sqrt{a}(1-\nu^2)},$$

where E represent the Young modulus of elasticity and ν the Poisson ratio. In Drasdo [19] it is assumed that $\nu = 0.33 - 0.5$ and $E = 400$. Hence the corresponding value of $\hat{k}$ is approximately 600. In Meineke et al. [47], where a linear force law is used to study cell dynamics in the colorectal crypt the value of k is chosen to be 30. These observations of parameter values used in other discrete model simulations are consistent with the trends identified in Table 5.5.

5.6 Discussion

In this chapter we generalised the mathematical model of nonlinear diffusion by considering

$$D(q) = \frac{nk\left(a - \frac{1}{aq}\right)^{n-1}}{q^2},$$

with a corresponding force law

$$F(x) = k(a-x)^n.$$

We derive asymptotic approximations for wave speed and proliferating rim width and show excellent agreement with numerical results. The form chosen for the force law in the underlying discrete model is of a general form. Here we have considered particular instances corresponding to linear, cubic and Hertz cell-cell interaction force laws.

The major difference between the results presented in this chapter and Chapter 4 is that here the power of the force law has a profound effect on the wave speed. To illustrate this point we demonstrate how the spring constant ought to vary with n so as to give biologically plausible behaviours. Such insight would be difficult to gain running brute force simulations.

We note that the problem is singular in the limit ε. This limiting case has been deal with by making the ansatz that $q_0 = 1$. The singular case could be deal with formally by returning to the derivation of the continuum model and considering higher order terms. Note that the main difference between these models and those Chapter 4 is that here the diffusion coefficient tends to 0 as $q \to 1/a$.

Chapter 6

Conclusion

In this thesis, we had the motivation of cell monolayers to explore the results from such a model of nonlinear diffusion and highlight the emergence of two tissue scale, experimentally measurable quantities: the speed of propagation of the edge of the tissue, c, and the proliferating rim width, ρ. Analysis of front dynamics can be used to infer proliferation and migration rates in a tumour, wound healing (tissue repair) studies. We described, in particular, the development of travelling wave solution with nonlinear boundary conditions show how monolayers in tissue occur. The population of the cell considering is observing in a one-dimensional chain of contact-inhibited cells where our choice of diffusion satisfied this condition. The cells' growth is near perfect in compact monolayers, while biochemicals from contact inhibition control it. We introduced the mathematical models to solve the problem, discrete (individual or agent) based models that explain the heterogeneity between cells at various scales, and continuum models which give the solution of density cells governed by the partial differential equation and discrete to continuum models. Reaction-diffusion problems with nonlinear boundary conditions considered in various applications discussed in literature review solving the mathematical model continuum or discrete.

In this thesis, we related the study in Murray et al. [49] to derive a model that described a one-dimensional chain of contact-inhibited cells that interact via a general nonlinear force law to the continuum model. This idea includes the condition of nonlinear Stefan problem in which a nonlinear diffusion coefficient represents the force law in the continuum limit.

We showed that a central non-proliferating region characterises the solutions with the density equal to the proliferation threshold density and a propagating outer proliferating rim of cells. The primary question is whether we could derive expressions that describe the wave speed and proliferating rim width. Discrete descriptions of cell behaviours allow for incorporation of experimental data at the cellular scale. Moreover, frameworks provide a natural framework to study heterogeneous cell populations, stochastic processes in cell populations and emergent behaviours. However, in some example, it is desirable to understand what population scale features of a simulation are continuum models.

The critical questions arise in this thesis, how does the choice of force law affect the front speed and the proliferation width?. How do the results affect the choice of parameters?.

Throughout Chapter 3 we considered the simplified case in which the diffusion coefficient is assumed to be a constant. We then discussed two different classes of boundary condition on the moving front and calculate asymptotic expressions for the wave speed and rim width. The analysis identifies a small parameter, the natural logarithm of the compression ratio of cells at which contact inhibition stops proliferation. We considered the case where the diffusion coefficient is a constant and consider two sub-cases: in Case 1 a nonlinear Robin boundary condition is replaced by a Dirichlet condition. This approach enables the computation of an exact solution and the identification of a small parameter which allows asymptotic expressions to derived for the wave speed and proliferating rim width. In Case 2 we returned to the nonlinear Robin boundary

condition, a second small parameter identified, and asymptotic methods are used to derive expressions for the wave speed and proliferating rim width.

We solved the system by solving the model numerically, then performing a travelling wave analysis using a shooting method. The essential method presented in this thesis is to investigate a travelling wave speed following the analysis of the asymptotic expressions using the perturbation method. After the identification of a small parameter ε: the log of the ratio of the proliferation threshold density to the equilibrium density. Hence we obtained asymptotic expressions for the travelling wave speed and proliferating rim width that show excellent agreement with numerical estimates of the wave speed computed using a shooting method. It is also notable that the density profile at leading order is a parabolic.

The assumption that D is constant is mathematically very convenient, but biologically is unrealistic since particle rates of cell movement are significantly affected by local attraction.

Meanwhile, Chapter 4 developed to nonlinear model, we retain the simplifying assumption of a constant diffusion coefficient, and we reintroduced the nonlinear boundary condition. We analysed the model by using a Perturbation theory approach, then we identified a second small parameter and again constructed asymptotic solutions that yielded excellent agreement with numerical approximations. Notably, in the limit $\alpha \ll 1$, we obtain the Dirichlet condition assumed in a previous study by Murray et al. [49].

Following the analysis by asymptotic and numerical solution, we compared the results with the previous chapter.

In Chapter 4, We considered a nonlinear diffusion free boundary problem that provides an approximation to behaviour in such discrete cell-based simulations; we calculated an asymptotic expression for the wave speed and rim width. The analysis identifies

a small parameter, the natural logarithm of the compression ratio of cells at which contact inhibition stops proliferation, from which asymptotic expressions for the wave speed and proliferating rim width obtained. In this chapter, we examined the solution for wave speed for dimensional case where

$$D(q) = \frac{k}{q^2},$$

with two cases of moving boundary condition following the force law condition generalise in this chapter

$$F = \frac{ka}{n-1}\left(1 - (\frac{1}{aq_0})^{n-1}\right).$$

The results of nonlinear diffusion model were computed without the exact solution as we did in constant diffusion. However, we illustrated the solution by using the perturbation method and numerical analysis approximation of a travelling wave. Then, we derived a new formula for wave speed solution and proliferation width.

We explored the effect of including nonlinear diffusion coefficient in Figure(4.9), then we compared asymptotic expansions for wave speed and proliferating rim width for both the constant diffusion $D = ka^2$ and linear spring diffusion coefficient ($D = k/q^2$) models.

Notably, the most pronounced effect of the nonlinearity is that for the case of the nonlinear diffusion coefficient, the proliferating rim width decreases with the parameter ε where α included. However, when we return the solution to the original parameters, the solution agreed to the leading order with the constant model. As a result that we could not find the exact solution, we investigated the results using the perturbation method. From the comparison with constant diffusion, we had found that the wave speed propagates in the same behaviour as $\varepsilon \ll 1$.

In Chapter 5 we reintroduced the non-linear diffusion coefficient corresponding to a nonlinear force law in the discrete simulation and derived the asymptotic expression

for the wave speed and proliferating rim width. This Chapter included a clear idea about general force law and related diffusion coefficient, for $n = 1$ we had linear force law, $n = 3/2$ Hertz force law and $n = 3$ Cubic force law (Murray 2009). In Chapter 5 we investigate every case numerically, and we found the effect in the speed of travelling wave when n increasing, the speed becomes much slower than linear force law.

The asymptotic approximations for the wave speed and proliferating rim width showed excellent agreement with numerical approximations. Moreover, the asymptotic results showed that the effect of the nonlinear diffusion coefficient is minor and that a constant diffusion model is likely a reasonable approximation to a linear spring discrete model for biologically relevant parameter values. However, the asymptotic expansions do show the leading order dependence of the proliferating rim width with the parameter ε changes as a result of using the nonlinear diffusion coefficient. We solve the general diffusion coefficient using Circulate boundary condition and Robin boundary condition for the random positive n number.

The main interesting results of this thesis observed in constant diffusion model where the wave speed and proliferation width at the leading order gives:

$$\rho = \sqrt{\frac{2D\varepsilon}{r}} \quad \text{and} \quad c = \sqrt{2rD\varepsilon}. \tag{6.1}$$

Notably, the wave speed is less than a wave speed obtained in a Fisher-KPP equation [22]. This result is possible because in this case, the domain on which the travelling wavefront defined is semi-infinite. It can show that the origin is a stable spiral, but this does not lead to minimum wave speed because the boundary condition enforced at $z = 0$. King and McCabe [39] study a modification of the Fisher-KPP equation with fast nonlinear diffusion that is given by

$$\frac{\partial q}{\partial t} = \nabla . \left(q^{-n} \nabla q \right) + q(1-q). \tag{6.2}$$

They explore travelling wave behaviours and estimate the wave speed and position of wavefront for small value n. Notably the boundary conditions from $-\infty$ to $+\infty$ different from those considered in this thesis. This model used logistic growth term and we have proliferation term.

Byrne and Drasdo [14] consider a model in which a discrete cell-based model simulation is compared with an analogous continuum model. In their work, the discrete force law was the JKR model. The authors note that simulation results showed an inverse correlation between wave speed and proliferating rim width for different values of proliferate rate. This is precisely the result derived in equation (5.62) except in our case the relationships are derived rather than observed in numerical simulations. Additionally, our results can be summarised as

$$c\rho = 2D\varepsilon \tag{6.3}$$

$$\frac{c}{\rho} = r. \tag{6.4}$$

Hence experimental measurement of the proliferating rim width, ρ, the front speed, c, and the threshold density q_c is sufficient to determine the proliferation rate and the diffusion coefficient, i.e.

$$D = \frac{c\rho}{2\varepsilon} r = \frac{c}{\rho}.$$

In the case where r is varied, as was performed in the simulations by Byrne and Drasdo, one obtains

$$c = \frac{2D\varepsilon}{\rho}.$$

Hence simulations for different values of r sit on a hyperbola in the $c\rho$ plane. However, if the parameter D was instead varied, one would observe simulation results sitting on

a straight line in the $c\rho$ plane, i.e.

$$c = r\rho.$$

6.1 Future work

We remark that in future work the diffusion in general form can be written as

$$D(q) = \frac{nk}{q^m}\left(1-\frac{1}{q}\right)^{n-1}, \tag{6.5}$$

with force law

$$F(x) = ka\left(1-\frac{x}{a}\right)^{n}. \tag{6.6}$$

For two dimensional, we can develop the model by introduce the diffusion coefficient

$$D(q) = \frac{nk}{q}\left(1-\frac{1}{q}\right)^{n-1}, \tag{6.7}$$

Meanwhile, following the methods we introduced in chapter 5, we consider the diffusion model for two dimensional

$$\frac{\partial q}{\partial t} = \nabla.\left(D(q)\nabla q\right) + \hat{r}qH(q_c - q). \tag{6.8}$$

Hence

$$\frac{\partial q}{\partial t} = \frac{\partial}{\partial r}\left(D(q)\frac{\partial q}{\partial r}\right) + \frac{D(q)}{r}\frac{\partial q}{\partial r} + \hat{r}qH(q_c - q), \tag{6.9}$$

where $r \to \infty$ we have

$$\frac{\partial q}{\partial t} = \frac{\partial}{\partial r}\left(D(q)\frac{\partial q}{\partial r}\right) + \hat{r}qH(q_c - q), \tag{6.10}$$

where $q(r,t)$ is the cell density, r is the position variable, t is time, $D(q)$ is a diffusion coefficient, $\hat{r}$ is a proliferation rate, q_c is the threshold cell density at which cells stop proliferating.

The boundary conditions are given by:

$$\left.\frac{\partial q}{\partial r}\right|_{r=0} = 0, \tag{6.11}$$

and

$$\left.\frac{\partial q}{\partial r}\right|_{r=s(t)} = -\frac{q(s(t),t)}{D(q(s(t),t))}\frac{ds}{dt}, \tag{6.12}$$

where $s(t)$ represents the position of moving boundary that satisfies the ordinary differential equation

$$\frac{ds}{dt} = F\left(q(s(t),t)\right). \tag{6.13}$$

The initial conditions are

$$s(0) = s_0, \tag{6.14}$$

and

$$q(x,0) = f(r), \quad r \in [0, s_0]. \tag{6.15}$$

There are many studies study wound healing, tumour growth and linked to cell proliferation and migration dynamic. The detail of this approaches the required analysis of cell dynamic and measure of cell movement and proliferation qualitatively. Ascione et al. [6] have this approaches by using cell imaging in *vitro* included several cell migration assays and image analysis.

However, the models we have introduced can also be used to investigate the impact on cell proliferation and wave speed.

Bibliography

[1] M. Alber, N. Chen, P. Lushnikov, and S. Newman. Continuous macroscopic limit of a discrete stochastic model for interaction of living cells. *Physical Review Letters*, 99(16):168102, 2007.

[2] W. Alt. Models for mutual attraction and aggregation of motile individuals. In *Mathematics in Biology and Medicine*, pages 33–38. Springer, 1985.

[3] A. Anderson. A hybrid mathematical model of solid tumour invasion: the importance of cell adhesion. *Mathematical Medicine and Biology: a Journal of the IMA*, 22(2):163–186, 2005.

[4] A. RA. Anderson, A. Weaver, P. Cummings, and V. Quaranta. Tumor morphology and phenotypic evolution driven by selective pressure from the microenvironment. *Cell*, 127(5):905–915, 2006.

[5] R. Araujo and D. McElwain. A history of the study of solid tumour growth: the contribution of mathematical modelling. *Bulletin of Mathematical Biology*, 66 (5):1039–1091, 2004.

[6] Flora Ascione, Sergio Caserta, and Stefano Guido. The wound healing assay revisited: A transport phenomena approach. *Chemical Engineering Science*, 160: 200–209, 2017.

[7] C. M Bender and S. A Orszag. Advanced mathematical methods for scientists

and engineers. i. asymptotic methods and perturbation theory. reprint of the 1978 original, 1999.

[8] A. Bergman, J. Yanai, J. Weiss, D. Bell, and M.P. David. Acceleration of wound healing by topical application of honey: an animal model. *The American journal of surgery*, 145(3):374–376, 1983.

[9] D. Boal. Mechanics of the cell cambridge university press. *New York, Cambridge, UK*, 2002.

[10] H. Georg Bock and K. Plitt. A multiple shooting algorithm for direct solution of optimal control problems. *IFAC Proceedings Volumes*, 17(2):1603–1608, 1984.

[11] M. Bodnar and J. Velazquez. Derivation of macroscopic equations for individual cell-based models: a formal approach. *Mathematical Methods in the Applied Sciences*, 28(15):1757–1779, 2005.

[12] N. Britton. *Essential mathematical biology*. Springer Science & Business Media, 2012.

[13] N. F. Britton et al. *Reaction-diffusion equations and their applications to biology.* Academic Press, 1986.

[14] H. Byrne and D. Drasdo. Individual-based and continuum models of growing cell populations: a comparison. *Journal of Mathematical Biology*, 58(4):657–687, 2009.

[15] A. Q. Cai, K. A. Landman, and B. D. Hughes. Multi-scale modeling of a wound-healing cell migration assay. *Journal of Theoretical Biology*, 245(3):576–594, 2007.

[16] F. Crick and J. Watson. What is dna? *Molecular biology*, 1961.

[17] A. Deutsch and S. Dormann. *Cellular automaton modeling of biological pattern formation: characterization, applications, and analysis*. Springer Science Business Media, 2007.

[18] D. Drasdo and S. Hohme. A single-cell-based model of tumor growth in vitro : monolayers and spheroids. *Physical Biology*, 2(3):133, 2005.

[19] D. Drasdo and S. Höhme. A single-cell-based model of tumor growth in vitro: monolayers and spheroids. *Physical Biology*, 2(3):133, 2005.

[20] S. Dunn, I. S Näthke, and J. M. Osborne. Computational models reveal a passive mechanism for cell migration in the crypt. *PLoS One*, 8(11):e80516, 2013.

[21] R. Erban and H. G. Othmer. From individual to collective behavior in bacterial chemotaxis. *SIAM Journal on Applied Mathematics*, 65(2):361–391, 2004.

[22] R. A. Fisher. The wave of advance of advantageous genes. *Annals of Eugenics*, 7(4):355–369, 1937.

[23] A. G. Fletcher, J.M. Osborne, P. K. Maini, and D.J. Gavaghan. Implementing vertex dynamics models of cell populations in biology within a consistent computational framework. *Progress in Biophysics and Molecular Biology*, 113(2): 299–326, 2013.

[24] JA. Fozard, HM. Byrne, OE. Jensen, and JR. King. Continuum approximations of individual-based models for epithelial monolayers. *Mathematical Medicine and Biology: a Journal of the IMA*, 27(1):39–74, 2009.

[25] J. Galle, M. Loeffler, and D. Drasdo. Modeling the effect of deregulated proliferation and apoptosis on the growth dynamics of epithelial cell populations in vitro. *Biophysical Journal*, 88(1):62–75, 2005.

[26] R. A. Gatenby and E. T. Gawlinski. A reaction-diffusion model of cancer invasion. *Cancer Research*, 56(24):5745–5753, 1996.

[27] J. A. Glazier and F. Graner. Simulation of the differential adhesion driven rearrangement of biological cells. *Physical Review E*, 47(3):2128, 1993.

[28] F. Graner and J. A. Glazier. Simulation of biological cell sorting using a two-dimensional extended potts model. *Physical Review Letters*, 69(13):2013, 1992.

[29] B. M Gumbiner. Cell adhesion: the molecular basis of tissue architecture and morphogenesis. *Cell*, 84(3):345–357, 1996.

[30] H. Hatzikirou and A. Deutsch. Cellular automata as microscopic models of cell migration in heterogeneous environments. *Current Topics in Developmental Biology*, 81:401–434, 2008.

[31] P. DN Hebert, A. Cywinska, Sh. L Ball, et al. Biological identifications through dna barcodes. *Proceedings of the Royal Society of London B: Biological Sciences*, 270(1512):313–321, 2003.

[32] E. John Hinch. *Perturbation methods*. Cambridge university press, 1991.

[33] H. Honda, M. Tanemura, and T. Nagai. A three-dimensional vertex dynamics cell model of space-filling polyhedra simulating cell behavior in a cell aggregate. *Journal of Theoretical Biology*, 226(4):439–453, 2004.

[34] G. Karp. *Cell and molecular biology: concepts and experiments*. John Wiley & Sons, 2009.

[35] M. Kearse, R. Moir, A. Wilson, S. Stones-Havas, M. Cheung, Sh. Sturrock, S. Buxton, A. Cooper, S. Markowitz, Ch. Duran, et al. Geneious basic: an integrated and extendable desktop software platform for the organization and analysis of sequence data. *Bioinformatics*, 28(12):1647–1649, 2012.

[36] E. F. Keller and L. A. Segel. Model for chemotaxis. *Journal of Theoretical Biology*, 30(2):225–234, 1971.

[37] J. Kevorkian and J. D Cole. *Perturbation methods in applied mathematics*, volume 34. Springer Science & Business Media, 2013.

[38] N. Khalilgharibi, M. Miodownik, and J. Green. A mathematical approach to tissue development. 2012.

[39] J. R King and Ph. M McCabe. On the fisher–kpp equation with fast nonlinear diffusion. In *Proceedings of the Royal Society of London A: Mathematical, Physical and Engineering Sciences*, volume 459, pages 2529–2546. The Royal Society, 2003.

[40] A. Kolmogorofl, I. Petrovsky, and N. Piscounofl. Study of the diffusion equation with growth of the quantity of matter and its application to a biology problem. *Dynamics of Curved Fronts*, page 105, 2012.

[41] C. Kuttler. Reaction-diffusion equations with applications. In *Internet Seminar*, 2011.

[42] CH. Liang, A. Y. Park, and J. Guan. In vitro scratch assay: a convenient and inexpensive method for analysis of cell migration in vitro. *Nature Protocols*, 2 (2):329, 2007.

[43] P. M. Lushnikov, N. Chen, and M. Alber. Macroscopic dynamics of biological cells interacting via chemotaxis and direct contact. *Physical Review E*, 78(6): 061904, 2008.

[44] P. K. Maini, DL. S. McElwain, and D. I. Leavesley. Traveling wave model to interpret a wound-healing cell migration assay for human peritoneal mesothelial cells. *Tissue Engineering*, 10(3-4):475–482, 2004.

[45] D. G. Mallet and L. De Pillis. A cellular automata model of tumor–immune system interactions. *Journal of Theoretical Biology*, 239(3):334–350, 2006.

[46] V. Maree, A. FM.and Grieneisen and P. Hogeweg. The cellular potts model and biophysical properties of cells, tissues and morphogenesis. In *Single-cell-based models in biology and medicine*, pages 107–136. Springer, 2007.

[47] F. A. Meineke, Ch. S. Potten, and M. Loeffler. Cell migration and organization in the intestinal crypt using a lattice-free model. *Cell Proliferation*, 34(4):253–266, 2001.

[48] A. M. Middleton, Ch. Fleck, and R. Grima. A continuum approximation to an off-lattice individual-cell based model of cell migration and adhesion. *Journal of Theoretical Biology*, 359:220–232, 2014.

[49] C. M. Murray, P. J.and Edwards, J. M. Tindall, and P. K. Maini. From a discrete to a continuum model of cell dynamics in one dimension. *Physical Review E*, 80 (3):031912, 2009.

[50] J. Murray, P. J.and Kang, G. R. Mirams, S. ShiN, H. M. Byrne, P. K. Maini, and K. Cho. Modelling spatially regulated β-catenin dynamics and invasion in intestinal crypts. *Biophysical Journal*, 99(3):716–725, 2010.

[51] J. D. Murray. *Mathematical biology. II Spatial models and biomedical applications* $\{$*Interdisciplinary Applied Mathematics V. 18*$\}$. Springer-Verlag New York Incorporated New York, 2001.

[52] P. J. Murray, A. Walter, A. G. Fletcher, C. M. Edwards, M. J. Tindall, and P. K. Maini. Comparing a discrete and continuum model of the intestinal crypt. *Physical Biology*, 8(2):026011, 2011.

[53] P. J. Murray, C. M. Edwards, M. J. Tindall, and P. K. Maini. Classifying general nonlinear force laws in cell-based models via the continuum limit. *Physical Review E*, 85(2):021921, 2012.

[54] A. A. Patel, E. T. Gawlinski, S. K. Lemieux, and R. A Gatenby. A cellular automaton model of early tumor growth and invasion: the effects of native tissue vascularity and increased anaerobic tumor metabolism. *Journal of theoretical biology*, 213(3):315–331, 2001.

[55] J. Pellerito and J. Polak. *Introduction to Vascular Ultrasonography E-Book*. Elsevier Health Sciences, 2012.

[56] R. B. Potts. Some generalized order-disorder transformations. In *Mathematical proceedings of the cambridge philosophical society*, volume 48, pages 106–109. Cambridge University Press, 1952.

[57] W. Press, S. Teukolsky, W. T. Vetterling, and B. Flannery. *Numerical recipes 3rd edition: The art of scientific computing*. Cambridge university press, 2007.

[58] D. Prieto, G. Aparicio, and J. Sotelo-Silveira. Cell migration analysis: A low-cost laboratory experiment for cell and developmental biology courses using keratocytes from fish scales. *Biochemistry and Molecular Biology Education*, 45(6): 475–482, 2017.

[59] T. Roose, S. Chapman, and Ph. K Maini. Mathematical models of avascular tumor growth. *SIAM review*, 49(2):179–208, 2007.

[60] SA Safran, N Gov, A Nicolas, US Schwarz, and T Tlusty. Physics of cell elasticity, shape and adhesion. *Physica A: Statistical Mechanics and its Applications*, 352(1):171–201, 2005.

[61] G. Schaller and M. Meyer-Hermann. Multicellular tumor spheroid in an off-lattice voronoi-delaunay cell model. *Physical Review E*, 71(5):051910, 2005.

[62] WE. Schiesser. The numerical methods of lines. *Integration of partial differential equations Academic Press San Diego*, 1991.

[63] M. Shakeel. Travelling wave solution of the fisher-kolmogorov equation with non-linear diffusion. *Applied Mathematics*, 4(08):148, 2013.

[64] D. Shao, H. Levine, and W. Rappel. Coupling actin flow, adhesion, and morphology in a computational cell motility model. *Proceedings of the National Academy of Sciences*, 109(18):6851–6856, 2012.

[65] M. J. Simpson, K. A. Landman, B. D. Hughes, and A. E. Fernando. A model for mesoscale patterns in motile populations. *Physica A: Statistical Mechanics and its Applications*, 389(7):1412–1424, 2010.

[66] W. G. Stetler-Stevenson, S. Aznavoorian, and L. A. Liotta. Tumor cell interactions with the extracellular matrix during invasion and metastasis. *Annual review of cell biology*, 9(1):541–573, 1993.

[67] A. M. Turing. The chemical basis of morphogenesis. *Philosophical Transactions of the Royal Society of London B: Biological Sciences*, 237(641):37–72, 1952.

[68] J D Victor. The dynamics of the cat retinal x cell centre. *The Journal of physiology*, 386(1):219–246, 1987.

[69] V. Volpert and S. Petrovskii. Reaction–diffusion waves in biology. *Physics of Life Reviews*, 6(4):267–310, 2009.

[70] J. P. Ward and JR. King. Mathematical modelling of avascular-tumour growth. *Mathematical Medicine and Biology: A Journal of the IMA*, 14(1):39–69, 1997.

[71] X. Zhang, Z. Pei, Ch. Ji, X. Zhang, J. Xu, and J. Wang. Novel insights into the role of the cytoskeleton in cancer. In *Cytoskeleton-Structure, Dynamics, Function and Disease*. InTech, 2017.